

## UvA-DARE (Digital Academic Repository)

### Hydrophilic interaction chromatography – mass spectrometry for metabolomics and proteomics

*state-of-the-art and current trends*

Kohler, I.; Verhoeven, M.; Haselberg, R.; Gargano, A.F.G.

#### DOI

[10.1016/j.microc.2021.106986](https://doi.org/10.1016/j.microc.2021.106986)

#### Publication date

2022

#### Document Version

Final published version

#### Published in

Microchemical Journal

#### License

CC BY

[Link to publication](#)

#### Citation for published version (APA):

Kohler, I., Verhoeven, M., Haselberg, R., & Gargano, A. F. G. (2022). Hydrophilic interaction chromatography – mass spectrometry for metabolomics and proteomics: state-of-the-art and current trends. *Microchemical Journal*, 175, [106986].  
<https://doi.org/10.1016/j.microc.2021.106986>

#### General rights

It is not permitted to download or to forward/distribute the text or part of it without the consent of the author(s) and/or copyright holder(s), other than for strictly personal, individual use, unless the work is under an open content license (like Creative Commons).

#### Disclaimer/Complaints regulations

If you believe that digital publication of certain material infringes any of your rights or (privacy) interests, please let the Library know, stating your reasons. In case of a legitimate complaint, the Library will make the material inaccessible and/or remove it from the website. Please Ask the Library: <https://uba.uva.nl/en/contact>, or a letter to: Library of the University of Amsterdam, Secretariat, Singel 425, 1012 WP Amsterdam, The Netherlands. You will be contacted as soon as possible.

*UvA-DARE is a service provided by the library of the University of Amsterdam (<https://dare.uva.nl>)*



# Hydrophilic interaction chromatography – mass spectrometry for metabolomics and proteomics: state-of-the-art and current trends

Isabelle Kohler<sup>a,c,\*</sup>, Michel Verhoeven<sup>a,b,c</sup>, Rob Haselberg<sup>a,c</sup>, Andrea F.G. Gargano<sup>b,c,\*</sup>

<sup>a</sup> Division of BioAnalytical Chemistry, Amsterdam Institute of Molecular and Life Sciences (AIMMS), Vrije Universiteit Amsterdam, Amsterdam, the Netherlands

<sup>b</sup> Van't Hoff Institute for Molecular Sciences, University of Amsterdam, Amsterdam, the Netherlands

<sup>c</sup> Centre for Analytical Sciences Amsterdam, Amsterdam, the Netherlands

## ARTICLE INFO

### Keywords:

Electrostatic repulsion – hydrophilic interaction chromatography  
Hydrophilic interaction chromatography  
HILIC-MS  
Metabolomics  
Proteomics  
Post-translational modifications  
Two-dimensional separations

## ABSTRACT

Among all the –omics approaches, proteomics and metabolomics have received increased attention over the last decade. Both approaches have reached a certain level of maturity, showing their relevance in numerous clinical applications, including biomarkers discovery, improved diagnosis, staging, and prognosis of diseases, as well as a better knowledge on various (patho-)physiological processes. Analytically, reversed-phase liquid chromatography – mass spectrometry (RPLC-MS) is considered the golden standard in proteomics and metabolomics, due to its ease of use and reproducibility. However, RPLC-MS alone is not sufficient to resolve the complexity of the proteome, while very polar metabolites are typically poorly retained. In this context, hydrophilic interaction chromatography (HILIC) represents an attractive complementary approach, due to its orthogonal separation mechanism. This review presents an overview of the literature reporting the application of HILIC-MS in metabolomics and proteomics. For metabolomics the focus is on the analysis of bioactive lipids, amino acids, organic acids, and nucleotides/nucleosides, whereas for proteomics the analysis of complex samples and protein post-translational modifications therein using bottom-up, middle up/down proteomics and intact protein analysis is discussed. The review handles the technological aspects related to the use of HILIC-MS in both proteomics and metabolomics, paying attention to stationary phases, mobile phase conditions, injection volume and column temperature. Recent trends and developments in the application of HILIC-MS in proteomics and metabolomics are also presented and discussed, highlighting the advantages the technique can provide in addition or complementary to RPLC-MS, as well as the current limitations and possible solutions.

## 1. Introduction

Among all –omics approaches, proteomics and metabolomics have gathered an increased attention from the clinical community over the recent years. Proteomics is defined as the comprehensive analysis of the proteome, i.e., all proteins produced or modified by an organism or living system [1–3]. By contrast to the genome (i.e., the genetic information of an organism), the proteome of an organism is not constant and dynamically changes over time. For this reason, the variation of the expression levels, the chemical modifications (post-translational modifications, PTMs) and conformational changes of proteins are frequently investigated as biological markers of alteration of the physiological conditions like the progression of diseases. Significant challenges in large-scale proteomics experiments include the high complexity of the

proteome and wide dynamic range [4,5]. Tens of thousands of proteins are present in a complex organism. Moreover, these distribute further due to variety in PTMs, giving origin to potentially hundreds of thousands of different protein species. In addition, the dynamic range of expression levels for different components of the proteome is estimated to result in differences in concentration in the order of  $10^7$ .

Proteins are most commonly identified and quantified using liquid chromatography coupled to mass spectrometry (LC-MS). The most common approach is bottom-up proteomics, where proteins are identified from peptides generated by the hydrolysis of specific enzymes. Other approaches include the use of enzymes that hydrolyze less frequent amino acids or characteristic sequences of subunits. The results are larger peptides or subunits that are analyzed during the so-called middle-down or middle-up proteomics. Lastly, proteins can be

\* Corresponding authors at: Vrije Universiteit Amsterdam, Division of Bioanalytical Chemistry, De Boelelaan 1085, 1081 HV Amsterdam, the Netherlands (I. Kohler). University of Amsterdam, van't Hoff Institute for Molecular Sciences, postbus 94157, 1090 GD Amsterdam, the Netherlands (A. Gargano).

E-mail addresses: [i.kohler@vu.nl](mailto:i.kohler@vu.nl) (I. Kohler), [a.gargano@uva.nl](mailto:a.gargano@uva.nl) (A.F.G. Gargano).

<https://doi.org/10.1016/j.microc.2021.106986>

Received 29 August 2021; Received in revised form 25 October 2021; Accepted 8 November 2021

Available online 15 November 2021

0026-265X/© 2021 The Author(s). Published by Elsevier B.V. This is an open access article under the CC BY license (<http://creativecommons.org/licenses/by/4.0/>).

analyzed in their intact form in top-down proteomics. Nowadays, LC-MS technology used in proteomics has reached a level of maturity that allowed its implementation into numerous application areas such as the discovery of biomarkers [6], personalized medicine [7], drug discovery and development [8], as well as system biology [9].

Metabolomics represents the large-scale study of metabolites (i.e., compounds with a mass lower than 1 kDa), intermediates, and products of cell metabolism in biological samples [10,11]. The metabolome includes lipids, amino acids, organic acids, vitamins, hormones, nucleosides/nucleotides, minerals, as well as xenobiotics such as drugs, food additives, and contaminants. It is very complex and reflects a great diversity of compounds with large differences in physicochemical properties, the presence of multiple isoforms and broad dynamic ranges between trace compounds and highly abundant species [10,12]. Metabolomics approaches are divided into targeted and untargeted approaches. Untargeted metabolomics involves the comprehensive and unbiased analysis of all metabolites present in a biological sample for the discovery of potential biomarkers, whereas targeted metabolomics involves the quantification of known biomarkers from one or more metabolic classes with high accuracy and reproducibility [13-15].

Numerous analytical approaches have been explored for proteomics and metabolomics studies, such as proton nuclear magnetic resonance spectroscopy ( $^1\text{H}$  NMR) or capillary electrophoresis (CE), gas chromatography (GC), and LC combined with MS [16,17]. Among these, LC-MS using atmospheric ionization interfaces, especially electrospray ionization (ESI), remains the most common technique. Compared with other techniques, LC-MS offers an expanded dynamic range and a higher sensitivity [18]. The LC-MS strategies used in proteomics and metabolomics typically show a high throughput (to cope with the needs in a clinical environment or a large number of samples) and/or high resolving power and selectivity (to adequately deal with the sample complexity) [19,20]. Similar to proteomics, metabolomics has been increasingly considered for the discovery of (new) biomarkers and drug targets, improved diagnosis, staging, and prognosis of diseases, as well as to provide better knowledge on (patho-)physiological processes [10].

Reversed phase (RP) LC-MS has been considered the golden standard in proteomics and metabolomics because of the ease of use and retention time reproducibility [10,21]. However, despite several attempts to increase the retention of polar compounds, a wide variety of highly polar and ionizable metabolites are not well retained using RPLC [21,22]. Moreover, the high complexity and dynamic range of the samples analyzed in proteomics cannot be solely resolved by RPLC-MS [4,23]. Therefore, when an in-depth analysis is needed, a complementary LC separation before RPLC-MS is often considered to either enrich for specific populations or to decrease the proteome complexity by fractionating the sample components into different sub-samples.

In metabolomics and proteomics, hydrophilic interaction liquid chromatography (HILIC) represents a valuable alternative and/or complementary separation technique to RPLC-MS, helping to overcome some of the aforementioned challenges. The term HILIC was first introduced by Alpert in 1990 [24]. HILIC is currently the second most common chromatographic mode used in LC-MS analysis due to its high separation peak capacity and selectivity [25]. HILIC can be considered as a hybrid technique between RPLC, normal phase LC (NPLC) and ion exchange chromatography (IEX), as it resembles NPLC in the polarity of the stationary phase, RPLC in the composition of the mobile phase, and IEX for the type of compounds analysed. The retention in HILIC is driven by the partition of analytes between a hydrophilic stationary phase and a relatively hydrophobic mobile phase. Common stationary phases used in HILIC are silica, aminopropyl, amide, diol, and zwitterionic columns. The mobile phase consists of a high proportion of water-miscible aprotic polar organic solvent (60–97%), mostly acetonitrile, and a low proportion of water or a volatile buffer (3–40%), forming a semi-immobilized aqueous layer on the stationary phase allowing for the hydrophilic partitioning. The exact mechanisms involved in HILIC retention and separation are quite complex, mostly involving hydrophilic partitioning,

dipole–dipole interactions, hydrogen bonding, and electrostatic interactions. These interactions depend on the nature of the stationary phase, the composition of the mobile phase, and the analytes [11,22,25].

HILIC shows several advantages, with the most obvious one being the possibility to serve as an orthogonal mechanism in online and offline 2D-LC separations. Other major benefits revolve around the lower mobile phase viscosity (2–3 times lower than RPLC), which results in lower back pressure and allows for the use of higher flow rates, longer columns and smaller particles size [21,22]. In addition, the higher mobile phase volatility improves the detection sensitivity in systems where evaporation of the mobile phase is employed, such as evaporative light scattering detection (ELSD) and ESI before MS detection [21,22,26]. Furthermore, the increased analyte diffusivity in the organic-rich mobile phase increases the B-term and lowers the C-term contribution to the Van Deemter equation. This translates to a lower efficiency at low flow rates and a higher efficiency at higher flow rates, which is especially beneficial in high-throughput workflows [21,22,25,27].

The use of HILIC for a various range of clinical applications has been growing in recent years [10,11,28]. However, the observed growth remained limited, which can be explained by the challenges commonly encountered in HILIC method development. Indeed, depending on the experimental conditions, the technique may suffer from poor peak shapes, lower intra- and inter-day retention time repeatability and it requires longer re-equilibration times than in RPLC. The retention times can be difficult to predict due to the complex retention mechanisms [29-31], although recent development using computer-aided approaches have shown progress in this area [32-36]. Nevertheless, significant technological advances in LC-MS over the last two decades have aided the implementation of HILIC in proteomics and metabolomics. These developments include the commercialization of dedicated HILIC columns along with improved particle chemistry and morphology (e.g., smaller particles, core-shell technology, etc.). Moreover, a better understanding of the retention mechanism and the effect of experimental parameters have contributed to the implementation of method development guidelines, helping users to become more experienced. Overall, this resulted in significant improvements in sensitivity, analyte coverage, throughput, analysis speed, and resolution [9,18]. HILIC thus offers excellent opportunities for the analysis of polar and/or ionizable metabolites, as well as hydrophilic proteins, such as glycoproteins [37].

This review discusses the recent developments in HILIC-MS for proteomics and metabolomics focusing on bioanalytical applications. The first section discusses the experimental parameters that are relevant for obtaining high-quality metabolomics and proteomics data, focusing on the stationary phase chemistries, mobile phase composition (i.e., solvents, buffer concentration and pH) and injection solvent. The section on metabolomics covers a selection of recent applications ( $\geq 2012$ ) of HILIC for the targeted analysis of specific metabolite classes, namely, bioactive lipids, amino acids, organic acids, and nucleosides/nucleotides, which have attracted much interest in clinical environments due to the important roles they play in multiple (patho-)physiological processes. The section on proteomics presents an overview of the research literature published in approximately the same time period and includes the analysis of reference proteins and complex cell digests and their analysis as intact proteins and as enzymatic digest (i.e., middle-up/down and bottom-up proteomics). Moreover, the selectivity and the most common approaches to analyze proteins using HILIC are discussed in the context of proteome-wide studies, as well as for targeted analysis of PTMs.

## 2. Technical aspects of HILIC separations in -omics

### 2.1. Metabolomics

#### 2.1.1. Stationary phase chemistries

The first HILIC applications were performed on normal phase (NPLC)

stationary phases, such as amino, diol and silica phases [38]. Most of the HILIC phases nowadays are silica- or polymer-based and are produced through the functionalization of silica gel or polymers with polar groups. These functional groups allow water to be retained through the formation of an immobilized layer on the stationary phase surface. Moreover, they introduce and tune the type of interactions occurring between the stationary phase and the analytes.

Many HILIC columns have been developed and commercialized in recent years for the analysis of polar and/or ionizable compounds. The phases can be divided into three categories: charged (anionic such as unmodified silica; cationic aminopropyl), neutral (amide or diol), and zwitterionic (sulfobetaine or phosphorylcholine). The stationary phases provide different characteristics in terms of hydrophilicity, formation of hydrogen bonds and electrostatic interactions. Table 1 summarizes the main characteristics of the different HILIC chemistries. Since the retention mechanism in HILIC is more complex than that of RPLC, different stationary phase chemistries should be investigated during method development as the retention behavior of targeted analytes is typically difficult to predict [22,29,30].

### 2.1.2. Injection solvent composition and volume

One of the major challenges in HILIC is related to the injection solvent, which may lead to relatively poor efficiency, poor peak shapes and reduced signal intensity if its composition and the injection volume are inadequate, both in metabolomics and proteomics applications.

The nature of the injection solvent in HILIC appears to be a more critical parameter than in RPLC [39]. Ruta et al. demonstrated that the water content in the injection solvent has a significant effect on peak shape and width (Fig. 1A) [39]. Their study showed that pure ACN and 10% water in the injection solvent provided the best results. However, increasing the amount of water in the injection solvent led to deteriorated peak shape, especially for the compounds eluting at the beginning of the gradient (i.e., 95% ACN). The effect was less important for late-eluting analytes (i.e., 95–75% ACN). Ideally, samples should therefore be reconstituted or dissolved in the mobile phase composition at the

start of the gradient, or at least in the highest proportion of ACN possible. The deleterious effect of the injection solvent on peak shape becomes more significant when the difference between the injection solvent and the mobile phase composition increases (so-called solvent mismatch) [40,41]. Note that this is often not an issue for relatively hydrophobic compounds that are easily soluble in a high proportion of ACN, but may become challenging for more polar compounds which have limited solubility in ACN, such as polar metabolites but also proteins (under their intact form, subunits or peptides). In metabolomics studies selecting the adequate injection solvent for a combination of metabolites with a large diversity in physico-chemical properties can thus be challenging. Using another organic solvent in the injection solvent may also lead to deteriorated peak shapes, as shown by Ruta et al. (Fig. 1B) [39]. This relatively poorer peak shape is explained by the hydrogen bonding capability. Indeed, polar protic solvents (e.g., MeOH, EtOH) have a strong ability to form hydrogen bonds, which can disrupt the water layer on the stationary phase surface, resulting in distorted peak shapes. On the other hand, isopropanol (IPA) is a polar protic solvent with a relatively low hydrogen bonding donor capability and can thus be used when the sample solubility of ACN is not sufficient, even though it leads to less satisfactory results compared with ACN. Finally, dimethyl-sulfoxide (DMSO) can also be considered in HILIC, as it has no hydrogen bonding capability and can solvate a wide range of organic compounds at a high concentration. Fully replacing ACN with DMSO generally results in poor peak shapes, but mixing ACN and DMSO up to a ratio of 70:30 (v/v) still provides acceptable peak shape while allowing sufficient solvation power for analytes that are poorly soluble in pure ACN [39].

In general, in metabolomics, the injection volume in HILIC should be kept as low as possible due to its susceptibility to volume overloading effects, which lead to peak distortion and tailing, especially in case of solvent mismatch, as illustrated in Fig. 2. Therefore, a maximum of 1% of the total column volume should be injected, regardless of the biological matrix or the composition of the injection solvent. If sensitivity is a concern, samples may be pre-concentrated to maximize the injected

**Table 1**

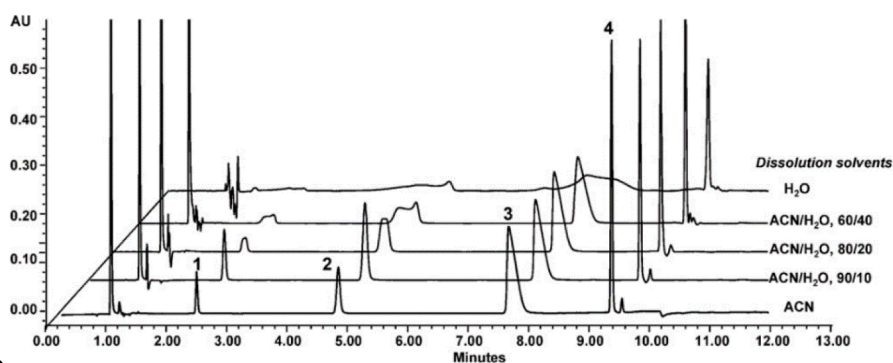
Commonly used stationary phase chemistries in hydrophilic interaction, electrostatic attraction, and electrostatic repulsion liquid separations. Modified from [29,180] and taking into account the literature discussed in this review.

Phase chemistry	Type of LC mode	Electrostatic interaction	Hydrogen bonds	Metabolomics	Proteomics
<i>Neutral phases</i>					
Amide	HILIC	/	A+D		
Diol	HILIC	/	A+D		
Crossed-linked diol	HILIC	/	A+D		
Polyhydroxyl	HILIC	/	A+D		
<i>Charged phases</i>					
Amino	HILIC (WAX)	pH < 9: strong (+) pH > 9: weak (+)	D		
Silica	HILIC (WCX)	pH < 4: weak (-) pH > 4-5: strong (-)	pH < 4: A+D pH 4-5: A		
Polyethyleneimine	ERLIC (WAX)	pH > 8: weak (+) pH < 8: strong (+)	D		
Strong anion exchange	ERLIC (SAX)	Strong (+)	D		
Polyaspartic acid	EALIC (WCX)	pH < 3: weak (-) pH > 3: strong (-)	pH < 3: A+D pH > 3: A		
<i>Zwitterionic phases</i>					
Sulfobetaine	HILIC	pH < 3: weak (-)	pH < 3: A pH > 3: A+D		
Phosphorylcholine	HILIC	pH < 3: weak (-)	pH < 3: A pH > 3: A+D		

A, Acceptor; D, Donor; WCX, Weak Cation Exchange; WAX, Weak Anion Exchange; SAX, Strong Anion Exchange; ERLIC, Electrostatic Repulsion Liquid Chromatography; EALIC, Electrostatic Attraction Interaction Chromatography. The colour code describes the frequency of which the stationary phase was used in the different application areas covered in this review: □ not observed, ◻ rare, ◻ moderate, ◻ frequent.



A.



B.

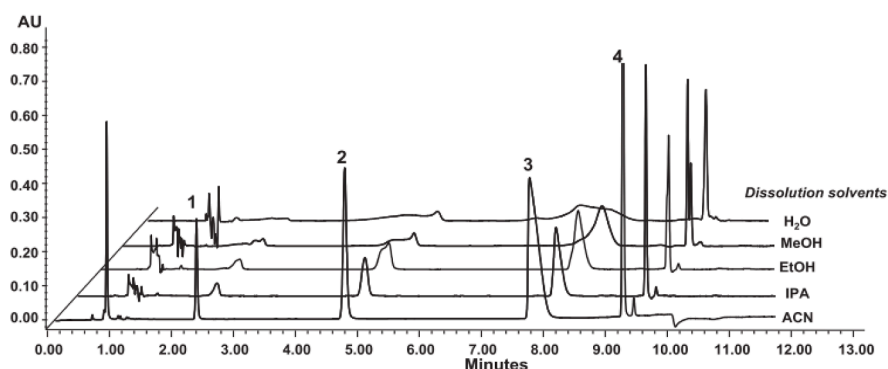
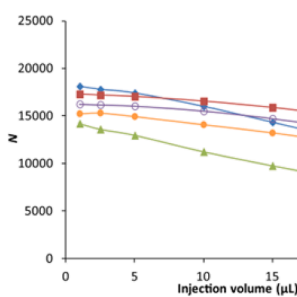
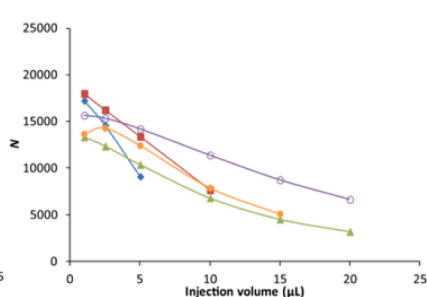


**Fig. 1.** Effect the injection solvent composition on peak shape. A. Effects observed with addition of water to the injection solvent; B. effects observed with alternative solvents, i.e., isopropanol (IPA), ethanol (EtOH) and methanol (MeOH). Experimental conditions: Acquity BEH HILIC column (2.1 mm × 150 mm, 1.7 μm); eluent A: ammonium formate (50 mM, pH 3.14), eluent B: ACN; gradient: 0–6.0 min. 95% B, 6.0–11.0 min. 95–75% B. Compounds: 1) hypoxanthine, 2) cytosine, 3) nicotinic acid, and 4) procainamide. Reproduced from [39] with permissions.

A.



B.



C.

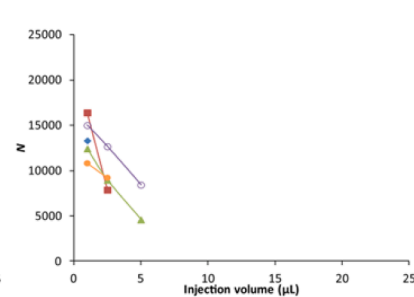


**Fig. 2.** Effects on efficiency (N) observed when increasing the injection volume from 1 to 20 μL depending on the composition of the injection solvent. (a) 95% ACN, (b) 90% ACN, and (c) 80% ACN. Mobile phase composed of a mixture of ACN/ 5 mM Ammonium acetate (95:5, v/v). Reproduced from Heaton and McCalley [41] with permissions.

quantity while keeping the injected volume to a minimum [21].

### 2.1.3. Mobile phase composition

**2.1.3.1. Organic solvent.** ACN is the most commonly used organic modifier in HILIC, as it is miscible with water and a polar aprotic solvent. Additional advantages include its high viscosity and volatility. The low hydrogen bond donor capability of ACN compared to other solvents allows for salts to be more easily solvated compared with polar protic solvents. Moreover, the aprotic nature of ACN facilitates the formation of a water layer on the stationary phase surface. This allows hydrogen-bond interactions to take place between the analyte and stationary phase, resulting in narrower and more symmetric peaks [39]. In HILIC, ACN is used as the weaker elutropic solvent in combination with an

aqueous buffer. Therefore, in contrast with RPLC, increasing the percentage of organic modifier in the mobile phase will increase analyte retention.

Other organic solvents have been considered as an alternative in order to tune the retention, selectivity, solubility and/or to decrease solvent consumption during times of ACN shortage, such as polar aprotic solvents (e.g., tetrahydrofuran (THF) and acetone) and polar protic solvents (e.g., IPA, MeOH, and EtOH) [39]. However, ACN is by far the most commonly used solvent in HILIC.

In metabolomics, the water content in HILIC typically ranges from 3 to 40%. A minimum of 2% water is always required in the mobile phase to allow the formation of the partially-immobilized water layer on the surface of the stationary phase. Higher water contents may cause a reduction or even prevent the retention of polar solutes. In specific cases,

a higher water content is needed to elute the highly polar compounds using gradients going as high as 90–95% water/buffer. However, such high-water contents cause the disruption of the water layer and, thus, the partitioning mechanism. When using such high concentration of water and running gradients starting at low water content (e.g., 3–5%), longer re-equilibration time (i.e., more than 20 column volumes) may be needed to restore the water layer prior to the next injection [42].

**2.1.3.2. Buffer salts, concentration and pH.** A variety of buffer salts may be used in HILIC, but the buffer must be soluble in high organic solvent-containing eluents. Ammonium formate (AF) and ammonium acetate (AmAc) are the most commonly used salts in metabolomics studies using HILIC. These buffers have a buffering capacity at the low pH range (i.e., pH of 3.8–5.8 for AmAc and 2.7–4.7 for AF, respectively), have a good solubility in high ACN-containing eluents and are volatile, which allows mass spectrometric and charged aerosol detection.

The choice between an AF and AmAc may influence the peak shape and depends on the physico-chemical properties of the targeted analytes. For example, Du et al. [43] showed the differences obtained for the analysis of nucleobases, nucleosides and nucleotides with an 0.8% acetic acid and 10 mM AmAc buffer compared with an 0.1% formic acid and 10 mM FA buffer. The latter buffer composition led to the formation of broad and split peaks for xanthosine and inosine, which was not observed with the former buffer. The authors hypothesized that this might be due to the gradual replacement of ACN by the aqueous buffer in gradient elution, causing analytes to partially ionize which changes the elution profile.

The concentration of salts in HILIC mobile phases changes the thickness of the water layer, which influences the hydrophilic partitioning and retention of compounds. More salt ions in the water layer causes the volume and hydrophilicity of this layer to increase or may contribute to shielding electrostatic attractions/repulsions, leading to a change in the retention of the analytes [44]. For example, when electrostatic interactions are prevalent, increasing the salt concentration may result in a decreased retention of anions on a column with strong cationic properties, such as an aminopropyl column, or weak cationic properties, such as the phosphorylcholine column, respectively, by shielding electrostatic attractions between the analyte and the stationary phase. Conversely, an increase in the salt concentration may increase the retention of anions on a column with anionic properties (e.g., bare silica) or a column with weak anionic properties, such as a sulfobetaine column, by shielding electrostatic repulsion instead [29,45].

Extra care should be taken when salts are used to improve the separation by tuning the retention to ensure reproducible results. The reproducibility in retention times in HILIC is challenging due to the occurrence of slight differences in the mobile phase composition over time (e.g., pH and buffer concentration). Such differences may arise from variations in buffer preparation, the evaporation of volatile salts, alterations in the pumping system over time, or the transfer of the method to other systems (which is often part of the validation of clinical methods). Moreover, retention time reproducibility is also challenging due to the limited solubility of salts in the presence of organic solvents which can lead to precipitation [39]. Salt concentrations generally vary between 0 and 50 mM. Some applications make use of a salt gradient by gradually increasing the content of the buffer in the mobile phase. When using a salt gradient, the water content in the mobile phase should be adjusted accordingly to ensure the solvation of the salt. For example, a higher concentration of salts require more water for sufficient solvation. Conversely, it may be necessary to keep the salt concentration in the mobile phase constant during separation. In order to do so, the mobile phase should contain a low percentage of water (ca. 5%) in the organic solvent and a low percentage of organic solvent in the buffer to completely solubilise the salts in the organic solvent. This ensures a constant concentration of salts throughout the run. For example, mobile phase A should contain 95% ACN and 5% buffer and mobile phase B

should contain 95% buffer and 5% ACN.

The pH of the mobile phase and the pKa of both the analyte and the stationary phase are crucial for the separation mechanism in HILIC. Therefore, buffer with a suitable and reproducible pH value should be used in the mobile phase. However, the apparent pH of the mobile phase may strongly vary after addition of an organic solvent in isocratic elution or during gradient elution. For this reason, it is difficult to predict the pH of the mobile phase. It is thus recommended to test multiple pH values during method development to achieve the desired separation. Most applications reported the screening of pH values of approx. 3.0, 4.5 and 6.0 during method development [31,46]. If a column allows for a higher pH value, such as the frequently used BEH amide column, a higher pH value up to pH 11 may be used. For example, Contrepolis et al. [46] tested five columns with different chemistries at three different pH values, i.e., i) acidic (pH 3.4), ii) neutral (pH 6.9), and iii) basic (pH 10.15). Various metabolic classes, such as organic acids, amino acids, nucleosides, and sugars, were used to assess the performance based on the retention time, peak shape, and MS signal intensity. The results, illustrated in Fig. 3, show that the best performance for the analysis of 43 model compounds was achieved with a sulfobetaine (ZIC-HILIC) column and a neutral pH value in the buffer.

#### 2.1.4. Mobile phase additives

The addition of organic acids such as 0.1–0.2% formic acid (FA) and 0.8% acetic acid (AcOH) to the mobile phase have been observed in a limited number of applications [13,47]. These acids are added instead of salt buffers to reduce ion suppression in MS. However, they may lead to poor peak shapes of some ionogenic solutes, such as acids and bases [48,49]. Moreover, the pH of these solutions is not buffered and susceptible to changes in the pH over the time, which results in poor retention time repeatability. Alternative mobile phase additives, such as trifluoroacetic acid (TFA), methane sulfonic acid (MSA), and phosphate have recently been investigated for their influence on the selectivity of the separation and their capability to improve peak shapes in HILIC. For example, phosphate showed to improve the peak shape of compounds that were negatively affected by strong electrostatic interactions. Adding 20 mM phosphate shielded the electrostatic interactions between the analytes and a ZIC-pHILIC stationary phase and expanded the metabolome coverage [50]. TFA and MSA showed to be useful in shielding electrostatic interactions of silanol groups on silica and amide columns. Using TFA results in anion exchange properties, which contrasts the cation exchange effects typically occurring when using ammonium salt buffers. MSA showed to results in cation exchange properties instead and has a different selectivity compared to ammonium salt buffers. The difference in selectivity may be useful for manipulating the retention [51]. However, the presence of TFA in the mobile phase is expected to lead to severe ion suppression during the analysis of metabolites, and should therefore be avoided or used with precautions.

#### 2.2. Proteomics

Similar to metabolites, proteins are polar species, typically having good solubility in water and, therefore, a class of analytes that can be successfully analyzed by HILIC. The polarity and chemophysical properties of proteins are determined by their amino acid (AA) composition (e.g., type, length, order, etc.), their PTMs, and the protein higher order organization. However, as a high proportion of ACN is used in the solvent, proteins are typically analyzed under denaturing conditions. Therefore, the protein higher-order organization is generally not contributing to the separation. Instead, the AA composition and the presence of PTMs are important to determine the protein or peptide retention. In particular, the most common PTMs, such as acetylation, glycosylation, phosphorylation, deamidation and methylation, can alter the local and overall charge as well as polarity of a protein. Therefore, HILIC can often resolve peptides or proteins with the same AA composition but presenting different PTMs (vide infra).

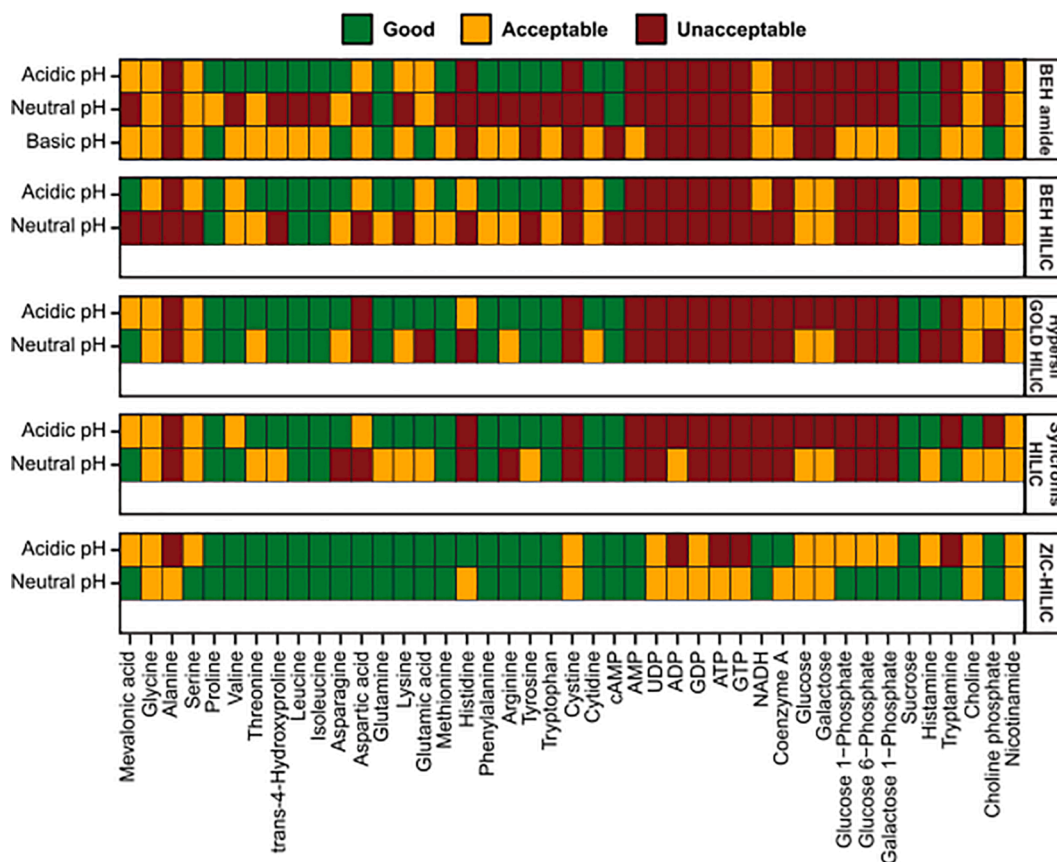


**Fig. 3.** Individual scores of the analysed metabolites from different classes. Experimental conditions obtained a good score in the following conditions: i) retention on the column to avoid ion suppression in the void volume zone; ii) have a narrow elution profile to provide optimal sensitivity and facilitate accurate peak integration; and iii) have an intense MS signal to be accurately extracted, aligned, quantified, and identified. If one of these parameters was not fulfilled, the score was acceptable. When multiple parameters could not be fulfilled, the score was considered unacceptable. Reproduced from Contrepois et al. [46] with permissions.

In proteomics, protein-containing samples are typically purified to filter protein components, which are subsequently analyzed either at the peptide level (i.e., bottom-up proteomics, using proteinases like trypsin),

at the subunit/large peptide level (i.e., middle-up or middle-down approaches) or as intact proteins (i.e., top-down proteomics). HILIC has been used in all these approaches, demonstrating alternative selectivity

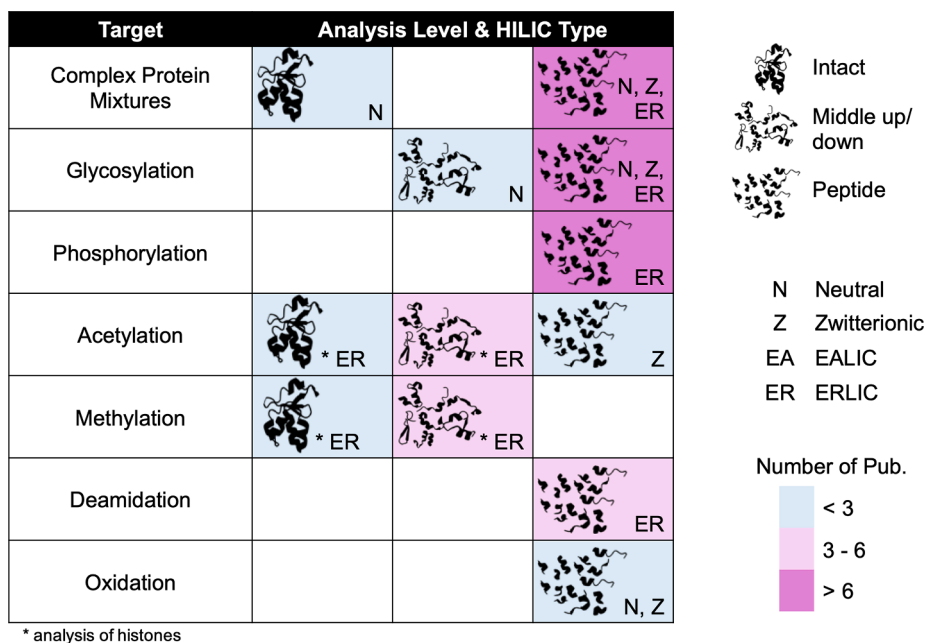


**Fig. 4.** Schematic representation of the different application areas of HILIC in proteomics, including direct HILIC-MS, 2D-LC and protein enrichment approaches. The literature discussed is reported in Table 3 and covers research articles from 2011 and June 2021 and is discussed further in Section 3.

compared with RPLC, satisfactory peak capacity and adequate MS compatibility.

Figure 4 shows an overview of the applications of HILIC in proteomics analysis covered in this review, classifying them according to the different protein level and the type of HILIC separation adopted.

### 2.2.1. Electrostatic attraction chromatography and electrostatic repulsion interaction chromatography

The chemistry of the stationary phase used in HILIC is important to determine the type and strength of interactions between proteins or peptides in the sample and the stationary phase [52]. Silica particles with chemically modified polar surfaces, either neutral or charged phases, are mostly used (Table 1). The neutral stationary phases mostly used for proteomics analysis use chemical selectors based on diol or amide. These phases, which exhibit low degree of ion-exchange interaction and resolve species mostly on the basis of their polarity, are typically used in proteomics for the analysis of complex peptides mixtures (e.g., cell lysate digest), intact proteins, as well as for the enrichment of glycopeptides.

When using charged stationary phases, similar to the analysis of metabolites, electrostatic attraction and repulsion play an important role in determining the retention of charge analytes. In particular, weak anion exchangers (WAX) and strong anion exchangers (SAX) have been used in the so-called electrostatic repulsion interaction chromatography (ERLIC) approach [53] for the separation or enrichment of modified peptides, such as phosphopeptides, deamidated peptides and glycopeptides.

Figure 5 shows two chromatograms from the work of Alpert that highlight in detail the use of electrostatic interactions in HILIC of peptides [53]. In Fig. 5A, a neutral stationary phase and a WAX stationary phase are used for the HILIC and ERLIC isocratic separation of 20 peptide standards, respectively, which showed different AA composition while some of them were phosphorylated. When using a neutral stationary phase (polyhydroxyethyl) and a mobile phase at pH of 2, the acidic peptides are eluting close to the void volume, while basic peptides are the most retained. Indeed, carboxylic acids (from Asp and Glu amino acids residues) are deprotonated and the basic groups have positive charges under acidic conditions. In ERLIC, however, the pH and buffer concentration are maintained constant over the run and the ACN content is increased. These conditions result in a decreased retention of basic

peptides due to repulsion with the stationary phase and an increased retention of the acidic peptides due to a decrease of the elution strength of the mobile phase. Fig. 5B illustrates the proposed interaction between the stationary phase and different peptide types. An exception to this mechanism is observed during the analysis of peptides containing groups that have negative charge at low pH, such as phosphate groups (pKa ~2.1), sialyl groups (pKa ~2.6) and isoaspartyl groups (pKa ~3.1; resulting from the deamidation of Asn). These groups confer electrostatic attraction in addition to the hydrophilic interaction. Therefore, peptides containing these groups may be pulled away from the rest of the peptide structure in a complex mixture, such as a protein digest, and can thus be used to enrich specific PTMs. The peculiar mixed-mode retention mechanism of ERLIC has been used in numerous studies as a fractionation approach to study specific portions of the proteome (e.g., phospho- and glyco-peptides [54]) as well as for the direct analysis of complex cell lysates [55].

Using the opposite electrostatic force (attraction), cation exchangers (WCX or SCX) have been used in the specific HILIC mode termed electrostatic attraction interaction chromatography (EALIC). EALIC has been mostly performed using cation anion exchangers in HILIC of acetylated and methylated proteins (in particular histones as in top-down [56] or middle-down [57] analysis).

### 2.2.2. Injection solvent composition and volume

In proteomics, injection solvent mixtures comprising 2 to 50% water (v/v) are often used to ensure for the complete dissolution of peptides, proteins subunits and intact proteins, while percentages between 2 and 5% are typically used in RPLC-MS. Similar to metabolomics, the direct injection of high percentages of water in HILIC leads to peak distortion and/or analyte breakthrough. This effect is more prominent for large injection volumes (i.e., more than 10% of column volume). Kozlik et al. described the effect of the injection solvent composition on the analysis of a glycopeptide of hemopexin using low flow HILIC-MS. The injection of 500 nL sample in 60% ACN (v/v) on a 75  $\mu\text{m}$   $\times$  150 mm column (ca. 100 % of column volume) resulted in the splitting of the glycopeptide peak [58]. The splitting could be circumvented by injecting samples in 80% ACN (v/v). Such ACN-rich solvent might work for (glyco)peptides, but this is often not possible for hydrophilic peptides. Indeed, high ACN percentages in the solvent may result in protein denaturation and precipitation, especially when keeping samples over a prolonged time (e.g.,

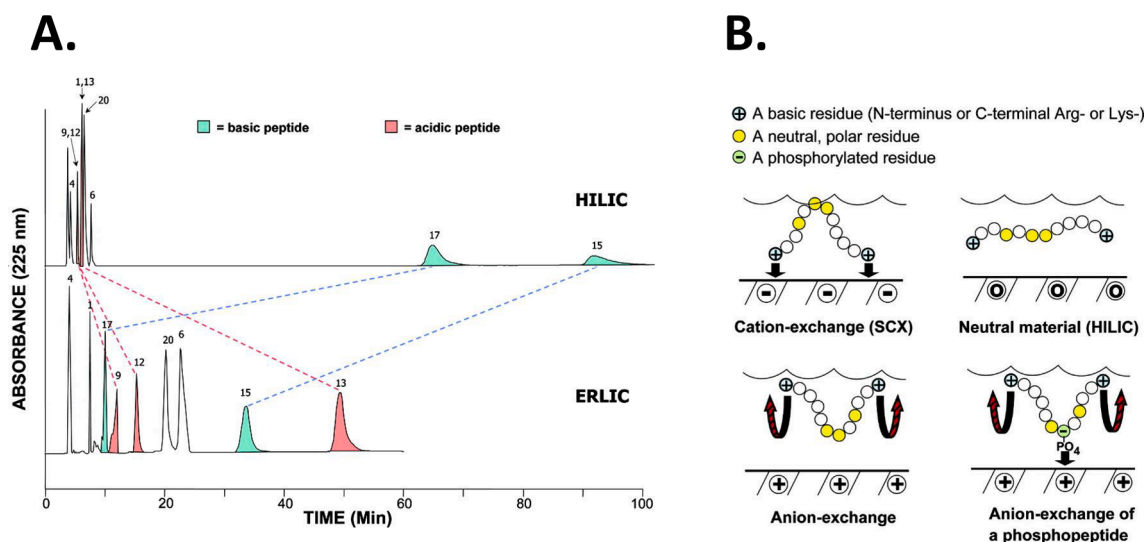


Fig. 5. A. HILIC vs ERLIC separation of acidic and basic reference peptides. HILIC mode (top panel): column: Polyhydroxyethyl A., mobile phase: 20 mM Na-MePO<sub>4</sub>, pH 2.0, with 63% ACN, flow rate: 1.0 mL/min. ERLIC mode (bottom panel): column: PolyWAX LP, mobile phase: 20 mM Na-MePO<sub>4</sub>, pH 2.0, with 70% ACN, flow rate: 1.0 mL/min. B. Hypothetical orientation of tryptic peptides on various stationary phases. The basic termini are attracted in cation exchange and repelled in anion exchange. Adapted from Alpert [53] with permissions (This is an unofficial adaptation of an article that appeared in an ACS publication. ACS has not endorsed the content of this adaptation or the context of its use).



1–2 days). Therefore, samples containing intact proteins are commonly dissolved in 80–90% water (v/v). As demonstrated by Gargano et al. with the analysis of several reference proteins using an amide HILIC column, a fraction of proteins elutes unretained when using an injection solvent of 90% water, indicating the presence of breakthroughs [59]. Analyte breakthroughs can be circumvented by injecting small sample volumes (i.e., below 1% of the column volume). Another way to avoid injection of too large volumes of strong solvent is to use a precolumn for trapping protein from highly aqueous samples. In this approach, a switching-valve setup is used to first concentrate the protein(s) on a small hydrophobic (e.g., C4) trap column using RPLC mobile phases (e.g., 5% ACN, 0.1% TFA). Subsequently, the trap column is online switched with the analytical column and the proteins are desorbed using the largely organic HILIC mobile phase. The analyte proteins can thus be dissolved in high percentages of water (e.g., 95%); after desorption from the RPLC trap column with weak HILIC solvent, the proteins are focused on the HILIC column prior to the actual separation [59]. This approach allows large sample volumes to be loaded, while actually resulting in minimal volumes injected onto the HILIC column. As this approach is accompanied by a significant preconcentration and reduction of injection volume, it is useful for analyzing low concentrations of glycoproteins using capillary HILIC-MS setups. This was recently demonstrated by Sénard et al. with the analysis of the Fc N-glycosylation of polyclonal IgGs from human blood [60].

### 2.2.3. Mobile phase composition and pH

In the analysis of peptides using HILIC and ERLIC-MS, the mobile phase often contains volatile salts and/or volatile acidic modifiers. In the selection of articles covered by this review, only two used salt systems regulated at pH higher than 4. In all other cases, the pH was kept low using either acidic modifiers solely (i.e., formic or acetic acid) or a combination of acids and salts (e.g., AmAc or AF with concentrations at ca. 10 mM). The pH of the buffer may influence the charge on the stationary phase and modify the charge state of peptides. In particular, low pH values reduce the ionization of carboxylic acids, favoring the ionization of basic peptides and therefore their retention, which is important to modulate the ion-exchange interactions as well as favor electrospray ionization of the peptides.

Mobile phases containing negatively charged ion-pairing agents, such as TFA, are often used in HILIC and ERLIC analysis or for the enrichment of glycopeptides and subunits of intact glycoproteins. For these analytes, the shielding of positively charged protein sites by TFA ions is essential to ensure sufficient efficiency and selectivity, especially when analyzing glycoproteins and peptides. Periat et al. [61] demonstrated this with the analysis of intact RNase B using an amide stationary phase in combination with a mobile phase containing formic acid (0.5% v/v), AF (50 mM) and TFA (0.1% v/v). The use of formic acid and AF in the eluent resulted in late elution and poor resolution of the glycoforms of RNase B. Moreover, the combination of formic acid (0.1% v/v) and AmAc (100 mM) in the mobile phase did not provide glycoform separation [62]. However, when adding 0.1% v/v TFA to the eluent, the retention of intact RNase B significantly decreased and almost baseline resolution of its five main glycoforms was achieved. This could be attributed to the reduced overall hydrophilicity of the protein when binding with TFA molecules. This observation is in line with other reports [63] on glycopeptide separations, indicating that under ion-pairing conditions, the retention and glycoform resolution of glycoproteins on a HILIC column is primarily driven by the glycan composition of the protein.

Both the pH and ionic strength are important for ERLIC enrichment of phosphopeptides or simultaneous enrichment of glyco- and phosphopeptides, where the type and concentration of salt additive are crucial to achieve efficient enrichment. In particular, buffers having well-hydrated cations, such as  $Mg^{2+}$ , and poorly hydrated anions, such as trifluoroacetate anion, increase the retention and selectivity for glyco- and phosphopeptides by several folds [64–66]. Under these conditions,

the well-hydrated  $Mg^{2+}$  cation helps enhancing the retention of phosphate, sialyl and isospartyl groups, while the trifluoroacetate anion reduces the unspecific retention of the basic amino acids.

## 3. Applications of HILIC

### 3.1. Metabolomics

HILIC has been increasingly used in untargeted and targeted metabolomics over the last years, expanding the metabolome coverage to metabolites classes that are not trivially analysed using RPLC-MS, such as amino acids and small organic acids [11]. In targeted clinical metabolomics, specific metabolite classes have gained an increasing interest due to their roles in multiple (patho)physiological processes, namely, bioactive lipids, nucleosides/nucleotides, and small organic acids, which will be discussed in the following sections.

#### 3.1.1. Bioactive lipids

Lipidomics is a sub-discipline of metabolomics focusing on the comprehensive analysis of lipids in biological fluids to study their structure and function, as well as their involvement in (patho)physiological processes [67]. Almost 70% of the plasma metabolome consists of lipids [68]. Lipids are not only involved in the formation of lipid bilayers in cell membrane structure or in energy storage, but also in signalling and regulation. Among all lipid classes, the so-called bioactive lipids are endogenous soluble mediators secreted by all cells involved in inflammatory processes and essential in multiple immune processes, due to their pivotal role in triggering, coordinating, and confining inflammatory mechanisms [69]. Moreover, bioactive lipids play a significant role in the transition from acute to chronic inflammation. They have been already linked to several chronic diseases, including atherosclerosis, diabetes, cancer, rheumatoid arthritis, inflammatory bowel disease, and multiple sclerosis [69]. The potential (patho)physiological roles played by some of these metabolites also remain unknown or not investigated yet [70].

Bioactive lipids are typically divided into four main sub-classes, i.e., eicosanoids, specialized pro-resolving lipid mediators (SPM), lysoglycerophospholipids, sphingolipids, and endocannabinoids (ECs). They are all generated from  $\omega$ -6 or  $\omega$ -3 polyunsaturated fatty acids precursors. The analysis of bioactive lipids in biosamples poses several challenges, such as (i) the large dynamic range of endogenous concentrations, e.g., very low concentrations for ECs and SPM vs. high concentrations for phospholipids, (ii) the presence of multiple isomers, which show similar physico-chemical properties but very different biological activity (e.g., the leukotriene LTB4 and its isomer 5S,12S-di-HETE) [71], (iii) the number of analytes targeted within this class, and (iv) the possible degradation of such compounds during the (pre-)analytical workflow, as observed for the EC 2-arachidonoyl glycerol (2-AG) that undergoes spontaneous isomerization to the biological inactive 1-AG during analysis [72].

Bioactive lipids and lipids in general are typically analysed using direct infusion MS or RPLC. Over the last years, both HILIC and SFC have shown their usefulness in bringing an orthogonal separation selectivity, which may be beneficial in both the identification and quantitation of lipids. HILIC enables the separation of the different lipid classes based on their polar head and charge, while RPLC leads to the separation of the different lipids within one class based on their hydrophobic tail.

Table 2 lists a selection of the recent applications of the analysis of bioactive lipids in different biosamples using HILIC-MS. The large majority of the applications reviewed did not focus on bioactive lipids solely but lipids in general, showing the relevance of using HILIC for the separation of polar lipid classes. An interesting example comes from the group of Holčapek and co-workers who compared ultrahigh-performance supercritical fluid chromatography-MS (UHPSFC-MS) with HILIC-UHPLC-MS for the analysis of different lipid classes, including mono-, di-, and triglycerides, ceramides, sphingomyelins,



**Table 2**  
Selected applications of HILIC for the analysis of bioactive lipids, amino acids, organic acids and nucleosides/nucleotides.

Sample matrix	Analytes	Sample preparation	Injection solvent/volume	Stationary phase	Mobile phase	Gradient conditions	LC-MS analysis	Ref., year
Human plasma	15 polar and non-polar lipid classes	LLE	ACN: 40 mM ammonium formate (pH = 4.0) 95:5, v/v), 2 µL	Acquity BEH Amide (100 × 2.1 mm, 1.7 µm); Waters.	A: 40 mM AF (pH = 4.0). B: 100% ACN	0–2.0 min. 96% B, 2.0–7.0 min. 96–70% B, 7.0–7.5 min. 70% B, 7.5–15.0 min. 96% B (at 0.25 mL/min.).	2D-LC UHPLC-MS	[20], 2018
				Acquity HSS T3 C <sub>18</sub> (150 × 2.1 mm, 1.8 µm); Waters	A: ACN/H <sub>2</sub> O (3:2, v/v) B: IPA/ACN (9:1, v/v) (both containing 0.1% FA and 10 mM AF)	0–4.5 min. 70% B, 4.5–6.0 min. 70–100% B, 6.0–9.0 min. 100% B, 9.0–15.0 min. 30% B		
Human plasma and porcine brain	7 lipid classes in human plasma and 10 in porcine brain	LLE	CHCl <sub>3</sub> /IPA (1:2, v/v), 1 µL	Acquity UHPLC BEH C <sub>18</sub> column (150 mm × 1 mm, 1.7 µm); Waters	A: 5 mM AmAc B: 99.5% ACN:IPA (1:2, v/v) and 0.5% 5 mM AmAc	0–150 min. 78.5–100% B (at 0.02 mL/min.)	2D-LCUHPLC-QTOF	[67], 2015
Kidney tissue	7 polar lipid classes	LLE	MeOH/H <sub>2</sub> O/ CHCl <sub>3</sub> (30:15:5; v/v), 0.5 µL	Core-shell silica CORTECS HILIC column (50 mm × 3 mm, 2.7 µm); Waters	A: 5 mM AmAc B: ACN	0–0.7 min. 92–80% B, 0.7–1.0 min. 80–92% B (at 5 mL/min.)	HPLC-QTOF	[181], 2018
				Ascentis Si column (150 × 2.1, 3.0 µm); Sigma-Aldrich	A: ACN B: 10 mM AmAc	0–10 min. 95–78% A (at 0.3 mL/min.)		
Human plasma and serum	8 polar and non-polar lipid classes	LLE	CHCl <sub>3</sub> /MeOH (1:1, v/v), 1 µL	Viridis BEH silica (100 × 3.0 mm, 1.7 µm); Waters	A: ACN/H <sub>2</sub> O (96:4, v/v) B: ACN/H <sub>2</sub> O (2:98, v/v) (both containing 8 mM AmAc)	0–5 min. 100–84% A, 5.0–5.5 min. 84% A, 5.5–5.51 min. 84–100% A, 5.51–10.5 min 100% A (at 0.5 mL/min.)	UHPLC-QTOF	[73], 2020
Heart, kidney and liver tissue	Polar lipids	Polar and nonpolar monophasic preparations and biphasic preparations	ACN:MeOH:H <sub>2</sub> O (1.5:1.5:1, v/v/v), injection volume unknown	Accucore 150-Amide-HILIC column (100 × 2.1 mm, 2.6 µm); Thermo Fisher Scientific	A: ACN:10 mM AF (95:5, v/v) + 0.1% FA B: ACN:10 mM AF (50:50, v/v) + 0.1% FA	0–1.0 min. 1% B, 1.0–3.0 min. 1–15% B, 3.0–6.0 min. 15–50% B, 6.0–9.0 min 50–95% B, 9.0–10.0 min 95% B, 10.0–10.5 min. 95–1% B, 10.5–14.0 min. 1% B (at 0.5 mL/min.)	UHPLC-Q-Orbitrap	[182], 2021
Human serum	Bioactive lipids, amino acids, organic acids	PP and LLE	ACN, 1 µL	Acquity BEH Amide column (100 × 2.1 mm, 1.7 µm); Waters	A: ACN B: H <sub>2</sub> O Both containing 0.1% FA and 10 mM AmAc	0–1.0 min. 95% A, 1.0–7.0 min. 95–50% A, 7.0–9.0 min. 50% A, 9.0–9.1 min. 50–95% A, 9.1–13.0 min. 95% A (at 0.3 mL/min.)	UHPLC-Q-Orbitrap	[183], 2020
Human blood and dog liver samples	Anandamide, arachidonic acid, ethanolamine	PP	1 µL	ZIC-HILIC (sulfobetaine) column (100 × 2.1 mm i.d., 3.5 µm) from Merck.	A: ACN B: 25 mM ammonium formate in water with 0.1% FA (w/v)	Isocratic elution at 0.2 mL/min	HPLC-QqQ	[76], 2012
Human plasma	36 amino acids	PP	Mobile Phase A, 2 µL	Acquity BEH Amide column (2.1 × 100 mm, 1.7 µm); Waters	A: ACN/10 mM AmF (85:15, v/v) B: H <sub>2</sub> O/10 mM AmF (85:15, v/v) pH 3.0(both containing 0.15% FA)	0–6 min. 100% A, 6.0–6.1 min. 94.1% A, 6.1–10.0 min. 94.1–82.4%, 10.0–12.0 min. 82.4–70.6%, 12–18 min. 70.6–100% A (at 0.4 mL/min.)	UHPLC-QqQ	[78], 2016
Human plasma	14 amino acids	PP	Mobile phase B, 5 µL	Acquity BEH Amide column (2.1 × 100 mm, 1.7 µm); Waters	A: 10 mM AF (pH 3.25) B: ACN/10 mM AF (80:20, v/v) (pH 3.25)	0–0.5 min. 100% B, 0.5–8.0 min. 100–60% B, 8.0–9.0 min. 60% B, 9.0–9.1 min. 60–100% B,	UHPLC-QqQ	[184], 2018

(continued on next page)

Table 2 (continued)

Sample matrix	Analytes	Sample preparation	Injection solvent/volume	Stationary phase	Mobile phase	Gradient conditions	LC-MS analysis	Ref., year
Human gastric cancer cell line MGC803	24 amino acids	PP	ACN/H <sub>2</sub> O (75:25, v/v), 4 µL	Acquity BEH Amide column (2.1 mm × 100 mm, 1.7 µm); Waters	A: 10 mM AmAc (pH 3.5) B: ACN	9.1–15.0 min. 100% B (at 0.3 mL/min.) 0.1–3.0 min. 75–40% B, 3.0–3.5 min. 40–75% B, 3.5–8.0 min. 75% B (at 0.2 mL/min.)	UHPLC-Q-IT	[185], 2019
Rat plasma and urine	19 amino acids	PP	Plasma/H <sub>2</sub> O/ACN (1:4:25, v/v/v) Urine/ACN (5:25, v/v), 10 µL	Acquity BEH Amide column (100 × 2.1 mm, 1.7 µm); Waters	A: Water + 0.2% FAB: ACN + 0.2% FA	0.1–4.5 min. 10–26% A, 4.5–5.5 min. 26–45% A, 5.5–6.5 min. 45% A, 6.5–10.0 min. 45–10% A (at 0.2 mL/min.)	UHPLC-QqQ	[47], 2019
Human tears	15 amino acids	PP + SPE	H <sub>2</sub> O + 0.2% FA, 5 µL	Acquity BEH Amide column (100 × 2.1 mm, 1.7 µm); Waters	A: ACN/H <sub>2</sub> O (50:50, v/v) B: ACN/MeOH/H <sub>2</sub> O (95:5:5, v/v/v) Both containing 8 mM AF and 0.2% FA	0–1.0 min. 90% B, 1.0–3.0 min. 90–30% B, 3.0–4.0 min. 30–60% B, 4.0–5.5 min. 60–95% B, 5.5–6.5 95% B, 6.5–8.0 min. 95–90% B (at 0.4 mL/min.)	UHPLC-Q-Orbitrap	[186], 2019
Breast cancer cells	40 amino acids	PP	Supernatant of ACN/MeOH (50:50, v/v) containing 0.2% FA and IS, 10 µL	Acquity BEH Amide column (100 × 2.1 mm, 1.7 µm); Waters	A: H <sub>2</sub> O/ACN (95:5, v/v) B: H <sub>2</sub> O/ACN (5:95, v/v) Both containing 0.2% FA and 5 mM AmAc (pH 2.78)	0–6.0 min. 98–60% B, 6.0–7.6 min. 60% B, 7.6–7.7 min. 60–98% B, 7.7–10.0 min. 98% B (at 0.4 mL/min.)	UHPLC-QqQ	[79], 2020
Whole blood	24 amino acids	Volumetric absorptive microsampling,	H <sub>2</sub> O, 2 µL	Acquity BEH Amide column (100 × 2.1 mm, 1.7 µm); Waters	A: 10 mM AF B: (ACN:100 mM AF (9:1, v/v) both containing 0.15% FA	0.0–3.0 min. 95% B; 3.0–6.0 min. 95–85% B; 6.0–7.0 min. 85–65% B; 7.0–8.5 min. 65% B. In-between runs the column was re-equilibrated at 95% B for 4 min.	UHPLC-QqQ	[187], 2019
Human plasma	26 organic acids	PP	ACN:H <sub>2</sub> O (5:1, v/v) containing 0.1% FA and IS, 10 µL	SeQuant ZIC-HILIC column (50 × 4.6 mm, 5 µm); Merck	A: H <sub>2</sub> O + 0.1% FA B: ACN + 0.1% FA	0–3.0 min. 90% B, 3.0–6.0 min. 90–20% B, 6.0–8.0 min. 20–5% B, 8.0–12.0 min. 5–90% B (at 0.3 mL/min.)	HPLC-QqQ	[13], 2020
Human urine	4 organic acids	PP	Mobile phase, 10 µL	SeQuant ZIC-HILIC column (250 × 4.6 mm, 3 µm); Merck	H <sub>2</sub> O:ACN (45:55, v/v) both containing 25 mM FA	Isocratic at a flow rate of 0.8 mL/min. Analysis time: 6 min.	HPLC-IT	[188], 2019
Exhaled breath condensate	Lactate	Dilution with mobile phase	Mobile phase, 10 µL	XBridge BEH Amide column (2.1 × 150 mm, 3.5 µm); Waters	A: ACN:10 mM AmAc pH 9.0 (50:50, v/v) B: ACN:10 mM AmAc pH 9.0 (50:50, v/v)	Isocratic; A:B (55:45, v/v) at a flow rate of 0.5 mL/min. Analysis time: 4 min.	HPLC-Q-IT	[17], 2017
Neonatal urine	organic acids	Dilution with mobile phase	Mobile phase, 2 µL	SeQuant ZIC-HILIC column (250 × 4.6 mm, 3 µm); Merck	ACN: H <sub>2</sub> O (55:45, v/v) containing 25 mM FA	Isocratic at a flow rate of 0.8 mL/min. Analysis time: 6 min.	HPLC-IT	[188], 2019
Rat urine	organic acids	PP	H <sub>2</sub> O/MeOH/ACN (40:5:55, v/v/v), 10 µL	SeQuant ZIC-HILIC column (250 mm × 4.6 mm, 5 µm); Merck	A: ACN B: 10 mM AmAc	Isocratic; A:B (70:30, v/v) at a flow rate of 0.5 mL/min. Analysis time: 14 min.	HPLC-QqQ	
Rat plasma	19 nucleobases and nucleosides	PP	Mobile phase B, 10 µL	XBridge Amide column (150 mm × 2.1 mm, 3.5 µm); Waters	A: H <sub>2</sub> O/ACN (50:50, v/v) B: H <sub>2</sub> O/ACN (5:95, v/v) Both containing 0.8% AcOH and 10 mM AmAc	0–10.0 min. 0% A, 10.0–15.0 min. 0–40% A, 15.0–18.0 min. 40–57% A, 18.0–19.0 min. 57–95% A (at 0.3 mL/min.) re-equilibration not reported.	HPLC-QqQ	[43], 2017

(continued on next page)

Table 2 (continued)

Sample matrix	Analytes	Sample preparation	Injection solvent/volume	Stationary phase	Mobile phase	Gradient conditions	LC-MS analysis	Ref., year
Human and rat urine	methylated nucleosides and nucleobases	PP	ACN, 5 $\mu$ L	SeQuant® ZIC®-HILIC column (50 mm $\times$ 2.1 mm, 5 $\mu$ m); Merck	A: 20 mM AmAc B: ACN + 0.2% FA	0.0–1.0 min. 95% B, 1.0–7.0 min. 95–50% B; 7.0–8.0 min. 50% B, 8.0–9.0 min. 50–95% B, 9.0–15.0 min. 95% B (at 0.5 mL/min.)	HPLC-QqQ-IT	[81], 2019
Calf thymus tissue	5 nucleobases and 1 methylated nucleobase	DNA extraction	ACN, 20 $\mu$ L	Diol (150 $\times$ 4.6 mm, 3 $\mu$ m); ProntoSIL Spherisorb s5 CN (250 $\times$ 4.6 mm, 5 $\mu$ m); Waters	A: 25 mM AmAc, pH 4.1 B: ACN	0–15.0 min. 2% A, 15.0–20.0 min. 5% A, 20.0–40.0 min. 5% A, 40.0–45.0 min. 30% A (at 0.5 mL/min.) re-equilibration not reported.	HPLC-DAD	[189], 2018
Human plasma	nucleotides and nucleosides	PP	ACN:MeOH:H <sub>2</sub> O (60:20:20, v/v) with 15 mM AmAc pH 9.7, 2 $\mu$ L	AdvanceBio MS Spent Media 2.1 $\times$ 100 mm, 2.7 $\mu$ m); Agilent	A: H <sub>2</sub> O:ACN (50:50, v/v) B: H <sub>2</sub> O:ACN (20:80, v/v), both with 15 mM AmAc adjusted to pH 9.7 with AH.	0.0–9.0 min. 10–65% A, 9.0–9.5 min 65–10% A, 9.5–14.0 min. (at 0.2 mL/min.)	UHPLC-QqQ	[190], 2020
Standards in H <sub>2</sub> O	nucleosides and nucleotides	Dilution of standards	ACN, 5 $\mu$ L	HILIC XBridge Amide (100 mm $\times$ 2.1 mm, 3.5 $\mu$ m); Waters	A: ACN 100 mM HFIP, 50 mM DEA w/w pH 9.0 – w/s pH 10.0 B: H <sub>2</sub> O, 100 mM HFIP, 50 mM DEA w/w pH 9.0	0–3.0 min. 82% B, fast gradient 82–78% B, 7 min. 78% B, back to initial conditions in 1 min. (at 0.35 mL/min.)	HPLC-QqQ	[82], 2015
RNA from various organisms	nucleosides	Digestion	ACN:20 mM trimethylamine-acetate (10:90, v/v), 23 $\mu$ L	ZIC-cHILIC column (150 mm $\times$ 2.1 mm, 3 $\mu$ m); Merck ZIC-cHILIC guard column (2.1 $\times$ 20 mm); Merck	A: 5 mM AmAc B: ACN	0–30.0 min. 90–40% B, 30.0–35.0 min. 40% B, 35–50 min. 40–90% B (at 0.1 mL/min.)	HPLC-QqQ- Orbitrap	[191], 2015
Feces	amino acids, amines, indole derivatives, fatty acids and carbohydrates	LLE	ACN/H <sub>2</sub> O (75:25, v/v), 1 $\mu$ L	Charge Modulated Hydroxyethyl Amide (zwitterionic) iHILIC-Fusion (100 $\times$ 2.1 mm, 1.8 $\mu$ m); Hilicon Acquity BEH Amide column (100 $\times$ 2.1 mm, 1.7 $\mu$ m); Waters CORTECS Solid Core (unbonded silica) HILIC Column (100 $\times$ 2.1 mm, 1.6 $\mu$ m); Waters	A: 5 mM AmAc/ACN (5:95, v/v) B: 5, 10 or 25 mM AmAc/ACN (95:5, v/v/v) Both A and B were prepared with pH 4.6, 6.8 and 9.0.	Pre-run time of 5 min. at 0.1% B, 0–2.0 min. 0.1% B, 2.0–9.5 min. 0.1–99.9% B, 9.5–12.0 min. 99.9% B, 12.0–12.1 min. 99.9–0.1% B (at 0.5 mL/min.)	UHPLC-Q-TOF	[31], 2019
Rat brain and serum	amino acids, neurotransmitters, purines, and pyrimidines	PP	ACN, 2 $\mu$ L	Acquity BEH Amide column (100 $\times$ 2.1 mm, 1.7 $\mu$ m); Waters Van Guard™ UHPLC BEH Amide pre-column (2.1 $\times$ 5 mm, 1.7 $\mu$ m); Waters	A: 20 Mm AF + 0.25% FA (pH 3.0) B: ACN:20 Mm AF (93:7, v/v) + 0.25% FA	0–2.6 min. 100% B, 2.7–4.0 min. 100–90% B, 4.1–6.5 min. 70% B (at 0.5 mL/min.)	UHPLC-QqQ	[77], 2016
Human urine	monosaccharides, organic acids, amino acids, quaternary ammonium compounds, and nucleic acids	PP	Urine/ACN/IS in H <sub>2</sub> O (15:80:5, v/v/v), 5 $\mu$ L	ZIC-HILIC column (150 mm $\times$ 2.1 mm, 3.5 $\mu$ m); SeQuant	A: 10 mM AF and FA B: ACN/10 mM AF and FA (95:5, v/v)	0–7.0 min. 20–30% A, 7.0–16.0 min. 30–50% A, 16.0–17.0 min. 50–20% A, 17.0–20.0 min. 20% A (at 0.25 mL/min.)	UHPLC-Q-IT	[19], 2019
Rat urine and feces	amino acids, organic acids, carbohydrates, and vitamins.	PP	Urine, diluted with ACN (1:3, v/v) Fecal samples:1-propanol:H <sub>2</sub> O (50:50, v/v) in a ratio of 1:4 sample weight to solvent volume	Acquity BEH Amide column (100 $\times$ 2.1 mm, 1.7 $\mu$ m); Waters Van Guard™ UHPLC BEH	A: ACN:H <sub>2</sub> O (95:5, v/v) B: ACN:H <sub>2</sub> O (95:5, v/v) both containing 10 mM AF	Unknown	UHPLC-QqQ	[192], 2019

(continued on next page)

Table 2 (continued)

Sample matrix	Analytes	Sample preparation	Injection solvent/volume	Stationary phase	Mobile phase	Gradient conditions	LC-MS analysis	Ref., year
Human serum	bioactive lipids, amino acids, organic acids	PP and LLE	ACN, 1 $\mu$ L	Amide pre-column (2.1 $\times$ 5 mm, 1.7 $\mu$ m); Waters Acquity BEH Amide column (100 $\times$ 2.1 mm, 1.7 $\mu$ m); Waters	A: ACN B: H <sub>2</sub> O Both containing 0.1% FA and 10 mM AmAc	0–1.0 min. 95% A, 1.0–7.0 min. 95–50% A, 7.0–9.0 min. 50% A, 9.0–9.1 min. 50–95% A, 9.1–13.0 min. 95% A (at 0.3 mL/min.)	UHPLC-Q-Orbitrap	[183], 2020
Breast cancer tissue	organic acids, amino acids, purines, pyrimidines	PP and LLE	Mobile phase, 10 $\mu$ L	SeQuant ZIC-HILIC column (250 $\times$ 4.6 mm, 3 $\mu$ m); Merck	A: H <sub>2</sub> O + 0.1% FA B: ACN + 0.1% FA	0–3.0 min. 90% B, 3.0–6.0 min. 90–20% B, 6.0–8.0 min. 20–5% B, 8.0–12.0 min. 5–90% B (at 0.3 mL/min.)	HPLC-QqQ	[13], 2020
Rat serum	organic acids and amino acids	PP	ACN:H <sub>2</sub> O (7:3, v/v), 5 $\mu$ L	SeQuant ZIC-eHILIC column (2.1 mm $\times$ 150 mm, 3 $\mu$ m); Merck	A: 10 mM AmAc (pH 3.25) B: ACN	0–8.0 min. 95–85% B, 8.0–10.0 min. 85–81% B, 10.0–22.0 min. 81–60% B, 22.0–22.5 min. 60–95% B, 22.5–25.0 min. 95% B (at 0.25 mL/min.)	HPLC-Q-Orbitrap	[193], 2020
Human plasma	3 lipid classes, nucleosides, nucleobases, amino acids, and sugars	PP, LLE (biphasic solvent, MeOH/ACN/Acetone (1:1:1, v/v/v))	MeOH:H <sub>2</sub> O (1:1, v/v), 15 and 5 $\mu$ L for standards and plasma samples respectively	Atlantis Silica HILIC column (100 $\times$ 2.1 mm, 3.0 $\mu$ m); Waters.	A: 100% ACN B: 50 mM AF	0–20 min. 5–50% B, 20–30 min. 5% B (at 0.2 mL/min.)	HPLC-LTQ-FTMS	[194], 2016

phosphatidylcholines, lysophosphatidylcholines, and phosphatidylethanolamines [73,74]. Fig. 6 shows the typical separation observed using both approaches. As expected, HILIC-MS is not suited for the analysis of non-polar lipid classes (e.g., triglycerides) and species with one hydroxyl group (e.g., mono- and diglycerides), which elute in the void volume (Fig. 6A, green trace). However, the positional isomers of more polar lysophospholipids (e.g., lysophosphoglycerols, lysophosphocholines and lysophosphoethanolamines) were well resolved using HILIC-MS (Fig. 6A, red trace) [74].

As reviewed by Tang et al., HILIC is well suited for the analysis of (lyso)phospholipids [11]. However, little has been published in the analysis of the other bioactive lipid classes, i.e., ECs, eicosanoids and SPM using HILIC-MS. An interesting example of the relevance of HILIC for the analysis of eicosanoids comes from Roy et al., who developed a HILIC method combined with charged aerosol detection for the analysis of the prostaglandin PGI<sub>2</sub> (prostacyclin) [75]. Prostacyclin is an important prostaglandin with antiplatelet and vasodilatory properties. However, it rapidly degrades in vitro and even faster in vivo in human plasma, a process accelerated with high temperature and low pH. The authors suggested that HILIC may be more adequate for the analysis of prostacyclin than RPLC, due to the dissolution of samples in organic solvents rather than water. Three column chemistries were considered for the separation of prostacyclin and its main metabolites 6-keto-PGF1 $\alpha$ , i.e., a hybrid silica, zwitterionic, and amine phases, which all provided satisfactory results depending on the composition of the mobile phase. The optimized method was applied to a kinetic study of the degradation of prostacyclin in a solution of dichloromethane:methanol:acetonitrile 7:2:1, showing a steady decrease of the parent compounds and increase of the degradation product 6-keto-PGF1 $\alpha$ . However, the stability of prostacyclin during the entire workflow using the optimized method has not been compared with RPLC, which renders any conclusion difficult. Moreover, this is the only study found on the analysis of PGI<sub>2</sub> using HILIC, and, to a larger extent, the only one reporting the analysis of an eicosanoid using HILIC.

Rakers et al. developed an HILIC-MS method for the analysis of the ECs anandamide and its downstream products arachidonic acid and ethanolamine to study to activity of the enzyme fatty acid amid hydrolase, using a sulfobetaine stationary phase [76]. No other studies have been reported where HILIC has been used for the analysis of ECs. The conclusion is similar for research related to the analysis of SPMs, where no studies have been reported so far.

Overall, RPLC appears to remain the gold standard for the analysis of bioactive lipids. HILIC may certainly play a role to achieve a better selectivity for the analysis of the more polar bioactive lipids, including the (lyso)phosphatidylcholine and (lyso)phosphatidylethanolamine classes. Moreover, more information is needed on the relative stability of bioactive lipids (mostly eicosanoids and ECs) during RPLC vs. HILIC workflow, as illustrated with the study on prostacyclin. Indeed, the use of high amount of ACN in the injection solvent and the mobile phase in HILIC may lead to a better stability of analytes during the entire analytical workflow, especially those who are prone to rapid hydrolysis.

### 3.1.2. Amino acids

AAs are essential in many biochemical processes and serve as the building blocks of peptides and proteins. Moreover, they can be used as energy sources, play a crucial role as biosynthetic precursors of neurotransmitters, purines, and pyrimidines, or can act as neurotransmitters themselves [77,78]. The concentration of AAs in plasma depends on a dynamic and balanced metabolic state. Changes in the AA concentrations within this equilibrium can be used for the diagnosis and treatment of a wide variety of inborn errors of metabolism. Several studies have reported the role that AAs may play in different diseases, including cancer, hepatic and renal disorders, and neurodegenerative diseases. For example, N-acetyl AA derivatives, such as N-acetyl leucine and N-acetyl isoleucine, have been used as potential biomarkers in patients with diabetes [79]. Moreover, several neurodegenerative

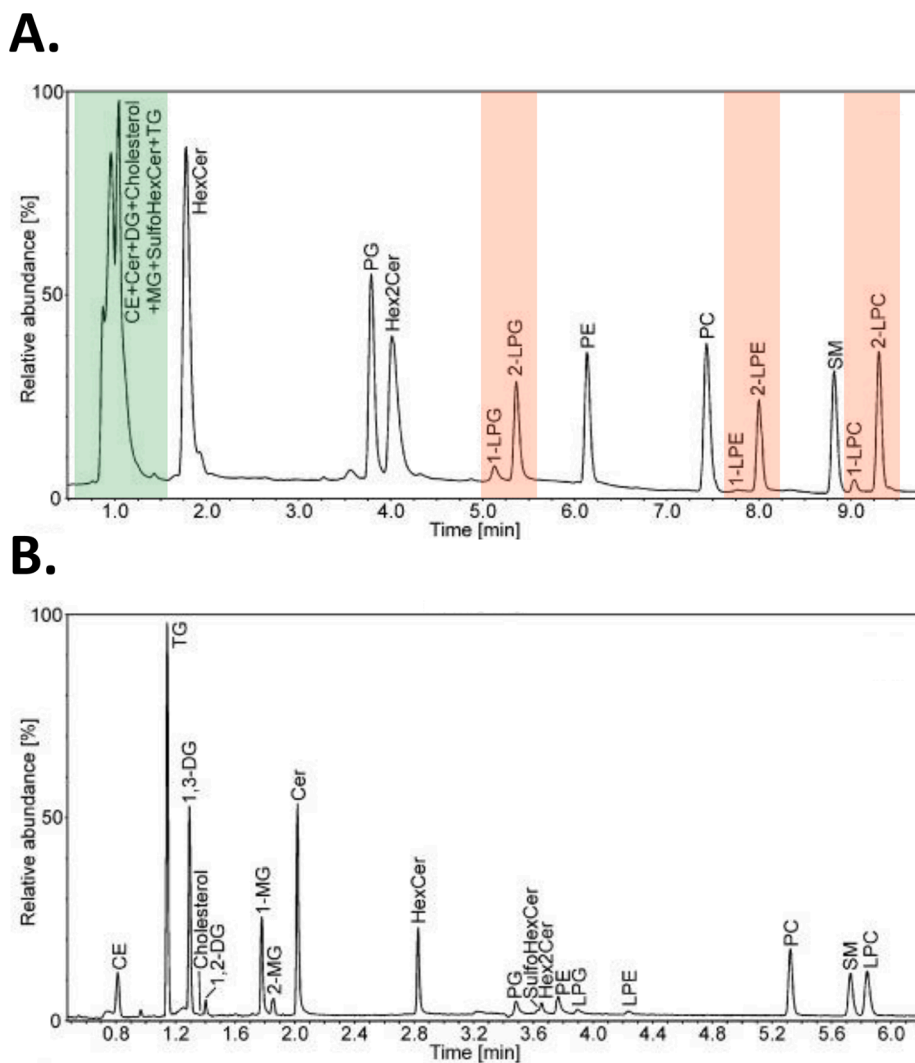


**Fig. 6.** Difference in selectivity for the analysis of lipid standards using A. HILIC-UHPLC-MS and B. Ultrahigh-performance supercritical fluid chromatography-MS (UHPSFC-MS). Non-polar lipid classes (e.g., triglycerides) and species with one hydroxyl group (e.g., mono- and diglycerides) elute in the void volume using HILIC-MS (green trace). However, the positional isomers of more polar lysophospholipids (e.g., lysophosphoglycerols, lysophosphocholines and lysophosphoethanolamines) are well resolved with HILIC-MS (red trace). Reproduced from ref. [74] with permissions. (For interpretation of the references to colour in this figure legend, the reader is referred to the web version of this article.)

diseases, including schizophrenia, Alzheimer's disease, and Parkinson's disease, involved altered levels of AAs and neurotransmitters [77].

AAs can be analysed using a large diversity of GC-MS and LC-MS/MS-based methods. Current strategies for AA analysis in LC include RPLC, IEX, NPLC, and HILIC [78]. A recent review by Violi et al. [78] investigated the advantages and disadvantages of these techniques for the analysis of AAs. Since most AAs have a high polarity and a low molecular weight, a derivatization step is frequently required in RPLC to improve separation and/or detection [40,78]. However, this procedure is often laborious and time consuming, making it less adequate for routine analysis in clinical applications [52]. On the other hand, HILIC allows for the analysis of AAs in their free (native) state, i.e., unbound from proteins or peptides and underivatized. Table 2 lists the recent metabolomics-based applications targeting AA analysis.

A review article from Periat et al. in 2015 reported that a baseline separation of the 20 natural amino acids allowing for accurate quantitation of AAs had not been published yet [52]. However, Prinsen et al. [78] published a year later a baseline separation of 36 underivatized AAs in human plasma within 18 min, including all 20 natural AAs and allowing for the baseline separation of leucine and *iso*-leucine. The developed method was validated, using UHPLC-MS to quantify all AAs except hydroxy-proline which could only be determined semi-quantitatively, using an Acquity BEH amide column (2.1 × 100 mm, 1.7 μm) coupled to a triple quadrupole. The LOD and LOQ ranged between (0.0002–0.11 μM) and (0.001–0.36 μM) respectively and

displayed excellent linearity. The CV were <7% for repeatability and <11% for reproducibility. Accuracy was between 78.8% and 121.8%. The reproducibility of hydroxy-proline was reported to be 16.7%, and therefore, labelled threonine was used for quantitation instead, making its determination semi-quantitative.

Zhu et al. [79] developed an UHPLC-HILIC-MS/MS method for the simultaneous quantification of 40 AAs and their derivatives within 10 min. Quantification was performed in selected reaction monitoring (SRM) mode using positive ionization. Specific transitions were found without interference allowing for detection. For the optimization of chromatographic conditions, three columns were tested: 1) Atlantis HILIC column (2.1 × 100 mm, 3 μm) from Waters, 2) ZIC-HILIC column (2.1 × 100 mm, 3.5 μm) from Merck SeQuant, and 3) Acquity UHPLC BEH Amide Column (2.1 × 100 mm, 1.7 μm) from Waters. The latter column was selected for further optimization. Notably, this was the only column with a smaller particle size and provided the best results in terms of separation and signal intensity. Moreover, better peak shape and separation were achieved when using 5 mM AmAc in the mobile phase buffer.

Based on the studies reported in Table 2, a column based on amide chemistry seems to be the more suited for the targeted analysis of AAs, as all reported applications involved the separation of AAs with an amide-based stationary phase.



### 3.1.3. Organic acids

Organic acids are used to assess health status, nutritional status, vitamin deficiencies, and response to xenobiotics because they reflect the activity of major metabolic pathways. The carboxylic acids, which contain at least one carboxyl ( $-\text{COOH}$ ) group, are the most common organic acids found in living organisms [80]. The tricarboxylic acid (TCA) cycle represents the major source of energy in the cell, after conversion of glucose into a cascade of downstream metabolites. The TCA cycle generates energy via ATP production, as well as other metabolites acting as building blocks for the cell. Multiple organic acids, including succinic, citric, *iso*-citric, fumaric, lactic, and malic acids are involved in these processes and have been shown to be altered in cancerous tissues. Another relevant example is D-2-hydroxyglutarate (D-2-HG), which has been the first oncometabolite (cancer-causing metabolite) ever reported. D-2-HG is produced in the presence of gain-of-function mutations of the enzyme isocitrate dehydrogenase, causing a cascade in the cell that leads to genetic perturbations and malignant transformations [10].

GC-MS has long been considered the gold standard for the measurement of organic acids in metabolomics, as these analytes are too polar to be analysed in their native state using RPLC. However, GC-MS required the derivatization of these compounds, which is a time-consuming process adding extra analytical variability, which is typically difficult to control when working with a large number of samples, as typically encountered in metabolomics studies. HILIC has therefore gained more attention from the community as an attractive method for the analysis of native organic acids. Table 2 lists the recent applications of HILIC-based metabolomics for the targeted analysis of organic acids. An interesting study comes from Jackson et al, who developed a targeted method for the analysis of lactate in exhaled breath condensate in less than 4 min, as potential marker to monitor the evolution of chronic obstructive pulmonary disease (COPD) [17]. An amide-based column ( $2.1 \times 150$  mm,  $3.5 \mu\text{m}$ ) was used for the separation using isocratic mode, with a basic mobile phase (i.e., ACN:10 mM AmAc pH 9.0 [50:50, v/v] and ACN:10 mM AmAc pH 9.0 [50:50, v/v]). The developed method led to a limit of quantification of  $0.5 \mu\text{M}$ , which was considered fit-for-purpose.

Interestingly, most of the applications involving the analysis of organic acids have been carried out using zwitterionic stationary phases (such as sulfobetaine), with an acidified mobile phase (mostly using FA). No study has been reported using amine-based columns, which have shown to allow for the retention of some organic acids that typically give unsatisfactory results using other phases [10]. Moreover, there is little information available in the literature on the effect of the composition of the mobile phase (especially its ionic strength and pH) on the retention of these analytes. Systematic studies are therefore further needed to further evaluate the role that HILIC-MS may play for the analysis of organic acids in metabolomics applications.

### 3.1.4. Nucleosides and nucleotides

Besides being the monomeric building blocks of nucleic acids (DNA and RNA), nucleosides and nucleotides play a role in the regulation and modulation of several biological processes. Nucleosides are built from nucleobases (purines and pyrimidines) joined by a sugar via a glycosidic bond. Phosphorylated nucleosides are referred to as nucleotides [43].

The level of nucleosides, nucleotides and their respective analogues can be used as potential biomarkers for metabolic diseases, including cancer. For example, methylation is the most common modification observed for these compounds. An elevation of the levels of methylated nucleosides has been observed in urine samples from patients with liver, breast, lung, ovarian, and colon cancer [81]. Moreover, a change in the level of nucleobases has been linked to diabetic nephropathy in patients with diabetes mellitus [43].

A variety of analytical techniques have been used for the determination of these compounds and include enzyme-linked immunosorbent assay (ELISA), LC-MS, GC-MS, capillary zone electrophoresis (CZE) and

micellar electrokinetic chromatography (MEKC) [81,82]. However, these techniques have some disadvantages. For example, ELISA can be used with only a limited number of antibodies for merely some nucleosides which can be of insufficient specificity. In addition, GC requires time-consuming derivatization [81]. Moreover, CE lacks the required separation power for the simultaneous determination of multiple nucleosides [82]. Among several LC techniques, such as RPLC and IEX, HILIC has been proposed as a promising alternative, leading to excellent results.

One of the most interesting applications is the quantitative determination of 21 nucleobases and nucleosides using an amide-based column ( $150$  mm  $\times$   $2.1$  mm,  $3.5 \mu\text{m}$ ) detected with a triple quadrupole mass spectrometer [43]. The mobile phase was composed of  $\text{H}_2\text{O}/\text{ACN}$  (50:50, v/v) and  $\text{H}_2\text{O}/\text{ACN}$  (5:95, v/v) with both containing 0.8% AcOH and 10 mM AmAc. After protein precipitation of the plasma samples using the mobile phase,  $10 \mu\text{L}$  was injected and the separation was achieved within 19 min using a gradient. The developed method was fully validated for its selectivity, linearity, LLOQ, precision, accuracy, extraction recovery, matrix effects and stability according to FDA guidelines. The developed HILIC method was compared with an RPLC separation ( $\text{C}_{18}$  column) of the same 19 nucleobases and nucleosides, with both chromatograms shown in Fig. 7. The observed selectivity and resolution were better using HILIC, which enabled correct integration and accurate quantification. Moreover, a comparison of the peak width and tailing factors of nearly all components proved that the amide column outperformed the RPLC  $\text{C}_{18}$  column. Last but not least, an improved separation efficiency may be achieved when using smaller particle sizes of the column, as amide-based columns as also available in sub- $2 \mu\text{m}$  format.

Mateos-Vivas et al. [82] established a fast method for the simultaneous determination of 20 nucleosides and nucleotides. Various buffer salts, concentrations and pH values were tested on each of the three columns selected. The peak shape, retention and intensity of the nucleosides were relatively unaffected by these changes in the mobile phase. However, the experimental conditions showed to be essential for nucleotides, as the separation efficiency and peak shape were strongly dependent on the conditions. The best results were achieved using a concentration of 100 mM hexafluoro-2-propano (HFIP) and 50 mM diethylamide (DEA) with a pH of 9.0 in the aqueous phase prior to addition of an organic solvent. Amide, silica, and zwitterionic columns were also compared using the optimal mobile phase conditions for the separation of nucleotide monophosphates. Among those columns, the amide-based stationary phase provided the best separation and was selected for analysis of all nucleosides and nucleotides.

Based on this study and the articles reported in Table 2, the choice of the most-suited column chemistry seems to depend on the application of the method. It is therefore important to screen different column chemistries and mobile phase composition during method development, allowing for the optimal separation and detection of nucleosides and nucleotides, as well as their derivatives.

## 3.2. Complex proteomes

### 3.2.1. Direct HILIC-MS analysis of cell lysates

(RP)LC-MS-based bottom up proteomics is the most common approach – used in studies from basic biology to precision medicine – to characterize the proteome and its changes in depth. Samples are first processed by digesting proteins into peptides, following standard protocols. Digested samples are then separated using RPLC-ESI-MS/MS, where both the  $m/z$  ratio (MS) and fragmentation pattern (MS/MS) of peptides are recorded. The generated MS and MS/MS are searched against databases, generating a list of identified peptides, from which the presence of proteins in a given sample can be inferred [83,84].

In the last 20 years, MS performance has drastically increased in terms of sensitivity, resolving power and scan speed. In particular, the scan speed, which determines the number of peptides that can be

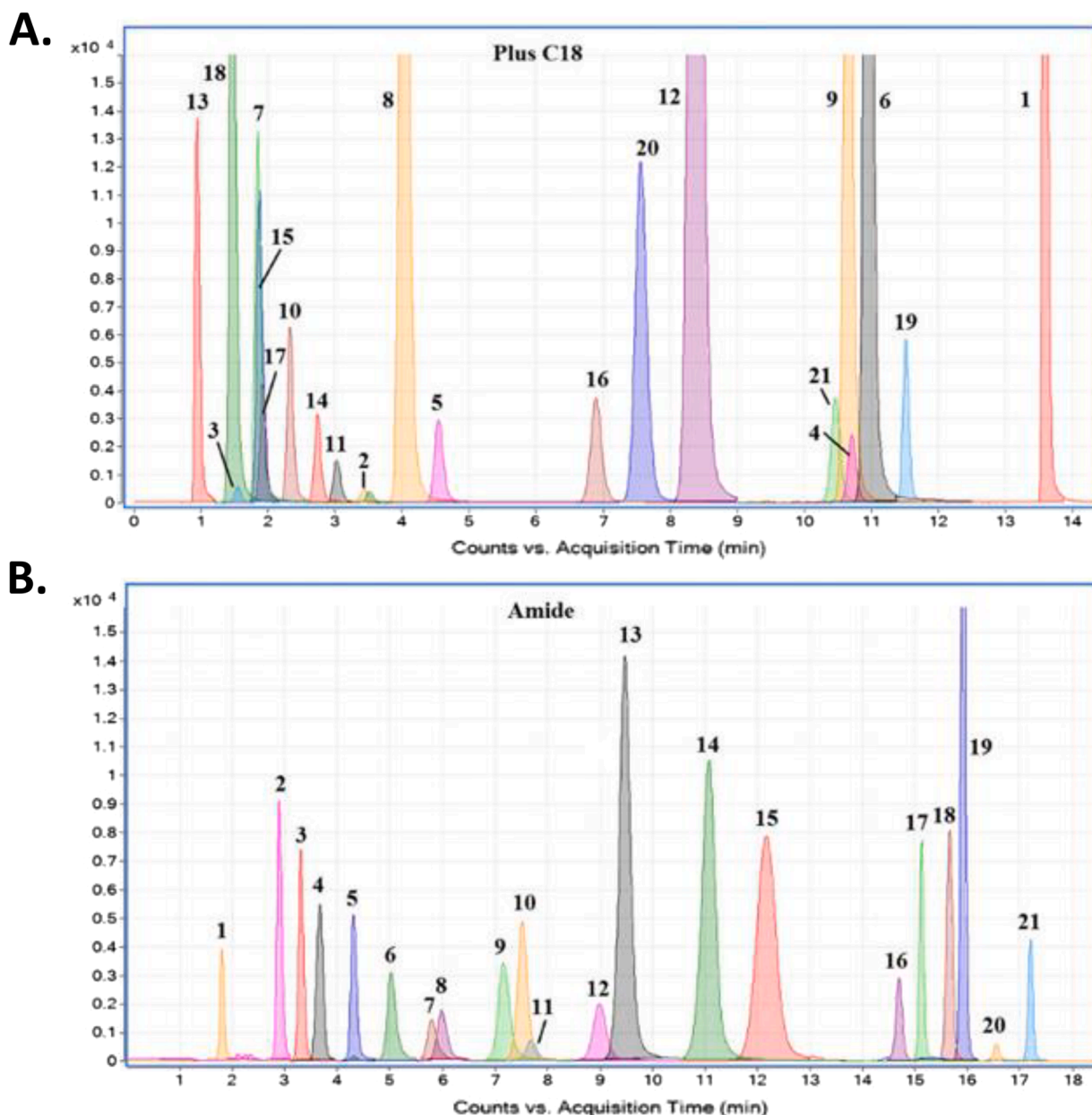


**Fig. 7.** Chromatograms of 21 nucleobases and nucleosides obtained with the analysis standard solutions using RPLC (A.) and HILIC (B.). Target analytes: 3- isobutyl-1-methylxanthine (1, internal standard); thymine (2); uracil (3); thymidine (4); 2'-deoxyuridine (5); 2'-deoxyadenosine (6); adenine (7); tubercidin (8, internal standard); adenosine (9); hypoxanthine (10); uridine (11); 2'-deoxyinosine (12); cytosine (13); xanthine (14); 2'-deoxycytidine (15); inosine (16); guanine (17); cytidine (18); 8-hydroxy-2'-deoxyguanosine (19); guanosine (20); and xanthosine (21). Reproduced from Du et al. [43] with permissions.

sequenced (and thus identified) in a certain analysis time, has grown from ca. 1 per second (1 Hz) in the end of the 1990s to more than 100 per second (100 Hz) in 2020 [85]. Hence, one of the challenges in proteomics is to achieve very high peak capacities in the LC separation (e.g., 1000) within a small time frame (e.g., 30 min to 1 h) [23].

Numerous studies have compared HILIC-MS with RPLC-MS for the characterization of complex protein digests. Table 3 shows a list of selected applications of HILIC for the proteomics-based analysis of complex protein mixtures.

Some of the advantages of HILIC described in the metabolomics section are also relevant in proteomics, such as the reduced viscosity of the mobile phase, allowing the use of longer column at reduced back pressure, and the facilitated evaporation in ESI. As stated previously, HILIC exhibits similar performance to RPLC for the analysis of small molecules, due to a increased B term and decreased C term contribution

in the Van Deemter equation [86,87]. However, peptides have higher molecular weights (typically between 3 and 9 kDa) and their analysis requires the use of MS-compatible mobile phase conditions (i.e., mostly based on acetic/formic acid or buffers such as ammonium acetate/formate), which often results in tailing and wider peak widths, due to secondary interactions with the stationary phase. Therefore, the peak capacity of HILIC separation of complex samples tend to be lower compared to RPLC-MS. Moreover, the expected improvement in intensity due to the high acetonitrile content [88] appears to be lower in practice than the one obtained for small molecules, especially for multiply charged species. Simion et al. observed a change of charge states of peptides in organic solvent with a shift from doubly or triply charged peptides in RPLC to monocharged species in HILIC-MS [89]. Singly charged ions are often excluded in proteomics experiments to reduce the fragmentation of contaminants or other small molecules in

**Table 3**

Selected applications of HILIC in proteomics analysis of complex protein mixtures and post translational modifications, covering the period from 2011 until July 2021.

Sample	Analytes	Analysis Level	Stationary phase	Mobile phase	LC-MS analysis	Ref., year
Human cells lysate (HeLa)	Complex Protein Mixtures	Peptides	ZIC-HILIC, ZIC-cHILIC (75 $\mu\text{m} \times 250 \text{ mm}$ , 3.5 $\mu\text{m}$ , 200 $\text{\AA}$ ); Sequant.	A: 95% ACN, 0.5% AcOH, 5 mM AmAc B: 5 mM AmAc (pH = 6.8) A: 95% ACN, 2% FA, 5 mM AmAc B: 0.07% FA, 5 mM AmAc (pH = 3.5)	HILIC(Z)-MS Offline 2D-LC-MS (HILIC(Z) $\times$ RPLC-MS)	[108,114],2011
Yeast cells lysate	Complex Protein Mixtures	Peptides	polyWAX (75 $\mu\text{m} \times 110 \text{ mm}$ , 5 $\mu\text{m}$ , 300 $\text{\AA}$ ); PolyLC.	A: 2% ACN, 0.1% FA, 5 mM AmAc B: 100% ACN 0.1% AmAc	ERLIC-MS	[55],2012
Human cells lysate (HeLa)	Complex Protein Mixtures	Peptides	Urea modified silica monolith (100 $\mu\text{m} \times 300$ and 2000 mm); custom made	A: 2% ACN, 0.1% FA, 5 mM AmAc B: 100% ACN 0.1% AmAc	HILIC(N)-MS	[90],2014
E. coli cells lysate	Complex Protein Mixtures	Intact Proteins	AdvanceBio glycan mapping (200 $\mu\text{m} \times 200 \text{ mm}$ 1.8 $\mu\text{m}$ , 300 $\text{\AA}$ ); Agilent	A: 98% ACN, 0.1% TFA B: 10% 2-propanol, 2% ACN, 0.1% TFA	HILIC(N)-MS	[195],2018
Human cells lysate (HeLa)	Complex Protein Mixtures	Peptides	TSK Amide- (100 $\mu\text{m} \times 150 \text{ mm}$ and 1000 mm, 5 $\mu\text{m}$ 80 $\text{\AA}$ ); TOSOH	A: 20% ACN, 0.1% FA B: 98% ACN	HILIC(N)-MS	[92],2019
Rat kidney	Complex Protein Mixtures	Peptides	polyWAX (4.6 mm $\times$ 200 mm, 5 $\mu\text{m}$ , 300 $\text{\AA}$ ); PolyLC.	A: 90% ACN, 0.1% AcOH B: 30% ACN 0.1% FA	Offline 2D-LC-MS (ERLIC $\times$ RPLC-MS)	[117],2013
Human serum	Complex Protein Mixtures	Peptides	polyWAX (4.6 mm $\times$ 100 mm, 5 $\mu\text{m}$ , 300 $\text{\AA}$ ); PolyLC.	A: 98% ACN, 0.2% AcOH, pH 3.4 B: 30% ACN 0.2% FA, pH 2.5	Offline 2D-LC-MS (ERLIC $\times$ RPLC-MS)	[118],2013
mouse fibroblasts	Complex Protein Mixtures (proteome & phosphoproteome)	Peptides	polyWAX (4.6 mm $\times$ 100 mm, 5 $\mu\text{m}$ , 300 $\text{\AA}$ ); PolyLC.	A: 70% ACN, 20 mM methyl phosphonic acid adjusted to pH 2 with 1 M NaOH B: 60% ACN 200 mM triethylamine phosphate, pH 2.0	Offline 2D-LC-MS (ERLIC $\times$ RPLC-MS)	[119],2015
Microbial Cells and Spores	Complex Protein Mixtures	Peptides	ZIC-HILIC (not described); Sequant.	A: 85% ACN, 0.4% AcOH, 5 mM AmAc pH 3.4 B: 30% ACN 0.5% AcOH, 5 mM AmAc pH 3.8	Offline 2D-LC-MS (HILIC(Z) $\times$ RPLC-MS)	[116],2018
synaptic vesicles of mammalian brane	Complex Protein Mixtures	Peptides	polyWAX (1.0 mm $\times$ 150 mm, 5 $\mu\text{m}$ , 300 $\text{\AA}$ ); PolyLC.	A: 90% ACN, 0.1% FA, adjusted to pH 4.5 with NH <sub>4</sub> OH B: 30% ACN 0.1% FA	Offline 2D-LC-MS (ERLIC $\times$ RPLC-MS)	[120],2020
Human immunoglobulin	Protein PTMs: Glycosylation	Peptides	ZIC-HILIC SPE; ProteaTips	A: 80% ACN, 2% FA B: 2% FA	Offline HILIC nanoESI-MS	[136],2011
Human cells (HeLa)	Protein PTMs: Phosphorylation	Peptides	TSKgel Amide-80 (4.6 mm $\times$ 250 mm, 5 $\mu\text{m}$ , 80 $\text{\AA}$ ); TOSOHpolyWAX (custom packed in Tricorn 5/100 column, 5 $\mu\text{m}$ , 300 $\text{\AA}$ ); PolyLC	A: 2% ACN, 0.1% TFA B: 98% ACN, 0.1% FA	Offline 2D-LC-MS (HILIC $\times$ RPLC-MSERLIC $\times$ RPLC-MS)	[196],2011
Rat kidney	Protein PTMs: Glycosylation & Phosphorylation	Peptides	polyWAX (4.6 mm $\times$ 200 mm, 5 $\mu\text{m}$ , 300 $\text{\AA}$ ); PolyLC	4 different combinations of mobile phases based on A: 80–85% ACN with AF 10 mM (pH 2–3) or FA A: 25–10 % ACN, 2% FA A: 70% ACN, 1% FA B: 70% ACN, 8% FA	Offline 2D-LC-MS (ERLIC $\times$ RPLC-MS)	[162],2011
Human core histones (HeLa)	Protein PTMs: Histone Acetylation & Methylation	Intact Proteins	polyCAT A (100 $\mu\text{m} \times 500 \text{ mm}$ , 5 $\mu\text{m}$ , 1000 $\text{\AA}$ ); PolyLC	A: 70% ACN, 1% FA B: 70% ACN, 8% FA	EALIC-MS	[56],2012
Rat liver tissue	Protein PTMs: Deamidation	Peptides	polyWAX (4.6 mm $\times$ 200 mm, 5 $\mu\text{m}$ , 300 $\text{\AA}$ ); PolyLC	A: 85% ACN, 0.1% AcOH B: 30% ACN, 0.2% FA	Offline 2D-LC-MS (RPLC $\times$ ERLIC-MS)	[168],2012
Human core histones (HeLa)	Protein PTMs: Histone Acetylation & Methylation	Middle down	polyCAT A (100 $\mu\text{m} \times 180 \text{ mm}$ , 3 $\mu\text{m}$ , 1500 $\text{\AA}$ ); PolyLC	A: 75% ACN 20 mM PA adjusted with NH <sub>4</sub> OH to pH 6 B: 25% ACN 20 mM PA pH 2.5	EALIC-MS	[149],2013
Human serum	Protein PTMs: Glycosylation	Peptides	XCharge SAX SPE (5 $\mu\text{m}$ , 100 $\text{\AA}$ ); Acchrom	A: 70% ACN, 0.1% AcOH B: 70% ACN, 0.1% AcOH, 10 mM AmmAc non glycop. C: 60% ACN, 0.1% AcOH, 10 mM AmmAc non glycop. D: 50% ACN, 10 mM AmmAc glycop.	Offline ERLIC nanoESI-MS	[137],2013
Pig plasma	Protein PTMs: Glycosylation	Peptides	polyWAX (4.6 mm $\times$ 200 mm, 5 $\mu\text{m}$ , 300 $\text{\AA}$ ); PolyLC	A: 85% ACN, 0.5% FA B: 30% ACN, 0.2% FA	Offline 2D-LC-MS (ERLIC $\times$ RPLC-MS)	[197],2015
Human cells (HeLa)	Protein PTMs: Phosphorylation	Peptides	polyWAX (4.6 mm $\times$ 100 mm, 5 $\mu\text{m}$ , 300 $\text{\AA}$ ); PolyLC	A: 75% ACN 20 mM methylphosphonic acid pH 2 B: 60% ACN, 200 mM triethylamine phosphate pH 2	Offline 2D-LC-MS (ERLIC $\times$ RPLC-MS)	[158],2015
Human cells (HeLa)	Protein PTMs: Phosphorylation	Peptides	polyWAX (4.6 mm $\times$ 200 mm, 5 $\mu\text{m}$ , 300 $\text{\AA}$ ); PolyLC	A: 70% ACN 20 mM sodium methylphosphonate pH 2 B: 10% ACN, 300 mM triethylamine phosphate pH 2	Offline 2D-LC-MS (ERLIC $\times$ RPLC-MS)	[141],2015
Rat liver		Peptides				[161],2015

(continued on next page)

Table 3 (continued)

Sample	Analytes	Analysis Level	Stationary phase	Mobile phase	LC-MS analysis	Ref., year
	Protein PTMs: Phosphorylation		TSK gel Amide-80 column (4.6 mm × 250 mm, 5 μm, 100 Å); TOSOH	A: 98% ACN, 0.1% TFA B: 2% ACN, 0.1% TFA	Offline 2D-LC-MS (HILIC × RPLC-MS)	
Histones from mouse organs: cerebrum, heart, kidney, spleen	Protein PTMs: Histone Acetylation & Methylation	Peptides	CORTECS HILIC column (2.1 mm × 100 mm, 2.7 μm, 120 Å); Waters	A: 0.2% FA, 10 mM AF in dH <sub>2</sub> O B: 60% ACN, 10% ACN, 0.2% FA, 10 mM AF	HILIC(N)-MS	[150],2016
Human brain tissue	Protein PTMs: Deamidation	Peptides	polyWAX (200 μm × 500 mm, 3 μm, 100 Å); PolyLC	A: 90% ACN, 0.1% FOA B: 0.1% FA	ERLIC-MS	[167],2016
Human brain tissue	Protein PTMs: Deamidation	Peptides	Amine column (data not reported); Shimadzu	A: 85% ACN, 0.1% AcOH B: 10% ACN, 0.1% FA	Offline 2D-LC-MS (ERLIC × RPLC-MS)	[166],2016
Mouse brain	Protein PTMs: N-Glycosylation	Peptides	ZIC-HILIC SPE (10 μm, 100 Å); Merck	IP-ZIC-HILICA: 80% ACN, 0.1% TFA B: 0.1% TFAFA-ZIC-HILIC A: 80% ACN, 0.1% FA B: 0.1% FA	Offline 2D-LC-MS (HILIC_RPLC-MS)	[133],2016
Human breast and brain cancer	Protein PTMs: N-Glycosylation	Peptides	HILIC: cotton wool packed tipsERLIC tips; PolyLC	HILICA: 90% ACN, 0.1% FA B: 0.5% FA ERLICA: 80% ACN, 0.1% FA B: 5% ACN, 2% FA	Offline 2D-LC-MS (ERLIC/HILIC_RPLC-MS)	[132],2016
Human primary lung fibroblast cells	Protein PTMs: Phosphorylation	Peptides	polyWAX (2.1 mm × 200 mm, 5 μm, 300 Å); PolyLC	A: 80% ACN, 0.1% FA B: 10% ACN, 2% FA	Offline 2D-LC-MS (ERLIC × RPLC-MS)	[159],2016
Human serum	Protein PTMs: N-Glycosylation	Peptides	Halo Penta-HILIC columns (2.1 mm × 150 mm, 2.7 μm); Advanced Materials Technology	A: ACN B: 5% ACN, 50 mM AmAc pH 4.4	HILIC (N)-MS	[138],2016
Human plasma	Protein PTMs: N-Glycosylation	Peptides	ERLIC: SOLA SAX SPE cartridges; ThermoFisher ScientificHILIC: Sepharose CL-4B media; Sigma-Aldrich	ERLICA: 95% ACN, 1%TFA B: 50% ACN, 0.1% TFA phosphop. C: 5% ACN, 0.1% TFA glycop. HILICA: 80% 1-butanol, 10% ethanol B: 50% ethanol	Offline 2D-LC-MS (ERLIC/HILIC_RPLC-MS)	[139],2017
Human immunoglobulins	Protein PTMs: Deamidation & Oxidation	Peptides	Halo Penta-HILIC (200 μm × 150 mm, 2.7 μm, 90 Å) Advanced Materials Technology	A: 100% ACN, 0.1% FA B: 0.1% FA	HILIC(N)-MS	[170],2017
Plasmodium falciparum	Protein PTMs: Methylation	Peptides	HILIC column (no further information) ; Agilent	A: 95% ACN, 0.1% FA B: 0.1% FA	Offline 2D-LC-MS (HILIC × RPLC-MS)	[156],2017
Human plasma	Protein PTMs: N-Glycosylation	Peptides	HILIC on a self-packed column (possibly ZIC-HILIC); Sequant/Merck	A: 80% ACN, 1% TFA B: 0.1% TFA	Offline 2D-LC-MS (SWATH) (HILIC_RPLC-MS)	[140],2018
Human core histones (HeLa)	Protein PTMs: Histone Acetylation & Methylation	Intact Proteins	polyCAT A (75 μm × 150 mm, 5 μm, 1000 Å); PolyLC	A: 70% ACN, 0.1% FA B: 70% ACN, 8% FA	EALIC-MS	[121],2018
Human core histones (HeLa)	Protein PTMs: Histone Acetylation & Methylation	Middle down	polyCAT A (75 μm × 150 mm, 3 μm, 1500 Å); PolyLC	A: 75% ACN, 20 mM PA adjusted with NH <sub>4</sub> OH to pH 6 B: 15% ACN, 0.2% FA PA pH 2.5	EALIC-MS	[198],2019
Human lung cancer cell	Protein PTMs: Glycosylation & Phosphorylation	Peptides	PolyWAX SPE (5 μm, 100 Å); PolyLC	A: 70% ACN 10 mM sodium methylphosphonate pH 2 B: 90% ACN 0.1% TFA phosphop. C: 20% ACN, 0.1% TFA glycop.	Offline 2D-LC-MS (ERLIC/HILIC_RPLC-MS)	[54],2019
Human multiple myeloma cell line (MM1)	Protein PTMs: Glycosylation & Phosphorylation	Peptides	PolySAX SPE (5 μm, 100 Å); PolyLC	1 Combinations of loading buffers (ACN 95–80% 1–0.1% TFA or 1–0.1% FA)4 Elution buffers in series:50% ACN,0.1% FA phosphop.0.1% FA in water,0.1% TFA in water,300 mM KH <sub>2</sub> PO <sub>4</sub> (pH = 2) glycop.	Offline 2D-LC-MS (ERLIC/HILIC_RPLC-MS)	[66],2019
Human serum	Protein PTMs: IgG Glycosylation	Middle up	AdvanceBio glycan mapping (200 μm × 300 mm 2.7 μm, 120 Å); Agilent	A: 98% ACN, 0.1% TFA B: 10% 2-propanol, 2% ACN, 0.1% TFA	HILIC(N) -MS	[60],2020
Human PSA	Protein PTMs: PSA Glycosylation	Peptides	Acquity glycan BEH amide (2.1 × 100 mm, 1.7 μm, 130 Å); Waters	A: 10 mM AF B: 90% ACN, 10 mM AF	HILIC(N)-MS	[147],2020
Mouse	Protein PTMs: Histone Acetylation & Methylation	Intact Proteins	polyCAT A (100 μm × 500 mm, 5 μm, 1000 Å); PolyLC	A: 70% ACN, 1% FA B: 70% ACN, 8% FA	EALIC-MS	[154],2020
IgG from human serum	Protein PTMs: IgG Glycosylation	Peptides	bare silica, polyhydroxy functionalized, aminopropyl functionalized (2.1 × 100 mm, 1.7 μm, 120 Å); ACE	A: 0.1% FA B: 100% ACN, 0.1% FA	HILIC(N)-MS	[146],2021
Mouse cortex	Protein PTMs: Glycosylation & Phosphorylation	Peptides	polyWAX or polySAX (2.1 mm × 200 mm, 5 μm, 300 Å); PolyLC	A: 80 % ACN, 20 mM magnesium trifluoroacetate B: 10 % ACN, 300 mM	Offline 2D-LC-MS (ERLIC/HILIC_RPLC-MS)	[64],2021

(continued on next page)



Table 3 (continued)

Sample	Analytes	Analysis Level	Stationary phase	Mobile phase	LC-MS analysis	Ref., year
				triethylammonium trifluoroacetate Other two mobile phase tested		

ACN, acetonitrile; PA, propionic acid; AcOH, acetic acid; FA, formic acid; AmAc, ammonium acetate; AF, ammonium formate; NH<sub>4</sub>OH, ammonium hydroxide; dH<sub>2</sub>O, deuterated water; IgG, immunoglobulin G; PSA, prostate-specific antigen; SPE, solid phase extraction; (N), neutral stationary phase, (Z), zwitterionic stationary phase. In the offline coupling, “.” indicates that HILIC was used as enrichment step (only a few fractions were analyzed), “×” indicates that a HILIC separation was performed and several fractions were collected and further analyzed. In the mobile phases, when not specified, the solvent is water.

the samples, while doubly charged ions are more readily dissociated than singly charged ions. This effect can also partially explain the lower identification rate observed when using HILIC-MS/MS compared with RPLC-MS/MS. Overall, the limited gains demonstrated so far by HILIC-MS in proteomics and the technical difficulties associated with the use of a technique different from RPLC (e.g., solvent and injection volume considerations [58]) have limited the application of HILIC-MS in proteomics.

In this context, the attempts to use HILIC-MS have focused on exploiting the low viscosity of the mobile phases for using longer separation columns. In particular, meter-long monolithic columns [90,91] and long-packed amide HILIC materials [92] have been used to separate complex protein digest. Except for one publication in which ERLIC separation outperformed RPLC-MS [55], the number of identified peptides in HILIC-MS was lower in the other reports (e.g., 911 unique peptides identified in HILIC vs. 2247 RPLC in [92] and 2529 vs. 2916 in [90], respectively). HILIC-MS has also been demonstrated for the analysis of proteomes without using enzymatic analysis (i.e., top-down analysis), reporting good separation capacities and orthogonal selectivity to RPLC [59]. However, the performance RPLC remains higher and the complication of using ion-pair agents like TFA in HILIC [93] are some of the reasons why this approach is not frequently used yet.

Nevertheless, the orthogonal selectivity offered by HILIC and its good separation capacity are beneficial in (offline/online) 2D-LC workflows and/or in the characterization of specific classes of PTMs of peptides and proteins.

### 3.2.2. HILIC in offline/online multidimensional protein separation methods

The analysis of the proteome of an organism requires to record MS and MS/MS signals from hundreds of thousands chemical species. Therefore, MS analysis benefits from having simpler and cleaner spectra. When coupling liquid separation approaches offline or online in a 2D-LC separation, the complexity of sample delivered to the MS in each time frame is reduced due to both an increased peak capacity and the coupling of different separation selectivities. This results in an increased number of peptides and proteins that can be identified [94]. Two important requisites are to be met to maximize the separation capacity when using 2D-LC in the analysis of complex samples, namely, (i) the two separation modes should target different sample dimensions (i.e., the two selectivity mechanisms have to be orthogonal [95]) and (ii) the peaks separated in the first dimension should not be mixed prior to the second separation dimension (i.e., the first separation should not be undersampled [96]).

2D-LC separations can be achieved either online or offline. The two approaches differ on how the separated fractions are sampled. Offline approaches may take place using SPE tips or collecting fractions from LC (-UV) separations. The fractions may then be dried and reconstituted (and in some cases mixed [97]) between the different separation dimensions, reducing incompatibility issues [98,99]. Moreover, there are no restrictions on the speed of analysis in the second dimension (<sup>2</sup>D), making this the best and simplest way to exploit the resolving power of both the separation dimensions and obtain a high proteome coverage. However, this is typically obtained by undersampling the first separation dimension (<sup>1</sup>D) to limit long analysis times.

Online 2D-LC has the advantage of significantly decreasing the analysis time necessary to obtain a high peak capacity, reducing the loss of sample (e.g., via adsorption on vials) and showing minimal sample dilution. In particular, online comprehensive 2D-LC (LC × LC) allows for the comprehensive analysis of samples, sampling extensively the <sup>1</sup>D and achieving high peak capacity per unit of time (in some cases exceeding 1000 per hour of analysis [100]). However, the tight constraints imposed by the coupling of the two chromatographic processes seriously limit the separation efficiency achievable in the second dimension (i.e., <sup>2</sup>D often occurs with a run time below 1 min). Moreover, proteomics analysis are typically performed at nanoflow rates to increase the MS sensitivity. The low flow rate, void volumes of valve and connection to realize LC × LC setup, pump dwell volumes and the sample dilution that are present in multiple places of the setup determine that only a limited amount of fractions (typically below 10) is collected from the <sup>1</sup>D and analyzed in the <sup>2</sup>D.

An additional complexity is present when coupling HILIC to RPLC separations, as the mobile phase have opposite elution strength, with ACN being a strong solvent in RPLC and a weak solvent in HILIC. For this reason, the online coupling of HILIC with RPLC requires dedicated solvent transfer solutions (modulation) to overcome potential issues such as the ones described in [101-103]. These HILIC-RPLC approaches are highly beneficial, as for HILIC and low pH RPLC of peptides and proteins the separation is highly orthogonal. An example of this is presented in Fig. 8, where the retention times obtained with HILIC and RPLC are normalized and compared using scatter plots.

Despite the advancements in low-flow online 2D-LC instrumentation since its first implementation in proteomics analysis [104], its application has been mostly limited to academic research. Only recently a first multilaboratory study has been reported [105]. For this reason, the majority of proteomics studies using 2D-LC adopt offline workflows.

As currently no application of the coupling of HILIC to RPLC at the intact or middle up/down level has been described outside the study of specific protein classes (e.g., histones), the next paragraphs focus on peptide separations.

The separation orthogonality and its effect on proteome coverage is discussed in the recent work of Yeung et al., where 16 different 2D-LC combinations were compared [106]. Retention data of approximately 30'000 peptides from a yeast digest were used to compare the different selectivities [106] of offline combinations such as RP-RP [107], HILIC-RP [108], IEC-RP [109] and mixed-mode separation-RP [110]. In this study, low pH RPLC-MS was used as second dimension, similar to the majority of 2D-LC applications in bottom-up proteomics. However, the study did not include ERLIC separation and compared 2D-LC separations using different numbers of first dimension fractions (40 to 70) and total MS analysis time (55 to 68 h). Nevertheless, it proved the high orthogonality of peptide separations in HILIC, using a buffer pH of 4.5. Separations using neutral and zwitterionic materials led to an orthogonality of ca. 60% [111], while SAX/IEC led to the highest orthogonality (around 70%) for peptides (40,000) and proteins (4100) identified, with high pH RPLC showing the highest numbers overall (60,000 peptides and 4600 proteins). Limited differences in terms of orthogonality were reported for the different silica phases studied, confirmed by the results obtained in a recent study from Roca et al. [112]. In addition, the



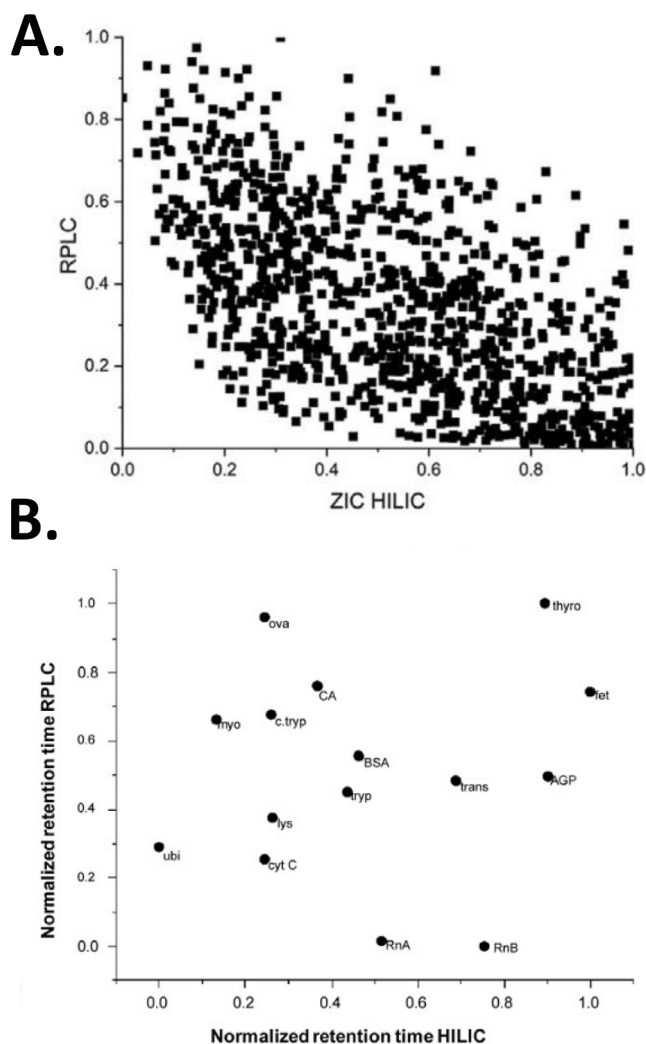


**Fig. 8.** Normalized retention times of peptides [37] (A.) and intact proteins (B.) observed with the analysis of a complex cell digest and reference intact proteins, respectively, in HILIC (x-axis) and RPLC (y-axis). Reprinted from [112,178] with permissions.

orthogonality between the HILIC and RPLC separations increased when increasing the pH of the mobile phase buffer while using neutral and zwitterionic stationary phases [108,113].

Because of these favorable characteristics, HILIC and ERLIC have been coupled offline to low pH separations and successfully applied to increase the number of proteins identified in the analysis of complex proteomes digests. In particular, HILIC applications include human cell digests analysis [108,114,115] and microbial cells and spores [116], whereas ERLIC was applied to the study of rat kidneys [117], serum samples [118], mouse fibroblasts [119], and mammalian brain [120]. Moreover, several publications describe the offline use of HILIC and ERLIC as fractionation method for the enrichment of glyco- and/or phosphopeptides (see section 3.3).

In contrast, the low-flow online coupling of HILIC to RPLC for complex proteome analysis have been reported in two instances only [112,113]. In both cases, trap columns (SCX [113] and RPLC [37]) were used to circumvent problems of sample loss in the injection in RPLC (breakthrough). In addition, similar setups have been used in the WCX-HILIC (EALIC) coupling with RPLC for the top-down analysis of histone proteoforms, helping to characterize their distribution in acetylated and methylated species [121,122].

### 3.3. Protein post-translational modifications in complex proteomes

When analyzing heterogeneous complex samples, the goal is generally to identify as many different peptides or proteins as possible. However, individual proteins are also inherently heterogeneous. Indeed, many proteins are actually a mixture of so-called proteoforms [123]. Proteins can undergo various post-translational and chemical (degradation) processes, leading to one protein backbone with numerous varying modifications. Typical examples of these modifications are glycosylation, phosphorylation, methylation, acetylation, oxidation, and deamidation. HILIC has shown high potential to separate or enrich these PTMs. Table 3 lists the applications reporting the use of HILIC for the analysis of PTMs in complex proteomics samples.

#### 3.3.1. Glycosylation

This section highlights the application of HILIC to glycoproteomic analysis by outlining selected examples where glycoproteins are analyzed at the peptide or protein level. The use of HILIC for glycan profiling (e.g., [124]) is not discussed.

Glycosylation is a post translational modification of proteins, where glycan structures are attached to a protein. Numerous biological functions are related to protein glycosylation, including cell-cell signaling, protein stability, protein localization, and immune response [125]. Modification of the glycoproteome are critical for physiological and pathological cellular functions in complex cells like mammalian (e.g., [126]). Therefore, it is of high interest to establish measurement approaches to monitor the presence and concentration of glycoproteins and their relationship with the development of diseases for which the early diagnosis is currently challenging [127,128].

HILIC is used in two principal ways to study glycoproteins, i.e., as enrichment to isolate glycopeptides in peptide mixtures, followed by an analysis typically by RPLC-MS to identify the glycopeptides, or as direct HILIC-MS method looking at mixture of (glyco)proteins with reduced complexity (e.g., immunoglobulins from serum) at the peptide or (less frequently) at the subunit level, allowing for an in-depth analysis of the protein glycoform distribution.

The most common approach to study the glycan composition and localization of glycoproteins is with glycopeptide analysis. Although the direct analysis of glycopeptides in peptide mixtures is possible, the sensitivity of MS detection is typically reduced by their lower abundance and due to their reduced ionization efficiency [129]. Therefore, an enrichment step is usually employed. Various methods are possible, such as lectin affinity chromatography, hydrazide chemistry and other chemical approaches [130], boronate affinity chromatography, and HILIC/ERLIC [131]. Generally, offline methods using HILIC/ERLIC for enrichment via solid phase extraction have proven to produce the highest number of glycopeptide identification [132,133], as illustrated in Fig. 9.A, showing no bias towards a large collection of different glycopeptide species and having good compatibility with MS [20,21]. However, when compared to methods such as chemical methods, they are less specific for solely glycopeptides and also capture other hydrophilic peptides [131]. The reduced selectivity of HILIC for glycopeptides makes HILIC enrichment suitable to isolate multiple PTMs. In particular, SPE-ERLIC enrichment of both glycol- and phosphopeptides has been reported. This is achieved by loading the sample using AX stationary phases (polyWAX/ polySAX) and ERLIC mobile phases (e.g., 70% ACN with 20 mM sodium methyl phosphonate at pH 2) and allowing for the phosphopeptides to be eluted first using HILIC weak mobile phases (e.g., 90% ACN, 0.1% TFA) followed by strong HILIC mobile phase (e.g., 20% ACN, 0.1% TFA) to elute the glycopeptides [54,66].

HILIC and ERLIC glycopeptide enrichments have been successfully applied in research to the analysis of glycoproteins in human blood [136-140], cancerous tissues [54,66,132], pig plasma [141], and mouse brain [133]. In recent years, the wide range of application that SPE-HILIC/ERLIC material have spurred interest in developing new format (e.g., magnetic beads) and chemistries to further improve the

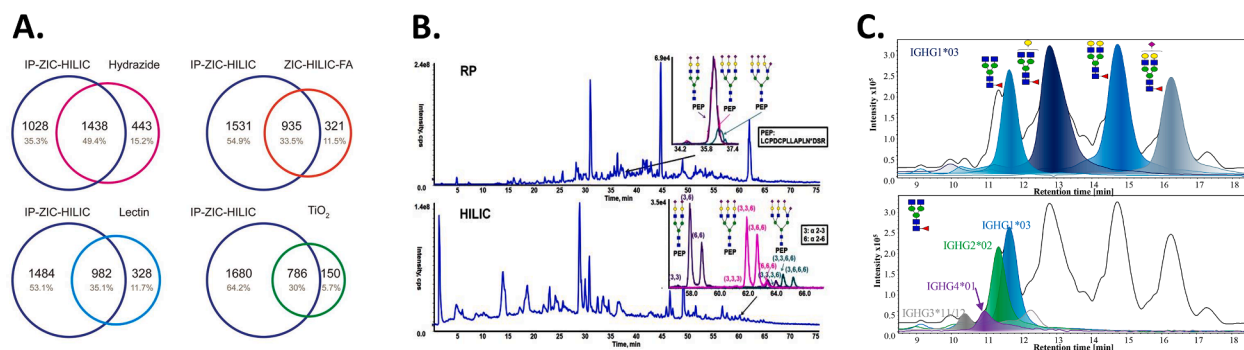


**Fig. 9.** A. Venn diagram of the identified N-glycosylation sites in mouse brain using ZIC-HILIC (ion-pair [IP] and using formic acid [FA]), hydrazide, lectins and titanium oxide ( $\text{TiO}_2$ ). The result of each method is the summation of three technical replicates. B. Separation of tryptic glycopeptides of fetuin observed with RPLC and HILIC-MS. Focus is placed on the peptide backbone of LCPDCPLLAPLNSR (GP15) modified with a bi/tri-antennary (Bi/Tri) N-glycan with variable number of sialic acids (SA; e.g., Bi-2SA). Top panel: total ion chromatogram (TIC; blue trace) and EIC (inset graph: purple trace of GP15-Bi-2SA; pink trace of GP15-Tri-3SA; green trace of GP15-Tri-4SA) from the RP separation. Bottom panel: TIC (blue trace) and EIC (inset graph: purple trace of GP15-Bi-2SA; pink trace of GP15-Tri-3SA; green trace of GP15-Tri-4SA) of HILIC separation of trypsin-digested fetuin. C. HILIC-MS analysis of IgG-Fc/2 proteoforms from human plasma from a single donor (Donor 1). The separation of Fc/2 subunits after IdeS digestion is visible through their base peak chromatograms (BPCs), which are represented by black lines. Extracted-ion chromatograms (EICs), from the same donor, of the different glycoforms (filled lines) of IGHG1\*03 illustrating the resolution of the different subclasses and allotypes. Reprinted from [60,133,138] with permissions. (For interpretation of the references to colour in this figure legend, the reader is referred to the web version of this article.)

enrichment properties of these materials [142-145].

The direct use of HILIC-MS to analyze glycopeptides is less common compared with RPLC-MS, based on similar reasons that are discussed in section 3.2.1. In HILIC, glycopeptides are typically more strongly retained, as well as separated from the non-glycosylated peptides. In addition, HILIC offers a unique selectivity towards the number and type of sugars present in the peptide or the glycoprotein. This is attractive for studies investigating the structural heterogeneity of glycoproteins. In particular, HILIC-MS analysis allows for the separation of the glycans isomers, which is true for many glycopeptides.

Huang et al. evaluated the use of HILIC-MS using neutral phases (diol) to separate isomers of glycopeptides using fetuin as model protein [138]. The presence of the peptide backbone did not significantly alter the relative retention of the different glycoforms with respect to the order obtained for the released glycans and the resolution obtained allowed to distinguish isomeric N-glycan structures, such as sialylated N-glycan isomers differing in  $\alpha_{2,3}$  and  $\alpha_{2,6}$  linkages (Fig. 9.B). Similarly, this was applied to the analysis of tryptic digests of the four subclasses of human serum IgGs (IgG<sub>1</sub>, IgG<sub>2</sub>, IgG<sub>3</sub>, and IgG<sub>4</sub>). The method was capable of resolving the peptides of the different classes due to their slightly different sequence, differing for a phenylalanine (F) to tyrosine (Y) substitution at one or two locations. In addition, the method allowed for a remarkable separation of isomeric glycoforms. Overall, at least ten different glycoforms on each individual IgG subtype were detected within a run time of 30 min. In a more recent study by Molnarova et al., the LC-MS-based separation of human serum IgG (IgG1 and 2) were compared using three different HILIC materials (charged and neutral) and a C18 column [146]. Moreover, the isomer resolving capacity of HILIC-MS (neutral, amide based) was applied in a recent article from van der Burgt et al. for the clinical characterization of human prostate specific antigen (PSA) as biomarker for prostate cancer using multiple reaction monitoring detection (MRM) [147]. Similar to IgG analysis, HILIC provided sufficient separating power to distinguish sialylated N-glycan isomers differing in  $\alpha_{2,3}$  and  $\alpha_{2,6}$  linkage. Using appropriate calibration, this HILIC-based method allowed for both the quantitation of PSA through its proteotypic peptides, as well as the identification of the presence and isomerism of glycopeptides.

Lastly, the use of HILIC-MS (neutral, amide based) has been successfully applied to the analysis of subunit/intact proteins in a clinical setting, opening potentially a new frontier in the use of HILIC analysis. Sénard et al. characterized the concomitant presence of sequence variance (allotype distributions) and glycoforms in the Fc portion of serum

IgG [60]. Human plasma IgG was isolated using Fc-specific beads, followed by an on-bead digestion with the enzyme IdeS. The obtained mixture of Fc subunits was analyzed by CE and HILIC hyphenated with MS. CE-MS provided separation of different IgG-subclasses and allotypes, while HILIC-MS allowed for the resolution of the different glycoforms and their oxidized variants (Fig. 9.C). The orthogonality of these techniques was crucial to reliably assign Fc allotypes. Samples obtained from five individual donors were analyzed using this approach. Heterozygosity was observed in all the analyzed donors resulting in a total of 12 allotypes identified. The assignments were further confirmed using recombinant monoclonal IgG allotypes as standards. While the glycosylation patterns were similar within allotypes of the same subclass, clear differences were observed between IgG subclasses and donors, highlighting the relevance of the proposed approach.

### 3.3.2. Acetylation and methylation

In HILIC-based studies of acetylation and methylation in proteomics, the focus has been almost exclusively on the characterization of histones [121,148-154]. Histones are important chromatin proteins that act as spools to package and order DNA into structural and manageable chromosomes. Core histones are modified by multiple PTMs, amongst others lysine acetylation and lysine or arginine methylation. These PTMs generate a so-called 'histone code' that is implicated in various chromatin-related cellular processes [155].

Histone acetylation and methylation have been mainly studied using middle-down [149,151-153] or top-down approaches [121,148,154]. As the complexity of these concurring PTMs is so vast, peptide mapping is less favorable. Although modifications can be pinpointed at the peptide level, the overall composition of the protein is lost. As histones have fairly low molecular weights (i.e., 11–18 kDa, for H2-4 families) intact separation and subsequent MS detection is seemingly easy. However, due to the potentially thousands of proteoforms, full characterization from a unidimensional separation is unlikely. Hence, intact analysis has been exclusively used using multidimensional separations RPLC and ERLIC are always combined, with the latter being either in the first [121] or second dimension [148,154]. RPLC is used to separate the histone families, whereas ERLIC allows for the differentiation based on degree of acetylation and/or methylation due to the loss of charged residues. Full fragmentation of the separated histones proteoforms should be achieved to obtain the highest amount of information. Hence, these workflows always include top-down proteomics approaches. They use either the combination of collision induced dissociation (CID) and

electron transfer dissociation (ETD) [148,154], or ultraviolet photodissociation (UVPD) [121] to (fully) fragment the proteins and obtain structural information. Reportedly over 700 histone proteoforms could be unambiguously identified with the single 2D-LC-MS/MS analysis of 7.5  $\mu$ g of purified core histones [148].

There are some hurdles associated with top-down approaches, which relate to the limited data analysis options for such heavily modified proteoforms. These shortcomings have accelerated the interest in middle-down MS methods that focus on the analysis of large peptides generated by specific proteases in conjunction with validated bioinformatics strategies to allow for the quantitation of isomeric isoforms. This has also gained traction for histone analysis using either unidimensional [151,153] or multidimensional separations [149,152] involving HILIC. Similar fragmentation approaches based on CID, ETD, and UVPD have been employed to obtain high sequence coverage for the large peptide fragments (ca. 6 kDa). A typical example of such a workflow is shown in Fig. 10 [152]. First, histone families are separated using RPLC. Subsequently, large peptide fragments are generated by the use of AspN digestion on a specific fraction, which can be again purified with RPLC

to focus on a specific region (e.g., the N-terminal tail of H4). The subsequent ERLIC separation of these fragments shows the clear separation based on degree of acetylation of the peptide. Through ETD-MS/MS experiments, the peptide can be fully sequenced and the presence of acetylation and methylation sites can be confirmed. In total, over 230 proteoforms of the histone H4 solely were identified and quantified with this approach. In another study, over 300 proteoforms were found in non-fractionated HeLa cell lysates using direct ERLIC-UVPD-MS/MS approach [151].

Only two studies show the use of HILIC for bottom-up proteomics. The first study focused on histone H3 modification [150], while the second looked at arginine methylation in the complete *Plasmodium falciparum* proteome [156]. In the former study, the authors specifically wanted to investigate K27/K36 modifications from all three different histone H3 variants. After digestion, the samples were analyzed with both RPLC-MS/MS and HILIC-MS/MS. This combined separation approach led to the full characterization of all combinatorically possible modifications (69 different options being possible on this single peptide). With HILIC, 34 peptides were identified and quantified,

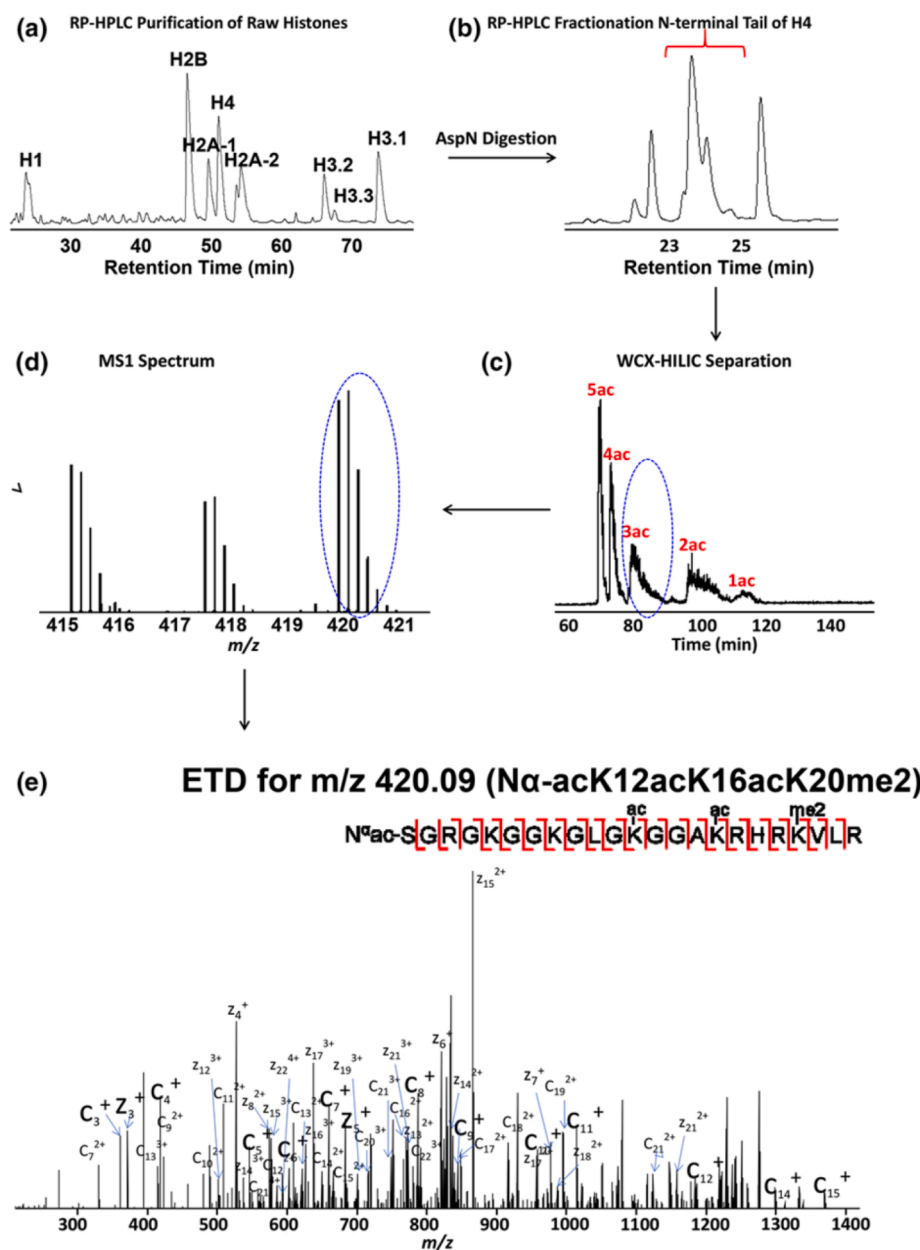


**Fig. 10.** Overall experimental workflow for the characterization of the histone H4  $N\alpha$ -acK12acK16-acK20me2 proteoform [6]. (a) RPLC allows for the separation of histones into different families, namely, H2A, H2B, H3.1, H3.2, H3.3, H4, and H1. (b) The target 23 amino acid peptide of the N-terminal tail is further purified by RP-HPLC. (c) Proteoforms are primarily separated by extent of acetylation, and then by methylation state and location by use of ERLIC. (d) Representative broadband mass spectrum of the desired 23 amino acid peptide of histone H4 at a retention time of 82.36 min. (e) Representative ETD product ion spectrum for precursor ion  $m/z$  420.09 with matched fragments marked. Reprinted from Jiang et al. [179] with permissions.

whereas RPLC enabled the same for the other 35 peptides. This approach was subsequently applied to investigate the pattern of the combinatorial K27/K36 marks for all histone H3 variants across five mouse organs. Distribution differences were observed not only between different H3 variants but also between different organs.

Notably, HILIC is not often used for acetylated peptide enrichment. A study showed the usefulness of enriching N-terminally acetylated peptides [157]. Acetylation of the N-terminus removes the positive charge of a peptide, modulating electrostatic and hydrophilic interactions with a zwitterionic HILIC phase. As a consequence, the elution of the acetylated peptides is pH dependent. Moreover, such an approach minimized co-elution of these peptides with phosphopeptides and interference due to the salts or buffers that might be present or required.

### 3.3.3. Phosphorylation

Phosphorylation of proteins is important for controlling cellular signaling and cell cycle regulatory events. The process is reversible and phosphoproteins normally constitute a minor part of the global proteome in a cell. Thus, sample preparation techniques tailored for phosphoproteome studies are highly relevant. ERLIC performed at a low pH results in unmodified peptides to elute in or near the void volume. However, peptides containing groups that retain some negative charge at low pH, such as the phosphate groups ( $pK_a \sim 2.1$ ), do show interaction with the material. Unsurprisingly, this ERLIC-based enrichment has been the main direction when studying phosphorylation with HILIC.

Cui et al. have shown that ERLIC material can be used for solid-phase extraction (SPE) in order to enrich phosphopeptides, besides glycopeptides [66]. They show that the choice of mobile phase dictated which compound class elute, by comparing 10 different eluent compositions. For both peptide classes, low pH elution conditions yielded the highest recovery, but phosphopeptides only eluted at high recovery when a competitive salt (potassium phosphate) was added to break the Coulombic interactions between the sorbent and the phosphopeptides.

Other studies make use of analytical ERLIC separations with [64,119,158-161] and without [162,163] additional enrichment/purification steps to obtain phospho-enriched fractions. In general, all these studies show a similar approach. By using ERLIC, an enriched fraction (or fractions) of phosphopeptides is obtained, due to their separation from unmodified peptides. Phosphopeptides tend to elute after unmodified peptides, due to their high hydrophilicity plus the electrostatic attraction with the column via the negatively charged phosphate group. After collecting fractions, they are occasionally purified or further enriched using  $TiO_2$ , RP, or SCX material, prior to subsequent RPLC-MS/MS analysis. These approaches have been used on rat kidney tissue [162], a mouse RAW 264.7 cell line [163], rat liver tissue [161], HeLa cells [158,160], adenovirus type 2 infected human cells [159], mouse cortex tissue [64], and murine fibroblasts [119]. Staggering amounts of phosphopeptides can be identified in these kind of workflows, with numbers ranging from several hundreds [162], thousands [64,119,158,163], just over 10,000 [160], and even close to 25,000 [161].

### 3.3.4. Deamidation

Deamidation is a protein modification that disrupts the structure and functions of proteins. While deamidation has long been recognized as a critical event in human aging and multiple degenerative diseases, research progress in this field has been restricted by the technical challenges associated with studying this PTM in complex biological samples. The main focus is often on asparagine (Asn) deamidation, generating L-aspartic acid (L-Asp), D-aspartic acid (D-Asp), L-isospartic acid (L-isoAsp) or D-isospartic acid (D-isoAsp) residues at the same position of Asn in the affected protein. Deamidation is most frequently studied on the peptide level, but typically the isomeric peptides cannot be resolved using RPLC, due to high similarity in hydrophobicity. Moreover, MS also fails to distinguish them when they coelute, due to the mass difference of only 0.984 Da being less than 20 mDa from the  $^{13}C$

isotope of the unmodified peptide. It is worth mentioning that the study of glutamine (Gln) deamidation faces the same analytical challenges.

Since the different residues have varying side-chain  $pK_a$  values, peptides should exhibit different  $pI$  values (e.g., isoAsp < n-Asp < Asn). Hence, separations driven by charge differences would be suitable to distinguish both Asn and Gln deamidation. Unsurprisingly, many studies have focused on the use of (L)ERLIC approaches to study deamidation [164-169]. However, the use of a hydroxyl-based (neutral) stationary phase for the separation of these variants also has shown promising results [170]. Interestingly, the retention behavior of peptides changes rather uniformly upon deamidation, so that the PTM can be reliably used in retention time prediction models [164,170]. Fig. 11 shows the separation that can be obtained using LERLIC for both Asn and Gln deamidated isomeric peptides. In this specific case, a 1200-min gradient was used to maximize the separation of all peptides in a tryptic digest of human brain tissue [167]. LERLIC-MS/MS displayed a consistent ability to separate the Asn deamidation products, where Asp eluted earlier than isoAsp (Fig. 11.A and 11.B), as expected based on  $pI$  differences. Moreover, more complex peptide combinations, including those showing two independently deamidated Asn and Gln proteoforms, were also successfully characterized by LERLIC-MS/MS (Fig. 11.C and 11.D). Overall, these results demonstrate that a single run of LERLIC-MS/MS allows for the combined characterization of Gln and Asn deamidated residues in proteins from highly complex biological samples, including brain tissues. After showing the separation efficiency obtained with ERLIC-MS in brain tissues, the same research group further used this approach to study dementia-linked amyloidosis [166]. Profiling of both soluble and aggregated amyloid plaque demonstrated significant enrichment and deamidation of various proteins [166]. The authors suggest that changes in charge state resulting from deamidation, leading to altered calcium-binding capacity of certain proteins, enhanced their aggregation and promotes neurodegeneration in the human brain.

Due to the complexity of proteomes, multidimensional approaches represent a valuable strategy to increase coverage. By making use of the difference in selectivity in the first and second dimension, a higher coverage of deamidated peptides (and consequently, proteins) can also be achieved. For example, using RPLC in the first dimension separates peptides on hydrophobicity, ensuring the coelution of a given peptide and its deamidated species. Sending this fraction to an ERLIC-based second dimension will resolve them and allows their identification. Hao et al applied this approach to probe for deamidation in rat liver tissues [168]. A 60-min nanoRPLC separation was off-line collected in 24 fractions that were subsequently subjected to ERLIC-MS/MS. They collected approximately 250'000 MS/MS spectra resulting in 1305 protein identifications via at least 2 unique peptides. Over 23'000 peptides were at the basis of that identification, with almost 4000 of them being unique. Of those unique peptides, over 300 were Asn-deamidated. Interestingly, 20 were identified via all three deamidation-related products and 70 of which were identified via two of them.

### 3.3.5. Oxidation

Oxidation of methionine is a common PTM. Due to the mass difference between modified and unmodified peptides (+16 Da), it is easier to study this PTM by ESI-MS than, for example, deamidation. Oxidation of methionine residues has been shown to affect the structure, stability, and biological functions of a variety of proteins [171]. Only two studies have focused on the effect of oxidation during HILIC separations of complex samples. Badgett et al. used a hydroxyl-based (neutral) stationary phase for their peptide separations [170]. As hydrophilic differences are the driving force of the separation of peptides when using neutral materials, they were able to separate both the modified peptide and their native form, allowing for confident quantitation of the peak areas or heights even with low-resolution mass spectrometers. Interestingly, they observed that the selectivity obtained for peptides that were oxidized was always highly similar ( $\alpha \sim 1.0-1.2$ ). This enabled them to include this PTM as a parameter in retention time modeling for



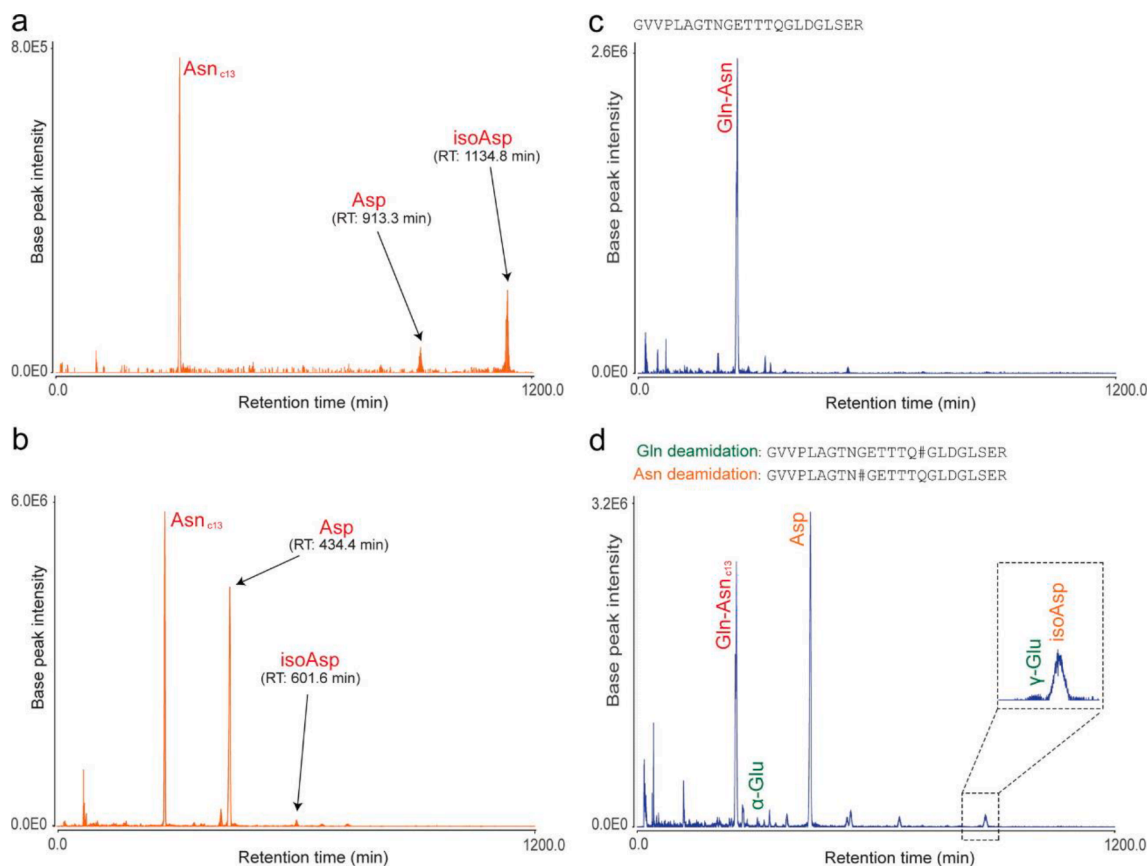


**Fig. 11.** Separation of Asn and Gln deamidation peptides from trypsin-digested human brain tissue using LERIC-MS/MS [25]. (a) EIC of N#GFDQCDYGWLSDASVR peptide showing Asn-deamidated peptides eluting at three different retention times (RT). (b) EIC of VDKGVVPLAGTN#GETTTQGLDGLSER peptide showing an inverted isoAsp/Asp ratio. (c) EIC of GVVPLAGTNGETTTQGLDGLSER nondeamidated peptide. (d) EIC of the two independently deamidated proteoforms with Asn and Gln deamidated residues (GVVPLAGTN#GETTTQGLDGLSER and GVVPLAGTNGETTTQ#GLDGLSER). Asnc13, carbon-13 peak of the nondeamidated peptide; Asp, Asp aspartyl isomer; isoAsp, isoaspartyl isomer; Gln-Asnc13, carbon-13 peak of the nondeamidated peptide; α-Glu, α-glutamyl isomer; γ-Glu, γ-glutamyl isomer. Reprinted from Serra et al. [167] with permissions.

#### HILIC separations.

On the other hand, Khaje and Sharp used a zwitterionic HILIC material in combination with a TFA-containing eluent in their study focusing on peptide oxidation [164]. This combination minimized the impact that the position of the oxidation has on the retention behavior of a specific peptide. As a consequence, isomeric peptide oxidation products are not separated. The authors show that in RPLC often only a partial separation is obtained. Due to differences in retention time and resulting fragmentation behavior, quantitation of the isomeric species is cumbersome. By ensuring that the isomeric peptides coelute a total amount of peptide oxidation can be readily achieved. Moreover, the resulting peptide fragmentation spectra can provide a reliable quantitative insight in the relative oxidation state of each isomer.

#### 4. Conclusions and perspectives

Owing to the numerous technological developments carried out over the last decade (notably the increased availability of dedicated stationary phases and columns equipped with sub-2 μm particle sizes), HILIC has become a relatively mature technique and has therefore been increasingly used in proteomics and metabolomics.

In metabolomics, multiple comparative studies have been published, reporting the advantages that HILIC may bring over RPLC for the analysis of polar metabolites, in both untargeted and targeted approaches. HILIC is now typically used by the metabolomics community, in addition to the gold-standard RPLC, to increase the metabolome coverage by enabling the analysis, identification and quantitation of

more polar classes that typically elute in the void volume in RPLC.

Among the metabolite classes showing a relevant interest in clinical practice, bioactive lipids, amino acids, organic acids, and nucleosides/nucleotides are currently very popular, as they have been reported to play a significant role in multiple pathological processes, including inflammation, cancer, obesity, diabetes, or neurodegenerative diseases. RPLC-MS remains the technique of choice for the analysis of bioactive lipids, especially the sub-classes eicosanoids, ECs, and SPMs. However, HILIC may be complementary to RPLC in two contexts, namely, (i) the analysis of lysophospholipids, which are difficult to separate with RPLC, and (ii) the analysis of eicosanoids (and likely ECs) which may show limited stability in water due to rapid hydrolysis, such as discussed for PGI<sub>2</sub>. More comparative studies are certainly needed, especially for the latter application, as stability remains one of the numerous challenges when analyzing these compounds. On the other hand, HILIC-MS shows improved performance for the analysis of amino acids (under their native form), organic acids, as well as nucleosides and nucleotides, and should be clearly considered in targeted approaches focusing on these classes of metabolites. However, the studies surveyed that there is no direct plug-and-play method that can be used for the analysis of such metabolites. Indeed, a rather extensive optimization step is often required, with careful screening of stationary phases and – especially – composition of the mobile phase buffer (e.g., pH, concentrations, additives, etc.). Moreover, these metabolites being relatively polar, careful optimization of the injection solvent composition and injection volume should be always carried out to find the best compromise between low solvent mismatch and sufficient solubility of the compounds in the



injection solvent.

With the commercialization of columns equipped with sub-2  $\mu\text{m}$  particle sizes, the equilibration times (which have long been considered a major drawback of the technique) have drastically decreased due to the possibility of using high flow rates and smaller columns. With such columns, HILIC-MS also enables high-throughput and high-resolution separations, which are typically required in metabolomics. In proteomics, the use of HILIC or ERLIC-MS to characterize complex proteomes has been explored at all levels (i.e., peptide and protein levels), revealing the unique separation and orthogonality of HILIC compared with RPLC in the analysis of peptides and proteins. However, the lower peak capacity observed in HILIC and the more complex conditions needed have so far limited its application in proteomics studies.

Nevertheless, the unique selectivity of HILIC has proven to be a valuable separation strategy to fractionate the complexity of protein samples, with performance comparable and often better compared with reference methods, such as SCX and high pH RPLC.

HILIC and ERLIC methods have shown to be excellent for the analysis of protein modifications. In particular, the ability of HILIC of retaining hydrophilic compounds can be exploited to enrich glycosylated and phosphorylated peptides, with several studies reporting the simultaneous enrichment of both PTMs. Moreover, HILIC separations have proven to be successful in separating and enhancing the detection of PTMs such as acetylation, deamidation, methylation and oxidation.

Overall, HILIC is expected to become further implemented in both proteomics and metabolomics, enabling access to (patho)physiological information that has remained so far underinvestigated.

Lastly, when it comes to possible technical developments, remarkable high-resolution separations have been achieved for omics separations in RPLC-UHPLC using long columns (i.e., 500 mm length) packed with sub 2  $\mu\text{m}$  particles (down to 1.1  $\mu\text{m}$ ) using extreme pressure over 3000 bar (45 kPsi) [172-175]. It will be interesting to follow whether such experiments will be tested for HILIC-UHPLC. Indeed, since less back-pressure is typically generated in HILIC compared with RPLC (depending on the composition of the gradient), longer columns and/or much higher flow rates or the use of smaller particles (e.g. 500 nm [176,177]) may be achieved with UHPLC instruments that can reach up to 3000 bar. Nowadays, the large majority of HILIC column formats (if not all) commercially available have a length of max. 250 mm (150 mm for sub 2  $\mu\text{m}$  particles). Ultra-high resolution or ultra-high throughput HILIC analysis will therefore only be possible – with adequate reproducibility – once longer HILIC columns will be commercially available, and this combined with the latest generation of UHPLC instruments.

## Declaration of Competing Interest

The authors declare that they have no known competing financial interests or personal relationships that could have appeared to influence the work reported in this paper.

## References

- [1] E.J. Dupree, M. Jayathirtha, H. Yorkey, M. Mihasan, B.A. Petre, C.C. Darie, A critical review of bottom-up proteomics: the good, the bad, and the future of this field, *Proteomes* 8 (2020) 1–26, <https://doi.org/10.3390/proteomes8030014>.
- [2] A.F.M. Altaalar, J. Munoz, A.J.R. Heck, Next-generation proteomics: towards an integrative view of proteome dynamics, *Nat. Rev. Genet.* 14 (2013) 35–48, <https://doi.org/10.1038/nrg3356>.
- [3] J.B. Müller, P.E. Geyer, A.R. Colaço, P.V. Treit, M.T. Strauss, M. Oroshi, S. Doll, S. Virreira Winter, J.M. Bader, N. Köhler, F. Theis, A. Santos, M. Mann, The proteome landscape of the kingdoms of life, *Nature* 582 (7813) (2020) 592–596, <https://doi.org/10.1038/s41586-020-2402-x>.
- [4] R.A. Zubarev, The challenge of the proteome dynamic range and its implications for in-depth proteomics, *Proteomics* 13 (5) (2013) 723–726, <https://doi.org/10.1002/pmic.201200451>.
- [5] J.W. Harper, E.J. Bennett, Proteome complexity and the forces that drive proteome imbalance, *Nature* 537 (7620) (2016) 328–338, <https://doi.org/10.1038/nature19947>.
- [6] C.A. Crutchfield, S.N. Thomas, L.J. Sokoll, D.W. Chan, Advances in mass spectrometry-based clinical biomarker discovery, *Clin. Proteomics* 13 (2016) 1–12, <https://doi.org/10.1186/s12014-015-9102-9>.
- [7] T.T. Duarte, C.T. Spencer, Personalized proteomics: the future of precision medicine, *Proteomes* 4 (2016), <https://doi.org/10.3390/proteomes4040029>.
- [8] M. Frantzi, A. Latosinska, H. Mischak, Proteomics in drug development: the dawn of a new era? *Proteomics - Clin. Appl.* 13 (2019) 1–13, <https://doi.org/10.1002/prca.201800087>.
- [9] H.A. Ehardt, A. Root, C. Sander, R. Aebersold, Applications of targeted proteomics in systems biology and translational medicine, *Proteomics* 15 (18) (2015) 3193–3208, <https://doi.org/10.1002/pmic.201500004>.
- [10] R. Haselberg, B.W.J. Pirok, A. Gargano, I. Kohler, Clinical metabolomics: expanding the metabolome coverage using advanced analytical techniques, *LC GC Eur.* 32 (2019) 465–480 (accessed April 17, 2020), <http://www.chromatographyonline.com/clinical-metabolomics-expanding-metabolome-coverage-using-a-dvanced-analytical-techniques>.
- [11] D. Tang, L. Zou, X. Yin, C.N. Ong, HILIC-MS for metabolomics: an attractive and complementary approach to RPLC-MS, *Mass Spectrom. Rev.* 35 (2016) 574–600, <https://doi.org/10.1002/mas.21445>.
- [12] M. Ma, X. Zhao, S. Chen, Y. Zhao, L.u. yang, Y.u. Feng, W. Qin, L. Li, C. Jia, Strategy based on deglycosylation, multiprotease, and hydrophilic interaction chromatography for large-scale profiling of protein methylation, *Anal. Chem.* 89 (23) (2017) 12909–12917, <https://doi.org/10.1021/acs.analchem.7b03673>.
- [13] T. Reçber, E. Nemutlu, K. Beksaç, S. Aksoy, S. Kır, Optimization and validation of a HILIC-LC-ESI-MS/MS method for the simultaneous analysis of targeted metabolites: Cross validation of untargeted metabolomic studies for early diagnosis of breast cancer, *Microchem. J.* 159 (2020), 105559, <https://doi.org/10.1016/j.microc.2020.105559>.
- [14] I. Kohler, A. Verhoeven, R.J.E. Derks, M. Giera, Analytical pitfalls and challenges in clinical metabolomics, *Bioanalysis* 8 (14) (2016) 1509–1532, <https://doi.org/10.4155/bio-2016-0090>.
- [15] I. Kohler, M. Giera, Recent advances in liquid-phase separations for clinical metabolomics, *J. Sep. Sci.* 40 (1) (2017) 93–108, <https://doi.org/10.1002/jssc.201600981>.
- [16] Z.-Z. Fang, F.J. Gonzalez, LC-MS-based metabolomics: an update, *Arch. Toxicol.* 88 (8) (2014) 1491–1502, <https://doi.org/10.1007/s00204-014-1234-6>.
- [17] T.C. Jackson, Y.V. Zhang, P.J. Sime, R.P. Phipps, R.M. Kottmann, Development of an accurate and sensitive method for lactate analysis in exhaled breath condensate by LC MS/MS, *J. Chromatogr. B Anal. Technol. Biomed. Life Sci.* 1061-1062 (2017) 468–473, <https://doi.org/10.1016/j.jchromb.2017.07.041>.
- [18] E. Iturrospe, K.M. Da Silva, B. Talavera Andújar, M. Cuykx, J. Boeckmans, T. Vanhaecke, A. Covaci, A.L.N. van Nuijs, An exploratory approach for an oriented development of an untargeted hydrophilic interaction liquid chromatography-mass spectrometry platform for polar metabolites in biological matrices, *J. Chromatogr. A.* 1637 (2021), 461807, <https://doi.org/10.1016/j.chroma.2020.461807>.
- [19] M.M. Khamis, D.J. Adamko, R.W. Purves, A. El-Aneed, Quantitative determination of potential urine biomarkers of respiratory illnesses using new targeted metabolomic approach, *Anal. Chim. Acta* 1047 (2019) 81–92, <https://doi.org/10.1016/j.aca.2018.09.035>.
- [20] E. Rampler, H. Schoeny, B.M. Mitić, Y. El Abiead, M. Schwaiger, G. Koellensperger, Simultaneous non-polar and polar lipid analysis by on-line combination of HILIC, RP and high resolution MS, *Analyst* 143 (5) (2018) 1250–1258, <https://doi.org/10.1039/C7AN01984J>.
- [21] I. Kohler, R.J.E. Derks, M. Giera, The rise of hydrophilic interaction chromatography in untargeted clinical metabolomics, *LC GC Eur.* 29 (2016) 60–75 (accessed April 17, 2020), <http://www.chromatographyonline.com/hydrophilic-interaction-chromatography-update?pageID=1>.
- [22] D.V. McCalley, Understanding and manipulating the separation in hydrophilic interaction liquid chromatography, *J. Chromatogr. A.* 1523 (2017) 49–71, <https://doi.org/10.1016/j.chroma.2017.06.026>.
- [23] E. Shishkova, A.S. Hebert, J.J. Coon, Now, more than ever, proteomics needs better chromatography, *Cell Syst.* 3 (4) (2016) 321–324, <https://doi.org/10.1016/j.cels.2016.10.007>.
- [24] A.J. Alpert, Hydrophilic-interaction chromatography for the separation of peptides, nucleic acids and other polar compounds, *J. Chromatogr. A.* 499 (1990) 177–196, [https://doi.org/10.1016/S0021-9673\(00\)96972-3](https://doi.org/10.1016/S0021-9673(00)96972-3).
- [25] I. Kohler, M. Sun, G. Groeneveld, A.F.G. Gargano, Not (Only) reversed-phase LC-MS: alternative LC-MS approaches, *LC-GC Eur.* 38 (2020) 507–519.
- [26] A. Periat, I. Kohler, D. Guilleme, J.L. Veuthey, Advances in hydrophilic interaction liquid chromatography for pharmaceutical analysis, *LC-GC Eur.* 26 (2013) 17–23.
- [27] J. Heaton, N. Gray, D.A. Cowan, R.S. Plumb, C. Legido-Quigley, N.W. Smith, Comparison of reversed-phase and hydrophilic interaction liquid chromatography for the separation of ephedrine, *J. Chromatogr. A.* 1228 (2012) 329–337, <https://doi.org/10.1016/j.chroma.2011.09.026>.
- [28] I. Kohler, M. Sun, G. Groeneveld, A.F.G. Gargano, Not (Only) reversed-phase LC-MS: alternative LC-MS approaches, *LC-GC North Am.* 38 (2020) 507–518, <https://www.chromatographyonline.com/view/not-only-reversed-phase-lc-ms-alternative-lc-ms-approaches>.
- [29] G. Greco, T. Letzel, Main interactions and influences of the chromatographic parameters in HILIC separations, *J. Chromatogr. Sci.* 51 (7) (2013) 684–693, <https://doi.org/10.1093/chromsci/bmt015>.
- [30] B. Buszewski, S. Noga, Hydrophilic interaction liquid chromatography (HILIC)-a powerful separation technique, *Anal. Bioanal. Chem.* 402 (1) (2012) 231–247, <https://doi.org/10.1007/s00216-011-5308-5>.

- [31] N. Sillner, A. Walker, E.-M. Harrieder, P. Schmitt-Kopplin, M. Witting, Development and application of a HILIC UHPLC-MS method for polar fecal metabolome profiling, *J. Chromatogr. B Anal. Technol. Biomed. Life Sci.* 1109 (2019) 142–148, <https://doi.org/10.1016/j.jchromb.2019.01.016>.
- [32] B.W.J. Pirok, S.R.A. Molenaar, R.E. van Outersterp, P.J. Schoenmakers, Applicability of retention modelling in hydrophilic-interaction liquid chromatography for algorithmic optimization programs with gradient-scanning techniques, *J. Chromatogr. A*. 1530 (2017) 104–111, <https://doi.org/10.1016/j.chroma.2017.11.017>.
- [33] G. van Schaick, B.W.J. Pirok, R. Haselberg, G.W. Somsen, A.F.G. Gargano, Computer-aided gradient optimization of hydrophilic interaction liquid chromatographic separations of intact proteins and protein glycoforms, *J. Chromatogr. A*. 1598 (2019) 67–76, <https://doi.org/10.1016/j.chroma.2019.03.038>.
- [34] L.S. Roca, S.E. Schoemaker, B.W.J. Pirok, A.F.G. Gargano, P.J. Schoenmakers, Accurate modelling of the retention behaviour of peptides in gradient-elution hydrophilic interaction liquid chromatography, *J. Chromatogr. A*. 1614 (2020), <https://doi.org/10.1016/j.chroma.2019.466050>.
- [35] M. Witting, S. Böcker, Current status of retention time prediction in metabolite identification, *J. Sep. Sci.* 43 (9–10) (2020) 1746–1754, <https://doi.org/10.1002/jssc.202000060>.
- [36] P. Bonini, T. Kind, H. Tsugawa, D.K. Barupal, O. Fiehn, Retip: retention time prediction for compound annotation in untargeted metabolomics, *Anal. Chem.* 92 (2020) 7515–7522, <https://doi.org/10.1021/acs.analchem.9b05765>.
- [37] A.F.G. Gargano, R. Haselberg, G.W. Somsen, Hydrophilic interaction liquid chromatography mass spectrometry methods for the characterization of glycoproteins: overview of the methods and applications for intact glycoproteins, glycopeptides and released glycan analysis, in: *Carbohydr. Anal. by Mod. Liq. Phase Sep. Tech.* 2nd Ed., Elsevier, 2021.
- [38] P. Hemström, K. Irgum, Hydrophilic interaction chromatography, *J. Sep. Sci.* 29 (12) (2006) 1784–1821, <https://doi.org/10.1002/jssc.200600199>.
- [39] J. Ruta, S. Rudaz, D.V. McCalley, J.-L. Veuthey, D. Guillarme, A systematic investigation of the effect of sample diluent on peak shape in hydrophilic interaction liquid chromatography, *J. Chromatogr. A*. 1217 (52) (2010) 8230–8240, <https://doi.org/10.1016/j.chroma.2010.10.106>.
- [40] J.P. Violi, D.P. Bishop, M.P. Padula, J.R. Steele, K.J. Rodgers, Considerations for amino acid analysis by liquid chromatography-tandem mass spectrometry: a tutorial review, *TrAC - Trends Anal. Chem.* 131 (2020) 116018, <https://doi.org/10.1016/j.trac.2020.116018>.
- [41] J.C. Heaton, D.V. McCalley, Some factors that can lead to poor peak shape in hydrophilic interaction chromatography, and possibilities for their remediation, *J. Chromatogr. A*. 1427 (2016) 37–44, <https://doi.org/10.1016/j.chroma.2015.10.056>.
- [42] D.V. McCalley, A study of column equilibration time in hydrophilic interaction chromatography, *J. Chromatogr. A*. 1554 (2018) 61–70, <https://doi.org/10.1016/j.chroma.2018.04.016>.
- [43] Y. Du, Y.J. Li, X.X. Hu, X. Deng, Z.T. Qian, Z. Li, M.Z. Guo, D.Q. Tang, Development and evaluation of a hydrophilic interaction liquid chromatography-MS/MS method to quantify 19 nucleobases and nucleosides in rat plasma, *Biomed. Chromatogr.* 31 (2017) 1–10, <https://doi.org/10.1002/bmc.3860>.
- [44] K. Kalfková, M. Boublík, G. Kucéřová, P. Kozlík, The effect of buffer concentration and cation type in the mobile phase on retention of amino acids and dipeptides in hydrophilic interaction liquid chromatography, *Chem. Pap.* 72 (1) (2018) 139–147, <https://doi.org/10.1007/s11696-017-0265-x>.
- [45] Y. Guo, S. Gaiki, Retention behavior of small polar compounds on polar stationary phases in hydrophilic interaction chromatography, *J. Chromatogr. A*. 1074 (1–2) (2005) 71–80, <https://doi.org/10.1016/j.chroma.2005.03.058>.
- [46] K. Contrepois, L. Jiang, M. Snyder, Optimized analytical procedures for the untargeted metabolomic profiling of human urine and plasma by combining hydrophilic interaction (HILIC) and reverse-phase liquid chromatography (RPLC)-mass spectrometry, *Mol. Cell. Proteomics* 14 (6) (2015) 1684–1695, <https://doi.org/10.1074/mcp.M114.046508>.
- [47] Y. Wen, X. Yuan, F. Qin, L. Zhao, Z. Xiong, Development and validation of a hydrophilic interaction ultra-high-performance liquid chromatography-tandem mass spectrometry method for rapid simultaneous determination of 19 free amino acids in rat plasma and urine, *Biomed. Chromatogr.* 33 (2019) 1–13, <https://doi.org/10.1002/bmc.4387>.
- [48] D.V. McCalley, Hydrophilic-interaction chromatography: an update, *LC-GC North Am.* 38 (2020) 173–181 (accessed April 17, 2020), <http://www.chromatographyonline.com/hydrophilic-interaction-chromatography-update?pageID=1>.
- [49] J.C. Heaton, J.J. Russell, T. Underwood, R. Boughtflower, D.V. McCalley, Comparison of peak shape in hydrophilic interaction chromatography using acidic salt buffers and simple acid solutions, *J. Chromatogr. A*. 1347 (2014) 39–48, <https://doi.org/10.1016/j.chroma.2014.04.026>.
- [50] J.L. Spalding, F.J. Naser, N.G. Mahieu, S.L. Johnson, G.J. Patti, Trace phosphate improves ZIC-PHILIC peak shape, sensitivity, and coverage for untargeted metabolomics, *J. Proteome Res.* 17 (10) (2018) 3537–3546, <https://doi.org/10.1021/acs.jproteome.8b00487>.
- [51] D.V. McCalley, Effect of mobile phase additives on solute retention at low aqueous pH in hydrophilic interaction liquid chromatography, *J. Chromatogr. A*. 1483 (2017) 71–79, <https://doi.org/10.1016/j.chroma.2016.12.035>.
- [52] A. Periat, I.S. Krull, D. Guillarme, Applications of hydrophilic interaction chromatography to amino acids, peptides, and proteins, *J. Sep. Sci.* 38 (3) (2015) 357–367, <https://doi.org/10.1002/jssc.201400969>.
- [53] A.J. Alpert, Electrostatic repulsion hydrophilic interaction chromatography for isocratic separation of charged solutes and selective isolation of phosphopeptides, *Anal. Chem.* 80 (1) (2008) 62–76, <https://doi.org/10.1021/ac070997p>.
- [54] R. Chen, S. Williamson, K.M. Fulton, S.M. Twine, J. Li, Simultaneous analysis of phosphopeptides and intact glycopeptides from secretome with mode switchable solid phase extraction, *Anal. Methods*. 11 (41) (2019) 5243–5249, <https://doi.org/10.1039/C9AY01756A>.
- [55] E.P. de Jong, T.J. Griffin, Online nanoscale ERLIC-MS outperforms RPLC-MS for shotgun proteomics in complex mixtures, *J. Proteome Res.* 11 (10) (2012) 5059–5064, <https://doi.org/10.1021/pr300638n>.
- [56] Z. Tian, N. Tolić, R. Zhao, R.J. Moore, S.M. Hengel, E.W. Robinson, D.L. Stenoien, S. Wu, R.D. Smith, L. Paša-Tolić, N. Toli, R. Zhao, R.J. Moore, S.M. Hengel, E. W. Robinson, D.L. Stenoien, S. Wu, R.D. Smith, L. Pa, Enhanced top-down characterization of histone post-translational modifications, *Genome Biol.* 13 (2012) R86, <https://doi.org/10.1186/gb-2012-13-10-r86>.
- [57] M. Benevento, P.D. Tonge, M.C. Puri, A. Nagy, A.J.R. Heck, J. Munoz, Fluctuations in histone H4 isoforms during cellular reprogramming monitored by middle-down proteomics, *Proteomics* 15 (2015) 3219–3231, <https://doi.org/10.1002/prot.201500031>.
- [58] P. Kozlik, M. Sanda, R. Goldman, Nano reversed phase versus nano hydrophilic interaction liquid chromatography on a chip in the analysis of hemopexin glycopeptides, *J. Chromatogr. A*. 1519 (2017) 152–155, <https://doi.org/10.1016/j.chroma.2017.08.066>.
- [59] A.F.G. Gargano, L.S. Roca, R.T. Fellers, M. Bocxe, E. Domínguez-Vega, G. W. Somsen, A.F.G. Gargano, L.S. Roca, R.T. Fellers, M. Bocxe, E. Domínguez-Vega, G.W. Somsen, A.F.G. Gargano, L.S. Roca, R.T. Fellers, M. Bocxe, E. Domínguez-Vega, G.W. Somsen, Capillary HILIC-MS: a new tool for sensitive top-down proteomics, *Anal. Chem.* 90 (2018) 6601–6609, <https://doi.org/10.1021/acs.analchem.8b00382>.
- [60] T. Sénard, A.F.G. Gargano, D. Falck, S.W. de Taeye, T. Rispens, G. Vidarsson, M. Wührer, G.W. Somsen, E. Domínguez-Vega, MS-based allotype-specific analysis of polyclonal IgG-Fc N-Glycosylation, *Front. Immunol.* 11 (2020) 1–13, <https://doi.org/10.3389/fimmu.2020.02049>.
- [61] A. Periat, S. Fekete, A. Cusumano, J.-L.-L. Veuthey, A. Beck, M. Lauber, D. Guillarme, Potential of hydrophilic interaction chromatography for the analytical characterization of protein biopharmaceuticals, *J. Chromatogr. A*. 1448 (2016) 81–92, <https://doi.org/10.1016/j.chroma.2016.04.056>.
- [62] J. Camperi, V. Pichon, T. Fournier, N. Delaunay, First profiling in hydrophilic interaction liquid chromatography of intact human chorionic gonadotropin isoforms, *J. Pharm. Biomed. Anal.* 174 (2019) 495–499, <https://doi.org/10.1016/j.jpba.2019.06.014>.
- [63] K. Furuki, T. Toyo'oka, Retention of glycopeptides analyzed using hydrophilic interaction chromatography is influenced by charge and carbon chain length of ion-pairing reagent for mobile phase, *Biomed. Chromatogr.* 31 (2017), <https://doi.org/10.1002/bmc.3988>.
- [64] Y. Cui, D.N. Tabang, Z. Zhang, M. Ma, A.J. Alpert, L. Li, Counterion optimization dramatically improves selectivity for phosphopeptides and glycopeptides in electrostatic repulsion-hydrophilic interaction chromatography, *Anal. Chem.* 93 (22) (2021) 7908–7916, <https://doi.org/10.1021/acs.analchem.1c00615>.
- [65] K.-C. Cho, L. Chen, Y. Hu, M. Schnaubelt, H. Zhang, Developing workflow for simultaneous analyses of phosphopeptides and glycopeptides, *ACS Chem. Biol.* 14 (1) (2019) 58–66, <https://doi.org/10.1021/acscmbio.8b00902>.
- [66] Y. Cui, K. Yang, D.N. Tabang, J. Huang, W. Tang, L. Li, Finding the sweet spot in ERLIC mobile phase for simultaneous enrichment of N-Glyco and phosphopeptides, *J. Am. Soc. Mass Spectrom.* 30 (12) (2019) 2491–2501, <https://doi.org/10.1007/s13361-019-02230-6>.
- [67] M. Holčápek, M. Ovcáčíková, M. Lísa, E. Cífková, T. Hájek, Continuous comprehensive two-dimensional liquid chromatography-electrospray ionization mass spectrometry of complex lipidomic samples, *Anal. Bioanal. Chem.* 407 (17) (2015) 5033–5043, <https://doi.org/10.1007/s00216-015-8528-2>.
- [68] J. Medina, V. van der Velpen, T. Teav, Y. Guitton, H. Gallart-Ayala, J. Ivanisevic, Single-step extraction coupled with targeted hilic-ms/ms approach for comprehensive analysis of human plasma lipidome and polar metabolome, *Metabolites* 10 (2020) 1–17, <https://doi.org/10.3390/metabo10120495>.
- [69] V. Chiurchiù, A. Leuti, M. Maccarrone, Bioactive lipids and chronic inflammation: managing the fire within, *Front. Immunol.* 9 (2018), <https://doi.org/10.3389/fimmu.2018.00038>.
- [70] K. Saito, Application of comprehensive lipidomics to biomarker research on adverse drug reactions, *Drug Metab. Pharmacokinet.* 37 (2021), <https://doi.org/10.1016/j.dmpk.2020.100377>.
- [71] H.S. Jónasdóttir, C. Papan, S. Fabritz, L. Balas, T. Durand, I. Hardardóttir, J. Freysdóttir, M. Giera, Differential mobility separation of leukotrienes and protectins, *Anal. Chem.* 87 (10) (2015) 5036–5040, <https://doi.org/10.1021/acs.analchem.5b00786>.
- [72] M. Vogeser, G. Schelling, Pitfalls in measuring the endocannabinoid 2-arachidonoylethanol glycerol in biological samples, *Clin. Chem. Lab. Med.* 45 (2007) 1023–1025, <https://doi.org/10.1515/CCLM.2007.197>.
- [73] D. Wolrab, M. Chochołousková, R. Jirásko, O. Peterka, M. Holčápek, Validation of lipidomic analysis of human plasma and serum by supercritical fluid chromatography-mass spectrometry and hydrophilic interaction liquid chromatography-mass spectrometry, *Anal. Bioanal. Chem.* (2020) 2375–2388, <https://doi.org/10.1007/s00216-020-02473-3>.
- [74] M. Lísa, E. Cífková, M. Khalikova, M. Ovcáčíková, M. Holčápek, Lipidomic analysis of biological samples: Comparison of liquid chromatography, supercritical fluid chromatography and direct infusion mass spectrometry

- methods, *J. Chromatogr. A*. 1525 (2017) 96–108, <https://doi.org/10.1016/j.chroma.2017.10.022>.
- [75] C.E. Roy, T. Kauss, S. Prevot, P. Barthelemy, K. Gaudin, Analysis of fatty acid samples by hydrophilic interaction liquid chromatography and charged aerosol detector, *J. Chromatogr. A*. 1383 (2015) 121–126, <https://doi.org/10.1016/j.chroma.2015.01.046>.
- [76] C. Rakers, A.A. Zoerner, S. Engeli, S. Batkai, J. Jordan, D. Tsikas, Stable isotope liquid chromatography-tandem mass spectrometry assay for fatty acid amide hydrolase activity, *Anal. Biochem.* 421 (2) (2012) 699–705, <https://doi.org/10.1016/j.ab.2011.11.003>.
- [77] J. Chen, W. Hou, B. Han, G. Liu, J. Gong, Y. Li, D. Zhong, Q. Liao, Z. Xie, Target-based metabolomics for the quantitative measurement of 37 pathway metabolites in rat brain and serum using hydrophilic interaction ultra-high-performance liquid chromatography-tandem mass spectrometry, *Anal. Bioanal. Chem.* 408 (10) (2016) 2527–2542, <https://doi.org/10.1007/s00216-016-9352-z>.
- [78] H.C.M.T. Prinsen, B.G.M. Schiebergen-Bronkhorst, M.W. Roelvelde, J.J.M. Jans, M.G.M. de Sain-van der Velden, G. Visser, P.M. van Hasselt, N.M. Verhoeven-Duif, Rapid quantification of underivatized amino acids in plasma by hydrophilic interaction liquid chromatography (HILIC) coupled with tandem mass spectrometry, *J. Inher. Metab. Dis.* 39 (5) (2016) 651–660, <https://doi.org/10.1007/s10545-016-9935-z>.
- [79] B. Zhu, L. Li, H. Wei, W. Zhou, W. Zhou, F. Li, P. Lin, J. Sheng, Q. Wang, C. Yan, Y. Cheng, A simultaneously quantitative profiling method for 40 endogenous amino acids and derivatives in cell lines using hydrophilic interaction liquid chromatography coupled with tandem mass spectrometry, *Talanta* 207 (2020), <https://doi.org/10.1016/j.talanta.2019.120256>.
- [80] D. Tsoukalas, A. Alegakis, P. Fragkiadaki, E. Papanikolaou, D. Nikitovic, A. Karataraki, A.E. Nosyrev, E.G. Papadakis, D.A. Spandidos, N. Drakoulis, A. M. Tsatsakis, Application of metabolomics: Focus on the quantification of organic acids in healthy adults, *Int. J. Mol. Med.* 40 (2017) 112–120, <https://doi.org/10.3892/ijmm.2017.2983>.
- [81] E. Račkowska, B. Bobrowska-Korczak, J. Giebutowicz, Development and validation of a rapid LC-MS/MS method for determination of methylated nucleosides and nucleobases in urine, *J. Chromatogr. B Anal. Technol. Biomed. Life Sci.* 1128 (2019) 121775, [10.1016/j.jchromb.2019.121775](https://doi.org/10.1016/j.jchromb.2019.121775).
- [82] M. Mateos-Vivas, E. Rodríguez-Gonzalo, D. García-Gómez, R. Carabias-Martínez, Hydrophilic interaction chromatography coupled to tandem mass spectrometry in the presence of hydrophilic ion-pairing reagents for the separation of nucleosides and nucleotide mono-, di- and triphosphates, *J. Chromatogr. A*. 1414 (2015) 129–137, <https://doi.org/10.1016/j.chroma.2015.08.040>.
- [83] F.M. Altelaar, J. Munoz, A.J.R. Heck, Next-generation proteomics: towards an integrative view of proteome dynamics, *Nat. Rev. Genet.* 14 (2013) 35–48, <https://doi.org/10.1038/nrg3356>.
- [84] M. Larance, A.I. Lamond, Multidimensional proteomics for cell biology, *Nat. Rev. Mol. Cell Biol.* 16 (5) (2015) 269–280, <https://doi.org/10.1038/nrm3970>.
- [85] F. Meier, A.-D. Brunner, S. Koch, H. Koch, M. Lubeck, M. Krause, N. Goedecke, J. Decker, T. Kosinski, M.A. Park, N. Bache, O. Hoerning, Jürgen Cox, O. Räther, M. Mann, Online parallel accumulation-serial fragmentation (PASEF) with a novel trapped ion mobility mass spectrometer, *Mol. Cell. Proteomics*. 17 (12) (2018) 2534–2545, <https://doi.org/10.1074/mcp.TIR118.000900>.
- [86] J.C. Heaton, X. Wang, W.E. Barber, S.M.C. Buckenmaier, D.V. McCalley, Practical observations on the performance of bare silica in hydrophilic interaction compared with C18 reversed-phase liquid chromatography, *J. Chromatogr. A*. 1328 (2014) 7–15, <https://doi.org/10.1016/j.chroma.2013.12.058>.
- [87] H. Song, E. Adams, G. Desmet, D. Cabooter, Evaluation and comparison of the kinetic performance of ultra-high performance liquid chromatography and high-performance liquid chromatography columns in hydrophilic interaction and reversed-phase liquid chromatography conditions, *J. Chromatogr. A*. 1369 (2014) 83–91, <https://doi.org/10.1016/j.chroma.2014.10.002>.
- [88] H.P. Nguyen, K.A. Schug, The advantages of ESI-MS detection in conjunction with HILIC mode separations: fundamentals and applications, *J. Sep. Sci.* 31 (2008) 1465–1480, <https://doi.org/10.1002/jssc.200700630>.
- [89] R. Simon, Q. Enjalbert, J. Biarc, J. Lemoine, A. Salvador, Evaluation of hydrophilic interaction chromatography (HILIC) versus C18 reversed-phase chromatography for targeted quantification of peptides by mass spectrometry, *J. Chromatogr. A*. 1264 (2012) 31–39, <https://doi.org/10.1016/j.chroma.2012.09.059>.
- [90] K. Horie, T. Kamakura, T. Ikegami, M. Wakabayashi, T. Kato, N. Tanaka, Y. Ishihama, Hydrophilic interaction chromatography using a metre-scale monolithic silica capillary column for proteomics LC-MS, *Anal. Chem.* (2014), <https://doi.org/10.1021/ac4038625>.
- [91] M.L. Chen, L.M. Li, B.F. Yuan, Q. Ma, Y.Q. Feng, Preparation and characterization of methacrylate-based monolith for capillary hydrophilic interaction chromatography, *J. Chromatogr. A*. 1230 (2012) 54–60, <https://doi.org/10.1016/j.chroma.2012.01.065>.
- [92] Y. Liu, X. Wang, Z. Chen, D.H. Liang, K. Sun, S. Huang, J. Zhu, X. Shi, J. Zeng, Q. Wang, B. Zhang, Towards a high peak capacity of 130 using nanoflow hydrophilic interaction liquid chromatography, *Anal. Chim. Acta.* 1062 (2019) 147–155, <https://doi.org/10.1016/j.aca.2019.01.060>.
- [93] S. Wouters, S. Eelink, R. Haselberg, G.W. Somsen, A.F.G. Gargano, Microfluidic ion stripper for removal of trifluoroacetic acid from mobile phases used in HILIC-MS of intact proteins, *Anal. Bioanal. Chem.* (2021), <https://doi.org/10.1007/s00216-021-03414-4>.
- [94] D.B. Bekker-Jensen, C.D. Kelstrup, T.S. Bath, S.C. Larsen, C. Haldrup, J. B. Bramsen, K.D. Sørensen, S. Høyer, T.F. Ørntoft, C.L. Andersen, M.L. Nielsen, J. V. Olsen, An optimized shotgun strategy for the rapid generation of comprehensive human proteomes, *Cell Syst.* 11 (2017) 214–221, <https://doi.org/10.1016/j.cels.2017.05.009>.
- [95] M. Gilar, P. Olivova, A.E. Daly, J.C. Gebler, Orthogonality of separation in two-dimensional liquid chromatography, *Anal. Chem.* 77 (19) (2005) 6426–6434, <https://doi.org/10.1021/ac050923i>.
- [96] J.M. Davis, D.R. Stoll, P.W. Carr, Effect of first-dimension undersampling on effective peak capacity in comprehensive two-dimensional separations, *Anal. Chem.* 80 (2) (2008) 461–473, <https://doi.org/10.1021/ac071504j>.
- [97] F. Yang, Y. Shen, D.G. Camp, R.D. Smith, High-pH reversed-phase chromatography with fraction concatenation for 2D proteomic analysis, *Expert Rev. Proteomics* 9 (2) (2012) 129–134, <https://doi.org/10.1586/epr.12.15>.
- [98] N. Marchetti, J.N. Fairchild, G. Guiochon, Comprehensive off-line, two-dimensional liquid chromatography: application to the separation of peptide digests, *Anal. Chem.* 80 (8) (2008) 2756–2767, <https://doi.org/10.1021/ac7022662>.
- [99] S. Eelink, S. Dolman, G. Vivo-Truyols, P. Schoenmakers, R. Swart, M. Ursem, G. Desmet, Selection of column dimensions and gradient conditions to maximize the peak-production rate in comprehensive off-line two-dimensional liquid chromatography using monolithic columns, *Anal. Chem.* 82 (16) (2010) 7015–7020, <https://doi.org/10.1021/ac101514d>.
- [100] D.R. Stoll, H.R. Lhotka, D.C. Harmes, B. Madigan, J.J. Hsiao, G.O. Staples, High resolution two-dimensional liquid chromatography coupled with mass spectrometry for robust and sensitive characterization of therapeutic antibodies at the peptide level, *J. Chromatogr. B Anal. Technol. Biomed. Life Sci.* 1134–1135 (2019) 121832, [10.1016/j.jchromb.2019.121832](https://doi.org/10.1016/j.jchromb.2019.121832).
- [101] R.J. Vonk, A.F.G. Gargano, E. Davydova, H.L. Dekker, S. Eelink, L.J. de Koning, P.J. Schoenmakers, Comprehensive two-dimensional liquid chromatography with stationary-phase-assisted modulation coupled to high-resolution mass spectrometry applied to proteome analysis of *Saccharomyces cerevisiae*, *Anal. Chem.* 87 (10) (2015) 5387–5394, <https://doi.org/10.1021/acs.analchem.5b00708>.
- [102] A.F.G. Gargano, M. Duffin, P. Navarro, P.J. Schoenmakers, Reducing dilution and analysis time in online comprehensive two-dimensional liquid chromatography by active modulation, *Anal. Chem.* 1 (2016) 1–16, <https://doi.org/10.1021/acs.analchem.5b04051>.
- [103] D.R. Stoll, K. Shoykhet, P. Petersson, S. Buckenmaier, Active solvent modulation: a valve-based approach to improve separation compatibility in two-dimensional liquid chromatography, *Anal. Chem.* 89 (2017) 9260–9267, <https://doi.org/10.1021/acs.analchem.7b02046>.
- [104] M.P. Washburn, D. Wolters, J.R. Yates, Large-scale analysis of the yeast proteome by multidimensional protein identification technology, *Nat. Biotechnol.* 19 (3) (2001) 242–247, <https://doi.org/10.1038/85686>.
- [105] R. Zheng, N. Govorukhina, T.N. Arrey, C. Pynn, A. van der Zee, G. Marko-Varga, R. Bischoff, A. Boychenko, Online-2D NanoLC-MS for crude serum proteome profiling: assessing sample preparation impact on proteome composition, *Anal. Chem.* 93 (2021) 9663–9668, <https://doi.org/10.1021/acs.analchem.1c01291>.
- [106] D. Yeung, B. Mizero, D. Gussakovskiy, N. Klaassen, Y. Lao, V. Spicer, O.V. Krokhin, Separation orthogonality in liquid chromatography-mass spectrometry for proteomic applications: comparison of 16 different two-dimensional combinations, *Anal. Chem.* 92 (2020) 3904–3912, <https://doi.org/10.1021/acs.analchem.9b05407>.
- [107] N. Delmotte, M. Lasaosa, A. Tholey, E. Heinzle, C.G. Huber, Two-dimensional reversed-phase x ion-pair reversed-phase HPLC: an alternative approach to high-resolution peptide separation for shotgun proteome analysis, *J. Proteome Res.* 6 (2007) 4363–4373, <https://doi.org/10.1021/pr070424t>.
- [108] S. Di Palma, P.J. Boersema, A.J.R. Heck, S. Mohammed, Zwitterionic hydrophilic interaction liquid chromatography (ZIC-HILIC and ZIC-CHILIC) provide high resolution separation and increase sensitivity in proteome analysis, *Anal. Chem.* 83 (9) (2011) 3440–3447, <https://doi.org/10.1021/ac103312e>.
- [109] M.S. Ritorito, K. Cook, K. Tyagi, P.G.A. Pedrioli, M. Trost, Hydrophilic strong anion exchange (hSAX) chromatography for highly orthogonal peptide separation of complex proteomes, *J. Proteome Res.* 12 (6) (2013) 2449–2457, <https://doi.org/10.1021/pr301011r>.
- [110] P. Yu, S. Petzoldt, M. Wilhelm, D. Zolg, R. Zheng, X. Sun, X. Liu, G. Schneider, A. F. Huhmer, B. Kuster, Trimodal mixed mode chromatography enables efficient offline 2D peptide fractionation for proteome analysis, *Anal. Chem.* (2017) [acs.analchem.7b01356](https://doi.org/10.1021/acs.analchem.7b01356), [10.1021/acs.analchem.7b01356](https://doi.org/10.1021/acs.analchem.7b01356).
- [111] M. Gilar, J. Fridrich, M.R. Schure, A. Jaworski, Comparison of orthogonality estimation methods for the two-dimensional separations of peptides, *Anal. Chem.* 84 (20) (2012) 8722–8732, <https://doi.org/10.1021/ac3020214>.
- [112] L.S. Roca, A.F.G. Gargano, P.J. Schoenmakers, Development of comprehensive two-dimensional low-flow liquid-chromatography setup coupled to high-resolution mass spectrometry for shotgun proteomics, *Anal. Chim. Acta.* 1156 (2021), 338349, <https://doi.org/10.1016/j.aca.2021.338349>.
- [113] Y. Zhao, R.P.W. Kong, G. Li, M.P.Y. Lam, C.H. Law, S.M.Y. Lee, H.C. Lam, I. K. Chu, Fully automatable two-dimensional hydrophilic interaction liquid chromatography-reversed phase liquid chromatography with online tandem mass spectrometry for shotgun proteomics, *J. Sep. Sci.* 35 (14) (2012) 1755–1763, <https://doi.org/10.1002/jssc.201200054>.
- [114] S. Di Palma, S. Mohammed, A.J.R. Heck, ZIC-CHILIC as a fractionation method for sensitive and powerful shotgun proteomics, *Nat. Protoc.* 7 (11) (2012) 2041–2055, <https://doi.org/10.1038/nprot.2012.124>.
- [115] S. Di Palma, D. Stange, M. van de Wetering, H. Clevers, A.J.R. Heck, S. Mohammed, Highly sensitive proteome analysis of FACS-sorted adult colon stem cells, *J. Proteome Res.* 10 (8) (2011) 3814–3819, <https://doi.org/10.1021/pr200367p>.



- [116] B.N. Swarge, W. Roseboom, L. Zheng, W.R. Abhyankar, S. Brul, C.G. de Koster, L. J. de Koning, "One-Pot" sample processing method for proteome-wide analysis of microbial cells and spores, *PROTEOMICS - Clin. Appl.* 12 (2018) 1700169, <https://doi.org/10.1002/prca.201700169>.
- [117] P. Hao, Y. Ren, B. Dutta, S.K. Sze, Comparative evaluation of electrostatic repulsion-hydrophilic interaction chromatography (ERLIC) and high-pH reversed phase (Hp-RP) chromatography in profiling of rat kidney proteome, *J. Proteomics* 82 (2013) 254–262, <https://doi.org/10.1016/j.jprot.2013.02.008>.
- [118] A.P. Boichenko, N. Govorukhina, A.G.J. van der Zee, R. Bischoff, Multidimensional separation of tryptic peptides from human serum proteins using reversed-phase, strong cation exchange, weak anion exchange, and fused-core fluorinated stationary phases, *J. Sep. Sci.* 36 (21–22) (2013) 3463–3470, <https://doi.org/10.1002/jssc.201300750>.
- [119] S. Loroch, T. Schommartz, W. Brune, René.P. Zahedi, A. Sickmann, Multidimensional electrostatic repulsion-hydrophilic interaction chromatography (ERLIC) for quantitative analysis of the proteome and phosphoproteome in clinical and biomedical research, *Biochim. Biophys. Acta.* 1854 (5) (2015) 460–468, <https://doi.org/10.1016/j.bbapap.2015.01.006>.
- [120] Z. Taoufiq, M. Ninov, A. Villar-Briones, H.-Y. Wang, T. Sasaki, M.C. Roy, F. Beauchain, Y. Mori, T. Yoshida, S. Takamori, R. Jahn, T. Takahashi, Hidden proteome of synaptic vesicles in the mammalian brain, *Proc. Natl. Acad. Sci.* 117 (52) (2020) 33586–33596, <https://doi.org/10.1073/pnas.2011870117>.
- [121] A.F.G. Gargano, J.B. Shaw, M. Zhou, C.S. Wilkins, T.L. Fillmore, R.J. Moore, G.W. Somsen, L. Paša-Tolić, Increasing the Separation Capacity of Intact Histone Proteoforms Chromatography Coupling Online Weak Cation Exchange-HILIC to Reversed Phase LC UVPD-HRMS, *J. Proteome Res.* 17 (2018) acs.jproteome.8b00458. [10.1021/acs.jproteome.8b00458](https://doi.org/10.1021/acs.jproteome.8b00458).
- [122] Z. Tian, R. Zhao, N. Tolić, R.J. Moore, D.L. Stenoien, E.W. Robinson, R.D. Smith, L. Paša-Tolić, Two-dimensional liquid chromatography system for online top-down mass spectrometry, *Proteomics* 10 (2010) 3610–3620, <https://doi.org/10.1002/pmic.201000367>.
- [123] L.M. Smith, N.L. Kelleher, Proteoform: a single term describing protein complexity, *Nat. Methods* 10 (2013) 186–187, <https://doi.org/10.1038/nmeth.2369>.
- [124] M.S. Bereman, D.D. Young, A. Deiters, D.C. Muddiman, Development of a robust and high throughput method for profiling N-linked glycans derived from plasma glycoproteins by nanoLC-FITCR mass spectrometry, *J. Proteome Res.* 8 (7) (2009) 3764–3770, <https://doi.org/10.1021/pr9002323>.
- [125] A. Helenius, M. Aebi, Intracellular functions of N-linked glycans, *Science* (80-). 291 (2001) 2364–2369. [10.1126/science.291.5512.2364](https://doi.org/10.1126/science.291.5512.2364).
- [126] C. Reilly, T.J. Stewart, M.B. Renfrow, J. Novak, Glycosylation in health and disease, *Nat. Rev. Nephrol.* 15 (6) (2019) 346–366, <https://doi.org/10.1038/s41581-019-0129-4>.
- [127] B.N. Vajaria, P.S. Patel, Glycosylation: a hallmark of cancer? *Glycoconj. J.* 34 (2) (2017) 147–156, <https://doi.org/10.1007/s10719-016-9755-2>.
- [128] J. Pan, Y. Hu, S. Sun, L. Chen, M. Schnaubelt, D. Clark, M. Ao, Z. Zhang, D. Chan, J. Qian, H. Zhang, Glycoproteomics-based signatures for tumor subtyping and clinical outcome prediction of high-grade serous ovarian cancer, *Nat. Commun.* 11 (2020) 1–13, <https://doi.org/10.1038/s41467-020-19976-3>.
- [129] S. Ongay, A. Boichenko, N. Govorukhina, R. Bischoff, Glycopeptide enrichment and separation for protein glycosylation analysis, *J. Sep. Sci.* 35 (2012) 2341–2372, <https://doi.org/10.1002/jssc.201200434>.
- [130] K.K. Palaniappan, C.R. Bertozzi, Chemical glycoproteomics, *Chem. Rev.* 116 (23) (2016) 14277–14306, <https://doi.org/10.1021/acs.chemrev.6b00023>.
- [131] R. Zhu, L. Zacharias, K.M. Wooding, W. Peng, Y. Mechref, Glycoprotein enrichment analytical techniques, *Methods Enzym.* (2017) 397–429, <https://doi.org/10.1016/bs.mie.2016.11.009>.
- [132] L.G. Zacharias, A.K. Hartmann, E. Song, J. Zhao, R. Zhu, P. Mirzaei, Y. Mechref, HILIC and ERLIC enrichment of glycopeptides derived from breast and brain cancer cells, *J. Proteome Res.* 15 (10) (2016) 3624–3634, <https://doi.org/10.1021/acs.jproteome.6b00429>.
- [133] C. Zhang, Z. Ye, P. Xue, Q. Shu, Y. Zhou, Y. Ji, Y. Fu, J. Wang, F. Yang, Evaluation of different N-glycopeptide enrichment methods for N-glycosylation site mapping in mouse brain, *J. Proteome Res.* 15 (9) (2016) 2960–2968, <https://doi.org/10.1021/acs.jproteome.6b00098>.
- [134] K. Neue, M. Mormann, J. Peter-Katalinić, G. Pohlentz, Elucidation of glycoprotein structures by unspecific proteolysis and direct nanoESI mass spectrometric analysis of ZIC-HILIC-enriched glycopeptides, *J. Proteome Res.* 10 (5) (2011) 2248–2260, <https://doi.org/10.1021/pr101082c>.
- [135] L. Cao, L. Yu, Z. Guo, X. Li, X. Xue, X. Liang, Application of a strong anion exchange material in electrostatic repulsion-hydrophilic interaction chromatography for selective enrichment of glycopeptides, *J. Chromatogr. A.* 1299 (2013) 18–24, <https://doi.org/10.1016/j.chroma.2013.05.037>.
- [136] Y. Huang, Y. Nie, B. Boyes, R. Orlando, Resolving isomeric glycopeptide glycoforms with hydrophilic interaction chromatography (HILIC), *J. Biomol. Tech.* 27 (3) (2016) 98–104, <https://doi.org/10.7171/jbt.16-2703-003>.
- [137] S.M. Totten, C.L. Feasley, A. Bermudez, S.J. Pitteri, Parallel comparison of N-linked glycopeptide enrichment techniques reveals extensive glycoproteomic analysis of plasma enabled by SAX-ERLIC, *J. Proteome Res.* 16 (3) (2017) 1249–1260, <https://doi.org/10.1021/acs.jproteome.6b00849>.
- [138] C.H. Lin, C. Krisp, N.H. Packer, M.P. Molloy, Development of a data independent acquisition mass spectrometry workflow to enable glycopeptide analysis without predefined glycan compositional knowledge, *J. Proteomics* 172 (2018) 68–75, <https://doi.org/10.1016/j.jprot.2017.10.011>.
- [139] A.J. Alpert, O. Hudecz, K. Mechtler, Anion-exchange chromatography of phosphopeptides: weak anion exchange versus strong anion exchange and anion-exchange chromatography versus electrostatic repulsion-hydrophilic interaction chromatography, *Anal. Chem.* 87 (2015) 4704–4711, <https://doi.org/10.1021/acs504420c>.
- [140] Y. Zhao, Y. Chen, Z. Xiong, X. Sun, Q. Zhang, Y. Gan, L. Zhang, W. Zhang, Synthesis of magnetic zwitterionic-hydrophilic material for the selective enrichment of N-linked glycopeptides, *J. Chromatogr. A.* 1482 (2017) 23–31, <https://doi.org/10.1016/j.chroma.2016.12.054>.
- [141] F. Jiao, F. Gao, H. Wang, Y. Deng, Y. Zhang, X. Qian, Y. Zhang, Ultrathin Au nanowires assisted magnetic graphene-silica ZIC-HILIC composites for highly specific enrichment of N-linked glycopeptides, *Anal. Chim. Acta.* 970 (2017) 47–56, <https://doi.org/10.1016/j.aca.2017.03.014>.
- [142] J. Wohlgenuth, M. Karas, T. Eichhorn, R. Hendriks, S. Andrecht, Quantitative site-specific analysis of protein glycosylation by LC-MS using different glycopeptide-enrichment strategies, *Anal. Biochem.* 395 (2) (2009) 178–188, <https://doi.org/10.1016/j.ab.2009.08.023>.
- [143] G. Qing, J. Yan, X. He, X. Li, X. Liang, Recent advances in hydrophilic interaction liquid chromatography materials for glycopeptide enrichment and glycan separation, *TrAC - Trends Anal. Chem.* 124 (2020), 115570, <https://doi.org/10.1016/j.trac.2019.06.020>.
- [144] K. Molnarova, A. Duris, T. Jecmen, P. Kozlik, Comparison of human IgG glycopeptides separation using mixed-mode hydrophilic interaction/ion-exchange liquid chromatography and reversed-phase mode, *Anal. Bioanal. Chem.* (2021) 8–14, <https://doi.org/10.1007/s00216-021-03388-3>.
- [145] Y.E.M. van der Burg, K.M. Siliakus, C.M. Cobbaert, L.R. Ruitaak, HILIC-MRM-MS for linkage-specific separation of sialylated glycopeptides to quantify prostate-specific antigen proteoforms, *J. Proteome Res.* 19 (7) (2020) 2708–2716, <https://doi.org/10.1021/acs.jproteome.0c00050>.
- [146] Z.X. Tian, N. Tolic, R. Zhao, R.J. Moore, S.M. Hengel, E.W. Robinson, D. L. Stenoien, S. Wu, R.D. Smith, L. Pasa-Tolic, Enhanced top-down characterization of histone post-translational modifications, *GENOME Biol.* 13 (2012), <https://doi.org/10.1186/gb-2012-13-10-R86>.
- [147] H.R. Jung, S. Sidoli, S. Haldbo, R.R. Sprenger, V. Schwämmle, D. Pasini, K. Helin, O.N. Jensen, Precision mapping of coexisting modifications in histone H3 tails from embryonic stem cells by ETD-MS/MS, *Anal. Chem.* 85 (17) (2013) 8232–8239, <https://doi.org/10.1021/ac401299w>.
- [148] Y. Yu, J. Chen, Y. Gao, J. Gao, R. Liao, Y. Wang, C. Oyang, E. Li, C. Zeng, S. Zhou, P. Yang, H. Jin, W. Yi, Quantitative profiling of combinational K27/K36 modifications on histone H3 variants in mouse organs, *J. Proteome Res.* 15 (3) (2016) 1070–1079, <https://doi.org/10.1021/acs.jproteome.5b01164>.
- [149] S.M. Greer, S. Sidoli, M. Coradin, M. Schack Jespersen, V. Schwämmle, O. N. Jensen, B.A. Garcia, J.S. Brodbelt, Extensive characterization of heavily modified histone tails by 193 nm ultraviolet photodissociation mass spectrometry via a middle-down strategy, *Anal. Chem.* 90 (17) (2018) 10425–10433, <https://doi.org/10.1021/acs.analchem.8b02320>.
- [150] T.T. Jiang, M.E. Hoover, M.V. Holt, M.A. Freitas, A.G. Marshall, N.L. Young, Middle-down characterization of the cell cycle dependence of histone H4 posttranslational modifications and proteoforms, *Proteomics* 18 (2018), <https://doi.org/10.1002/pmic.201700442>.
- [151] M. Coradin, M.R. Mendoza, S. Sidoli, A.J. Alpert, C.C. Lu, B.A. Garcia, Bullet points to evaluate the performance of the middle-down proteomics workflow for histone modification analysis, *Methods* 184 (2020) 86–92, <https://doi.org/10.1016/j.ymeth.2020.01.013>.
- [152] S. Rezinčinc, Z. Tian, S. Wu, S. Hengel, L. Pasa-Tolic, H.S. Smallwood, Mapping influenza-induced posttranslational modifications on histones from cd8+ t cells, *Viruses* 12 (2020), <https://doi.org/10.3390/v12121409>.
- [153] B.D. Strahl, C.D. Allis, The language of covalent histone modifications, *Nature* 403 (6765) (2000) 41–45, <https://doi.org/10.1038/47412>.
- [154] M. Zeeshan, I. Kaur, J. Joy, E. Saini, G. Paul, A. Kaushik, S. Dabral, A. Mohammed, D. Gupta, P. Malhotra, Proteomic identification and analysis of arginine-methylated proteins of plasmodium falciparum at asexual blood stages, *J. Proteome Res.* 16 (2) (2017) 368–383, <https://doi.org/10.1021/acs.jproteome.5b01052>.
- [155] P.J. Boersema, N. Divecha, A.J.R. Heck, S. Mohammed, Evaluation and optimization of ZIC-HILIC-RP as an alternative MudPIT strategy, *J. Proteome Res.* 6 (3) (2007) 937–946, <https://doi.org/10.1021/pr060589m>.
- [156] S. Loroch, R.P. Zahedi, A. Sickmann, Highly sensitive phosphoproteomics by tailoring solid-phase extraction to electrostatic repulsion-hydrophilic interaction chromatography, *Anal. Chem.* 87 (3) (2015) 1596–1604, <https://doi.org/10.1021/ac502708m>.
- [157] M. Källsten, J. Bergquist, H. Zhao, A. Konzer, S.B. Lind, A comparative study of phosphopeptide-selective techniques for a sub-proteome of a complex biological sample, *Anal. Bioanal. Chem.* 408 (9) (2016) 2347–2356, <https://doi.org/10.1007/s00216-016-9333-2>.
- [158] M. Wakabayashi, Y. Kyono, N. Sugiyama, Y. Ishihama, Extended coverage of singly and multiply phosphorylated peptides from a single titanium dioxide microcolumn, *Anal. Chem.* 87 (20) (2015) 10213–10221, <https://doi.org/10.1021/acs.analchem.5b01216>.
- [159] F. Zappacosta, G.F. Scott, M.J. Huddleston, R.S. Annan, An optimized platform for hydrophilic interaction chromatography-immobilized metal affinity chromatography enables deep coverage of the rat liver phosphoproteome, *J. Proteome Res.* 14 (2) (2015) 997–1009, <https://doi.org/10.1021/pr501025e>.
- [160] P.L. Hao, T.N. Guo, S.K. Sze, Simultaneous analysis of proteome, phospho- and glycoproteome of rat kidney tissue with electrostatic repulsion hydrophilic interaction chromatography, *PLoS One* 6 (2011), <https://doi.org/10.1371/journal.pone.0016884>.

- [163] T.-T. Yeh, M.-Y. Ho, W.-Y. Chen, Y.-C. Hsu, W.-C. Ku, H.-W. Tseng, S.-T. Chen, S.-F. Chen, Comparison of different fractionation strategies for in-depth phosphoproteomics by liquid chromatography tandem mass spectrometry, *Anal. Bioanal. Chem.* 411 (15) (2019) 3417–3424, <https://doi.org/10.1007/s00216-019-01823-0>.
- [164] C. Villacrés, V. Spicer, O.V. Krokhnin, Confident identification of citrullination and carbamylation assisted by peptide retention time prediction, *J. Proteome Res.* 20 (3) (2021) 1571–1581, <https://doi.org/10.1021/acs.jproteome.0c00775>.
- [165] X. Gallart-Palau, A. Serra, S.K. Sze, LERLIC-MS/MS for in-depth characterization and quantification of glutamine and asparagine deamidation in shotgun proteomics, *JOVE-JOURNAL Vis. Exp.* (2017), <https://doi.org/10.3791/55626>.
- [166] S.S. Adav, X. Gallart-Palau, K.H. Tan, S.K. Lim, J.P. Tam, S.K. Sze, Dementia-linked amyloidosis is associated with brain protein deamidation as revealed by proteomic profiling of human brain tissues, *Mol. Brain* 9 (2016), <https://doi.org/10.1186/s13041-016-0200-z>.
- [167] A. Serra, X. Gallart-Palau, J. Wei, S.K. Sze, Characterization of glutamine deamidation by long-length electrostatic repulsion-hydrophilic interaction chromatography-tandem mass spectrometry (LERLIC-MS/MS) in Shotgun Proteomics, *Anal. Chem.* 88 (21) (2016) 10573–10582, <https://doi.org/10.1021/acs.analchem.6b02688>.
- [168] P. Hao, J. Qian, B. Dutta, E.S.H. Cheow, K.H. Sim, W. Meng, S.S. Adav, A. Alpert, S.K. Sze, Enhanced separation and characterization of deamidated peptides with RP-ERLIC-based multidimensional chromatography coupled with tandem mass spectrometry, *J. Proteome Res.* 11 (3) (2012) 1804–1811, <https://doi.org/10.1021/pr201048c>.
- [169] P.L. Hao, Y. Ren, A.J. Alpert, S.K. Sze, Detection, evaluation and minimization of nonenzymatic deamidation in proteomic sample preparation, *Mol. Cell. Proteomics* 10 (2011), <https://doi.org/10.1074/mcp.O111.009381>.
- [170] M.J. Badgett, B. Boyes, R. Orlando, The separation and quantitation of peptides with and without oxidation of methionine and deamidation of asparagine using hydrophilic interaction liquid chromatography with mass spectrometry (HILIC-MS), *J. Am. Soc. Mass Spectrom.* 28 (5) (2017) 818–826, <https://doi.org/10.1007/s13361-016-1565-z>.
- [171] W. Vogt, Oxidation of methionyl residues in proteins: tools, targets, and reversal, *Free Radic. Biol. Med.* 18 (1) (1995) 93–105, [https://doi.org/10.1016/0891-5849\(94\)00158-G](https://doi.org/10.1016/0891-5849(94)00158-G).
- [172] R. De Pauw, B. Degreef, H. Ritchie, S. Eelink, G. Desmet, K. Broeckhoven, Extending the limits of operating pressure of narrow-bore column liquid chromatography instrumentation, *J. Chromatogr. A* 1347 (2014) 56–62, <https://doi.org/10.1016/j.chroma.2014.04.056>.
- [173] K.M. Grinias, J.M. Godinho, E.G. Franklin, J.T. Stobaugh, J.W. Jorgenson, Development of a 45 kpsi ultrahigh pressure liquid chromatography instrument for gradient separations of peptides using long microcapillary columns and sub-2 μm particles, *J. Chromatogr. A* 1469 (2016) 60–67, <https://doi.org/10.1016/j.chroma.2016.09.053>.
- [174] M.J. Sorensen, R.T. Kennedy, Capillary ultrahigh-pressure liquid chromatography-mass spectrometry for fast and high resolution metabolomics separations, *J. Chromatogr. A* 1635 (2021), 461706, <https://doi.org/10.1016/j.chroma.2020.461706>.
- [175] M.J. Sorensen, K.E. Miller, J.W. Jorgenson, R.T. Kennedy, Ultrahigh-performance capillary liquid chromatography-mass spectrometry at 35 kpsi for separation of lipids, *J. Chromatogr. A* (2019), 460575, <https://doi.org/10.1016/j.chroma.2019.460575>.
- [176] Z. Wu, B. Wei, X. Zhang, M.J. Wirth, Efficient separations of intact proteins using slip-flow with nano-liquid chromatography-mass spectrometry, *Anal. Chem.* 86 (3) (2014) 1592–1598, <https://doi.org/10.1021/ac403233d>.
- [177] B.A. Rogers, Z. Wu, B. Wei, X. Zhang, X. Cao, O. Alabi, M.J. Wirth, Submicrometer particles and slip flow in liquid chromatography, *Anal. Chem.* 87 (5) (2015) 2520–2526, <https://doi.org/10.1021/ac504683d>.
- [178] G. van Schaick, B.W.J. Pirok, R. Haselberg, G.W. Somsen, A.F.G. Gargano, Computer-aided gradient optimization of hydrophilic interaction liquid chromatographic separations of intact proteins and protein glycoforms, *J. Chromatogr. A* (2019) 67–76, <https://doi.org/10.1016/j.chroma.2019.03.038>.
- [179] T. Jiang, M.E. Hoover, M.V. Holt, M.A. Freitas, A.G. Marshall, N.L. Young, Middle-down characterization of the cell cycle dependence of histone H4 posttranslational modifications and proteoforms, *Proteomics* 18 (11) (2018) 1700442, <https://doi.org/10.1002/pmic.201700442>.
- [180] P. Jandera, Stationary and mobile phases in hydrophilic interaction chromatography: a review, *Anal. Chim. Acta* 692 (1–2) (2011) 1–25, <https://doi.org/10.1016/j.aca.2011.02.047>.
- [181] R. Hájek, M. Lída, M. Khalikova, R. Jirásko, E. Cífková, V. Študent, D. Vrána, L. Opálka, K. Vávrová, M. Matzenauer, B. Melichar, M. Holčápek, HILIC/ESI-MS determination of gangliosides and other polar lipid classes in renal cell carcinoma and surrounding normal tissues, *Anal. Bioanal. Chem.* 410 (25) (2018) 6585–6594, <https://doi.org/10.1007/s00216-018-1263-8>.
- [182] A.D. Southam, H. Pursell, G. Frigerio, A. Jankevics, R.J.M. Weber, W.B. Dunn, Characterization of monophasic solvent-based tissue extractions for the detection of polar metabolites and lipids applying ultrahigh-performance liquid chromatography-mass spectrometry clinical metabolic phenotyping assays, *J. Proteome Res.* 20 (1) (2021) 831–840, <https://doi.org/10.1021/acs.jproteome.0c00660>.
- [183] Y. rong Ma, M. yan Xin, K. Li, H. Wang, Z. Rao, T. xi Liu, X. an Wu, An LC-MS/MS analytical method for the determination of uremic toxins in patients with end-stage renal disease, *J. Pharm. Biomed. Anal.* 191 (2020) 113551. 10.1016/j.jpba.2020.113551.
- [184] G. Hermann, M. Schwaiger, P. Volejnik, G. Koellensperger, <sup>13</sup>C-labelled yeast as internal standard for LC-MS/MS and LC high resolution MS based amino acid quantification in human plasma, *J. Pharm. Biomed. Anal.* 155 (2018) 329–334, <https://doi.org/10.1016/j.jpba.2018.03.050>.
- [185] J. Li, Q.L. Wang, Y. Liu, Y. Ke, Q.Q. Fan, P. Zhou, M.C. An, H.M. Liu, Simultaneous determination of 24 free amino acids in MGC803 cells by hydrophilic interaction liquid chromatography with tandem mass spectrometry, *J. Chromatogr. B Anal. Technol. Biomed. Life Sci.* 1132 (2019) 1–9. 10.1016/j.jchromb.2019.121792.
- [186] C.-X. Du, Z. Huang, Analysis of amino acids in human tears by hydrophilic interaction liquid chromatography and quadrupole orbitrap mass spectrometry, *RSC Adv.* 9 (63) (2019) 36539–36545, <https://doi.org/10.1039/C9RA05956C>.
- [187] M.G.M. Kok, C. Nix, G. Nys, M. Fillet, Targeted metabolomics of whole blood using volumetric absorptive microsampling, *Talanta* 197 (2019) 49–58, <https://doi.org/10.1016/j.talanta.2019.01.014>.
- [188] E.M. Mathew, L. Lewis, P. Rao, K. Nalini, A. Kamath, S. Moorkoth, Novel HILIC-ESI-MS method for urinary profiling of MSUD and methylmalonic aciduria biomarkers, *J. Chromatogr. Sci.* 57 (2019) 715–723, <https://doi.org/10.1093/chromsci/bmz045>.
- [189] L. Rastegar, H. Mighani, A. Ghassempour, A comparison and column selection of Hydrophilic Interaction Liquid Chromatography and Reversed-Phase High-Performance Liquid Chromatography for detection of DNA methylation, *Anal. Biochem.* 557 (2018) 123–130, <https://doi.org/10.1016/j.ab.2018.07.013>.
- [190] L.M. Rest, A. Shafaei, K. Fuchino, P. Bruheim, Zwitterionic HILIC tandem mass spectrometry with isotope dilution for rapid, sensitive and robust quantification of pyridine nucleotides in biological extracts, *J. Chromatogr. B Anal. Technol. Biomed. Life Sci.* 1144 (2020) 122078. 10.1016/j.jchromb.2020.122078.
- [191] Y. Sakaguchi, K. Miyauchi, B. Il Kang, T. Suzuki, Nucleoside Analysis by Hydrophilic Interaction Liquid Chromatography Coupled with Mass Spectrometry, 1st ed., Elsevier Inc., 2015. 10.1016/bs.mie.2015.03.015.
- [192] O. Begou, O. Deda, A. Agapiou, I. Taitzoglou, H. Gika, G. Theodoridis, Urine and fecal samples targeted metabolomics of carobs treated rats, *J. Chromatogr. B Anal. Technol. Biomed. Life Sci.* 1114–1115 (2019) 76–85, <https://doi.org/10.1016/j.jchromb.2019.03.028>.
- [193] T. Linghu, Y. Gao, A. Li, B. Shi, J. Tian, X. Qin, A unique insight for energy metabolism disorders in depression based on chronic unpredictable mild stress rats using stable isotope-resolved metabolomics, *J. Pharm. Biomed. Anal.* 191 (2020), 113588, <https://doi.org/10.1016/j.jpba.2020.113588>.
- [194] X. Cai, R. Li, Concurrent profiling of polar metabolites and lipids in human plasma using HILIC-FTMS, *Sci. Rep.* 6 (2016) 1–10, <https://doi.org/10.1038/srep36490>.
- [195] A.F.G. Gargano, L.S. Roca, R.T. Fellers, M. Bocxe, E. Domínguez-Vega, G. W. Somsen, Capillary HILIC-MS: a new tool for sensitive top-down proteomics, *Anal. Chem.* 90 (2018) 6601–6609, <https://doi.org/10.1021/acs.analchem.8b00382>.
- [196] M. Zarei, A. Sprenger, F. Metzger, C. Gretzmeier, J. Dengjel, Comparison of ERLIC-TiO<sub>2</sub>, HILIC-TiO<sub>2</sub>, and SCX-TiO<sub>2</sub> for global phosphoproteomics approaches, *J. Proteome Res.* 10 (8) (2011) 3474–3483, <https://doi.org/10.1021/pr200092z>.
- [197] S.S. Adav, H.H. Hwa, D. de Kleijn, S.K. Sze, Improving blood plasma glycoproteome coverage by coupling ultracentrifugation fractionation to electrostatic repulsion-hydrophilic interaction chromatography enrichment, *J. Proteome Res.* 14 (7) (2015) 2828–2838, <https://doi.org/10.1021/acs.jproteome.5b00102>.
- [198] K.A. Janssen, M. Coradin, C. Lu, S. Sidoli, B.A. Garcia, Quantitation of Single and combinatorial histone modifications by integrated chromatography of bottom-up peptides and middle-down polypeptide tails, *J. Am. Soc. Mass Spectrom.* 30 (12) (2019) 2449–2459, <https://doi.org/10.1007/s13361-019-02303-6>.